THE THERMAL DEHYDRATION OF NATURAL ZEOLITES

L. P. VAN REEUWIJK

L. P. VAN REEUWIJK

THE THERMAL DEHYDRATION OF NATURAL ZEOLITES

PROEFSCHRIFT

TER VERKRIJGING VAN DE GRAAD VAN DOCTOR IN DE LANDBOUWWETENSCHAPPEN, OP GEZAG VAN DE RECTOR MAGNIFICUS, PROF. DR. IR. H. A. LENIGER, HOOGLERAAR IN DE TECHNOLOGIE, IN HET OPENBAAR TE VERDEDIGEN OP WOENSDAG 29 MEI 1974 DES NAMIDDAGS TE VIER UUR IN DE AULA VAN DE LANDBOUWHOGESCHOOL TE WAGENINGEN

H. VEENMAN & ZONEN B.V. - WAGENINGEN - 1974

STELLINGEN

1

Vanwege hun unieke eigenschappen verdienen natuurlijke zeolieten meer onderzoek van hun toepassingsmogelijkheden dan thans het geval is.

2

Het bepalen van het z.g. H_2O- van zeolieten door het gewichtsverlies van monsters na verhitting tot 110°C te meten, zoals voorgesteld door MARGARET FOSTER, is zinloos.

FOSTER, M. D. (1965) U.S. Geol. Surv. Prof. Paper **504-D,E.**

3

In tegenstelling tot de bewering van ZEN, hebben in zeolieten geadsorbeerde watermoleculen geen grotere entropie dan die in de vloeibare fase.

ZEN, E-AN (1972) Amer. Miner. **57**: 524.

4

Bij publicatie van differentiëel thermische analyse (DTA) curves van reacties waarbij gassen zijn betrokken, dient van deze gassen de (partiële) druk te worden vermeld, ook wanneer die gassen zijn samengesteld uit de lucht in het laboratorium en de gassen die bij de reactie vrijkomen of worden opgenomen.

MCADIE, H. G. (1967) Zeitschr. anal. Chem. **231**: 35.

5

Bij het geven van nieuwe namen aan mineralen die slechts in symmetrie een weinig blijken af te wijken van eerder bekende mineralen, moet grote terughoudendheid betracht worden.

ANDERSEN, E. K., M. DANØ en O. V. PETERSEN (1969) Medd. *Grønland* **181** *no.* 10:1.

6

Bij de preferentiële onttrekking van kaliumionen uit zeewater spelen amorfe aluminosilicaten in het bodemslib een belangrijke rol.

7

De pH-afhankelijkheid van de adsorptiecapaciteit van allofaan is niet slechts het gevolg van protonatie of deprotonatie van de functionele eindgroepen van hydroxy-aluminium polymeren, maar tevens van het verschuiven van de polymerisatiegraad van deze fase.

DE VILLIERS, J. M. en M. L. JACKSON (1967) Soil Sci. Soc. Amer. Proc. **31**: 473.
VAN REEUWIJK, L. P. en J. M. DE VILLIERS (1970) Agrochemophysica **2**: 77.

8

Texturele banden of lamellae van een banden-B in zandige bodems verplaatsen zich van beneden naar boven in het profiel.

9

Vijfenzeventig jaar na de oproep van Hopkins om tot standaardisatie van korrelgrootteklassen in de korrelgrootteanalyse van grondmonsters te komen, dient hier thans in de bodemkunde zowel als in de sedimentologie onverwijld toe te worden overgegaan.

HOPKINS, C. G. (1899) U. S. Dept. Agric. Bull. 56: 64.

10

De geologische positie van Nederland, een bekken dat gedeeltelijk opgevuld is met grofkorrelige zandige afzettingen met daaronder niet-diagenetisch verharde fijnerkorrelige afzettingen, maakt het niet verantwoord schadelijke afvalstoffen in deze afzettingen te persen.

11

De educatieve waarde van botanische tuinen is aanmerkelijk groter indien de naamsaanduidingen bij de planten niet slechts in het latijn zijn gesteld doch tevens, voor zover deze bestaan, in de landstaal.

12

Indien wegen in wooncentra met klinkers moeten worden bestraat, dan dienen ter vermindering van geluidsoverlast de klinkers volgens een diagonaalpatroon te worden gelegd en niet loodrecht op de rijrichting van het verkeer.

13

Dat volwassenen een lager lichaamsvochtgehalte hebben dan babies houdt niet in dat zij daardoor minder uit hun duim kunnen zuigen.

LYKLEMA, J. Diesrede Landbouwhogeschool 1974.

L. P. VAN REEUWIJK
Wageningen, 29 mei 1974.

CONTENTS

1. INTRODUCTION

1.1. HISTORY

Investigation of zeolites by heat treatment dates back to the middle of the 18th century. CRONSTEDT (1756) at that time noted that on heating certain minerals seemed to melt and boil simultaneously with an intense production of water vapour. He therefore called these minerals zeolites, a combination of the Greek words *zein*, to boil, and *lithos*, stone.

Zeolites could be broadly defined as hydrated aluminosilicates of the alkalies and alkaline earths, with a three-dimensional anion network. By consequence, they belong to the tectosilicates together with such minerals as feldspars and felspathoids.

The first direct investigation on zeolites was carried out by DAMOUR (1857) who reported on the reversibility of dehydration of these minerals. Ever since, the character of water in zeolites has been a topic of discussion and research (for early literature see HINTZE, 1897).

Almost simultaneously, EICHHORN (1858), studied the property of zeolites to exchange ions with salt solutions. However, it was not until 1905 that his property was applied on an industrial scale for softening hard water. In 1890, DOELTER was the first to synthesize zeolites from solutions whereas FRIEDEL (1896) shortly after that succeeded to adsorb gases, alcohol and several other substances on dehydrated zeolites.

The term 'soil zeolites' was introduced by GANS (1915) who ascribed the ion exchange properties of soils to amorphous weathering products similar to synthetic permutites and zeolites. It should be realized that at that time X-ray analysis had not yet revealed the crystallinity of soil clay particles. This soil zeolite theory persisted for a surprisingly long time (STEBUTT, 1930).

Structure analysis using X-ray techniques (e.g., PAULING, 1930; TAYLOR, 1930; TAYLOR et al., 1933) revealed that zeolite structures contain channels and cages of molecular size, roughly from 3–10 Å. These voids are occupied by charge balancing cations and by water molecules. These both have considerable freedom of movement and thus permit ion exchange, reversible dehydration and replacement of water by certain other substances. The dimensions of these cavities are fixed and specific for each zeolite species which thus facilitates preferential adsorption i.e., accepting one kind of ions or molecules and excluding others. For this reason zeolites are often appropriately referred to as 'molecular sieves'.

Synthetic zeolites appeared to have distinct technical advantages over the natural ones in that they are pure, consisting of one type, and commercially available in virtually unlimited amounts often synthesized to a required pore size specification. Therefore, the emphasis of recent research has considerably shifted towards these materials. Of late, however, large and relatively pure

deposits of technically useful zeolites have been discovered in various parts of the world, notably in the United States, and therefore the interest in natural zeolites is rapidly reviving. This interest is also stimulated by the fact that they may become available at a price up to a hundred times lower than their synthetic analogues (DEFFEYES, 1967). Exploitation, however, is still in its infancy.

1.2. GENESIS AND OCCURRENCE OF NATURAL ZEOLITES

The genesis and paragenesis of zeolites have been the field of study of many geologists. Recent contributions are given by COOMBS (1970), COOMBS et al. (1959), DEER et al. (1963), DEFFEYES (1959), AUMENTO (1966), HOOVER (1969), SEKI (1969), IJIMA and HARADA (1968), SHEPPARD and GUDE (1968), KOSSOWSKAYA (1973). It was soon realized that the zeolite facies was bridging a wide gap between processes in sediments under atmospheric conditions and the hitherto recognized metamorphic facies. However, the continuous discovery of new sources of zeolites of different origin has repeatedly made necessary the modification and extension of the theories concerning the genetical processes.

Because zeolites are hydrous mineral phases of low specific density (ranging from 1.9 to 2.3 g/cm^3) they are relatively sensitive to pressure and temperature. Thus, it is to be expected that a vertical pressure-temperature gradient in a rock column results in a vertical zonation of zeolite types from least dense and most hydrous at the surface to most dense and least hydrous at depth. The picture is usually complicated by the behaviour of water (i.e., water pressure) which is influenced by such factors as permeability, porosity and osmotic effects.

The chemical environment is of equal importance in determining the species to be formed. The prime factors in this respect are the host rock and the water chemistry (pH, salinity); usually, components are supplied from elsewhere by percolating water.

At the present state of knowledge the following state functions, largely following COOMBS (1970), may be distinguished:

a. *Transformation and neoformation of minerals under the influence of hydrothermal processes caused by active volcanism (late-stage hydrothermal environment)*

This produced the often well-developed show-case zeolites occurring in amygdales, veins and fissures of mainly, but not exclusively, basic volcanic rocks as a result of rising hydrothermal solutions through stationary but still liquid magma. Though they are perhaps the best known occurrences, the paragenesis in this case is the least well systematized. Almost any type of zeolite may be formed in this environment.

b. *Hydrothermal alteration of rocks in so-called geothermal fields*

Several of these areas have been described in the Japanese literature and by Coombs and his coworkers. The study of the relation between the occurrence

of certain species and the prevailing temperature and pressure has led to the construction of useful phase diagrams describing the paragenesis. An example of a sequence towards the heat centre of such a geothermal field may be: analcite, mordenite, laumontite, wairakite and less hydrous phases, feldspars.

c. *Alteration by burial metamorphism*

This results from a vertical pressure-temperature gradient as mentioned earlier, caused by increasing thickness of sediment with time. The zeolites may replace detrital feldspars, organic and inorganic calcite together with aluminous clay minerals, glass and vitric tuffs. The sequences found in such cases are similar to those in geothermal fields although gross overlapping appears to be common.

d. *Alteration caused by the processes in a column of sediments*

Petrographers call this process *diagenesis*. Zeolites are common authigenic silicate minerals in sedimentary deposits of different age, lithology and depositional environment. This is particularly so in those sediments originally rich in silicic pyroclasts such as vitric tuffs. Most zeolites in sedimentary rocks are formed during diagenesis by the reaction of aluminosilicates with pore water. This water can be either alkalic groundwater or alkalic lake water. Hence, these zeolites are often found as cementing agents filling pores and interstices of the host rock. Gel-like materials as an interstage of such crystallization processes have been observed, for instance during formation of phillipsite, and suggests a dissolution-reprecipitation mechanism at least in some cases. This is fully in agreement with the preferential adsorption of alkalies by such gels (VAN REEUWIJK & DE VILLIERS, 1968) and the finding of the present author that the amorphous colloidal fraction of fresh marine sediments contain relatively large amounts of potassium despite the unfavourable Na/K ratio in sea water (VAN REEUWIJK, 1967). However, during analcite crystallization no such interstage has been observed (R. A. SHEPPARD, oral comm.).

It is fortunate that a number of technically interesting zeolites such as clinoptilolite, mordenite, erionite, chabazite and phillipsite are abundantly present in several of these sediments as virtually monomineralic beds (altered tuffs) rendering them suitable for exploitation.

e. *Formation by chemical sedimentation*

Under this heading is described the 'primary' crystallization of zeolites in sediments. Since this process may, to a greater or lesser extent, also occur during all the earlier mentioned situations, this case may be somewhat cryptic. It is generally accepted that analcite, occurring commonly in rocks varying widely in lithology, age and environment, is formed by this process. Another example is the wide occurrence of phillipsite and harmotome in palagonitic bottom sediments of the Pacific Ocean.

The occurrence of analcite in soils has been reported by SCHULZ et al. (1965) and BALDAR and WHITTIG (1968). In both cases the zeolite was found in highly

alkaline soils containing Na_2CO_3 and with a pH above 9. This can safely be considered as a primary crystallization.

1.3. Structural classification

To date, a satisfactory detailed classification of the more than 30 known zeolites is still lacking despite several attempts that have been made. This could be due to the relatively limited interest mineralogists have shown to this group. Non-mineralogists, especially chemists, have made classification schemes but they are based on a limited number of characteristics, usually not more than one, serving a specific purpose. Classification schemes of this type are, for example, those based on the effective diameter of the structural channels, or on a derived property, such as the size of molecules activated (i.e., dehydrated) zeolites can absorb (Barrer, 1964; Hersch, 1961). Pécsi-Donáth (1968) suggested classification on the basis of the type of water bonding and the related rehydration properties. Barrer (1973) suggested a new nomenclature of synthetic and natural zeolites essentially based on the structural type but including information about cation exchange, isomorphous substitution and chemical lattice defects.

The modern mineralogical classifications relate to natural substances only and are of crystallochemical nature in that that they employ the functional relationship existing between the chemical composition and the structure of a mineral. Because the structures of several zeolites have remained undetermined or are still subject to revision, their classification is not yet finished. Even the recent descriptive mineralogy book by Kostov (1969) appears to ignore such recognized and seemingly sound classification schemes as those of Smith (1963), Deer et al. (1963) and Meier (1968). Based mainly on these latter references the following tentative classification may be given (table 1.1.).

The sodalite group of minerals is not included in this scheme. These do have related properties but are generally classified as felspathoids.

The geometrical pattern of the zeolite aluminosilicate frameworks can in most cases be visualized in at least one of three different ways: in terms of chains, layers, and polyhedra, all formed by the linking of silica and alumina tetrahedra. To illustrate this a few examples of each type will be given in brief.

Chain structures. Three different possibilities are found in zeolites (fig. 1.1.). All minerals of the natrolite group, which will be dealt with in greater detail in chapter 4, are constructed by different lateral combinations of the chain type of figure 1.1a. by sharing apical oxygens. Thus, the linking between chains is less prominent than that within them which results in a fibrous habit of these minerals.

Zeolites of the phillipsite group are constructed by different cross-linkings of 'double crankshaft" chains (fig. 1.1b.). The cross-linking can occur in several ways and is not restricted to zeolites but is also found in feldspars.

TABLE 1.1. Tentative classification scheme of natural zeolites.

Group	Members	Structure type designation[1]	Approx. chemical formula[2]
Analcite	Analcite	*ANA*	$NaAlSi_2O_6 . H_2O$
	Wairakite	*ANA*	$Ca(AlSi_2O_6)_2 . 2H_2O$
	Viséite	*ANA*	$NaCa_5Al_{10}Si_3P_5O_{30}(OH)_{18}.8H_2O$
	Kehoeite[3]	*ANA*	$Zn_{5.5}Ca_{2.5}Al_{16}P_{16}H_{48}O_{96}.16H_2O$
Natrolite	Natrolite[4]	*NAT*	$Na_2Al_2Si_3O_{10} . 2H_2O$
	Scolecite	*NAT*	$CaAl_2Si_3O_{10} . 3H_2O$
	Mesolite	*NAT*	$Na_2Ca_2(Al_2Si_3O_{10})_3 . 8H_2O$
	Thomsonite	*THO*	$NaCa_2Al_5Si_5O_{20} . 6H_2O$
	Gonnardite	*THO*	$Na_2CaAl_4Si_6O_{20} . 6H_2O$
	Edingtonite	*EDI*	$BaAl_2Si_3O_{10} . 4H_2O$
Chabazite	Chabazite	*CHA*	$CaAl_2Si_4O_{12} . 6H_2O$
	Gmelinite	*GME*	$NaAlSi_2O_6 . 3H_2O$
	Erionite	*ERI*	$(Na_2,Ca,K_2)_{0.5}AlSi_3O_8 . 3H_2O$
	Offretite	*OFF*	ditto
	Levynite	*LEV*	$CaAl_2Si_4O_{12} . 6H_2O$
Phillipsite	Phillipsite	*PHI*	$(Na,K)CaAl_3Si_5O_{16} . 6H_2O$
	Harmotome	*PHI*	$BaAl_2Si_6O_{16} . 6H_2O$
	Wellsite	*PHI*	$(K,Ca,Ba)Al_3Si_5O_{16} . 6H_2O$
	Gismondite	*GIS*	$CaAl_2Si_2O_8 . 4H_2O$
	Garronite	*GIS*?	$Na_{0.5}CaAl_3Si_5O_{16} . 7H_2O$
Heulandite	Heulandite	*HEU*	$(Ca,Na_2,K_2)Al_2Si_7O_{18} . 6H_2O$
	Clinoptilolite	*HEU*	ditto
	Stilbite	*STI*	$NaCa_2Al_5Si_{13}O_{36} . 14H_2O$
	Stellerite	?	$CaAl_2Si_7O_{18} . 7H_2O$
	Epistilbite	*EPI*	$CaAl_2Si_6O_{16} . 5H_2O$
	Dachiardite	*DAC*	$Na_5Al_5Si_{19}O_{48} . 12H_2O$
	Ferrierite	*FER*	$(Na,K)_2MgAl_3Si_{15}O_{36}(OH).9H_2O$
	Brewsterite	*BRE*	$(Sr,Ba,Ca)Al_2Si_6O_{16} . 6H_2O$
Miscellaneous	Mordenite	*MOR*	$NaAlSi_5O_{12} . 3H_2O$
	Laumontite	*LAU*	$CaAl_2Si_4O_{12} . 4H_2O$
	Faujasite	*FAU*	$Na_2CaAl_2Si_4O_{12} . 8H_2O$
	Paulingite	*PAU*	$(K,Na,Ca)_6(Al,Si)_{39}O_{58}.15H_2O$
	Bikitaite	*BIK*	$LiAlSi_2O_6 . H_2O$
	Yugawaralite	*YUG*	$Ca_4Al_7Si_{20}O_{54} . 14H_2O$
	Cancrinite	*CAN*	$Na_6Al_6Si_6O_{24} . 5H_2O$
	Rhodesite[3]	?	$(Ca,Na_2,K_2)_8Si_{16}O_{40} . 11H_2O$
	Mountainite[3]	?	$(Ca,Na_2,K_2)_8Si_{16}O_{40} . 12H_2O$

[1] From BARRER (1973)

[2] The simple chemical formula, not necessarily the unit-cell content.

[3] These minerals are not aluminosilicates.

[4] Very recently the name tetranatrolite was approved for a tetragonal natrolite. Ref.: ANDERSEN, E. K., M. DANØ and O.V. PETERSEN (1969) A tetragonal natrolite. Medd. Grønland **181** no. 10: 1-18.

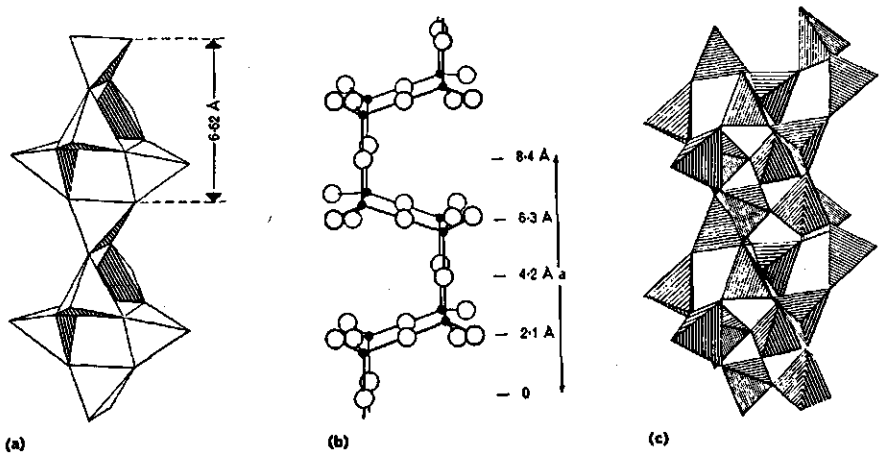

FIG. 1.1. Three types of chains of linked tetrahedra found in zeolite structures.: (*a*) natrolite, (*b*) phillipsite, (*c*) mordenite. (From BARRER,1964).

The third type of chain (fig. 1.1c.) is found in mordenite and can be described in terms of individual tetrahedra. The cross-linking in mordenite results in wide non-intersecting channels running parallel to the *c* axis (fig. 1.2.).

Layer structures. A layered habit is obtained when linking between parallel structural units of some two-dimensional extent is less prominent than within them. Minerals of the heulandite group show this habit very clearly. The struc-

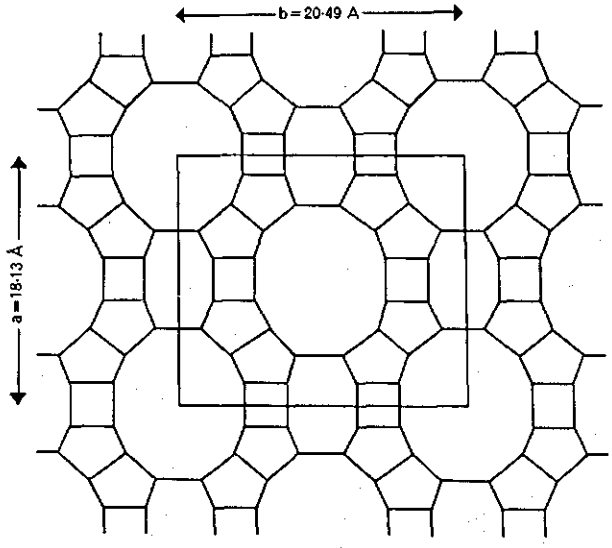

FIG. 1.2. A section of the mordenite structure normal to the *c* axis and the wide channels. Large square delimits unit-cell. (From BARRER, 1964.)

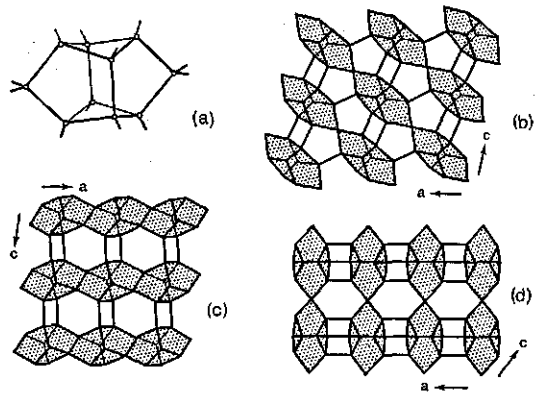

FIG. 1.3. Different ways of stacking of the structural unit (*a*) in minerals of the heulandite group: (*b*) heulandite, (*c*) brewsterite, (*d*) stilbite. (After MEIER, 1968.)

ture of some members of this group is schematically represented in figure 1.3., and consists basically of cages of 10 tetrahedra linked to form sheets which are appropriately stacked in the different species.

Structures formed by polyhedra. Such structures are built up by appropriate stacking and linking of polyhedra such as cubes, cubo-octahedra, prisms etc. formed by the silica and alumina tetrahedra. A typical example of this type is faujasite (fig. 1.4.) which is composed of cubo-octahedra and hexagonal prisms. Because of the relatively large stability of these structures, many prominent synthetic molecular sieves, such as types A, X and Y, belong to this group.

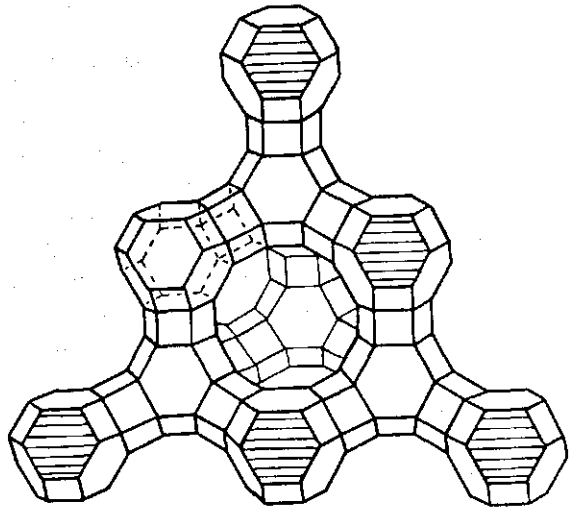

FIG. 1.4. The structure of faujasite. (From ROELOFSEN, 1972.)

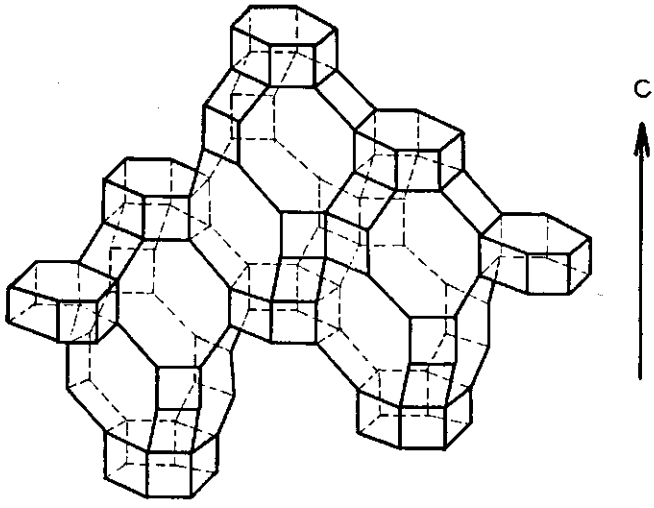

FIG. 1.5. The structure of chabazite. (From MARCILLY, 1969.)

Some zeolites may be described in terms of more than one of these structural features. The chabazite structure, for instance, consists of 'sheets' containing hexagonal prisms in which two six-membered rings are united by sharing spical oxygens of the tetrahedra (fig. 1.5.). Each layer of prisms is linked to identical layers above and below by bonds forming four-membered rings. Thus large cages are formed accommodating cations and water molecules. It can easily be seen that there are in fact two pore diameters, one determined by the hexagonal prisms and one by the non-planar eight-membered rings.

1.4. PRACTICAL APPLICATIONS OF ZEOLITES

No mineral group is as versatile in its application possibilities as the zeolites. Especially during the past two decades the development of their practical use has been extensive and is expected to continue. Underlying this versatility is the combination of a few favourable properties, each of which may be found in other agents as a single property but seldom in combination. Zeolites have ordered and rigid frameworks, may undergo ion exchange, have strong and specific sorptive properties, may be powdered or pelletized, are relatively thermally stable, do not corrode, sulfonate or oxidize and contact with reactants can be effected in several ways. A major disadvantage is their relatively weak resistance to acid conditions (dissolution). Depending on Si/Al ratio of the framework (Si-rich zeolites are more stable) they are stable in aqueous solutions in the pH-range of 4 to 12.

The most important of the known practical applications are listed below. For a recent summary see also LEE (1973).

Ion exchange. As a basic property, ion exchange has many derived applications. The mechanism of ion exchange on zeolites differs from that on materials such as clay minerals in that it can be highly specific: some cations may be exchanged to full capacity whereas others are almost totally excluded. Hence, base exchange capacity values are to be treated with care. In general, depending on the kind of zeolite, they may vary from 100 to 400 me/100 g or higher. The effective pore diameter determines the kind of ion sieve action. In so-called 'small-port' zeolites (relatively compact, small apertures) such as analcite exclusion depends on the size of the non-solvated ions because the lattice forces are strong enough to overcome solvation. The so-called 'open' zeolites such as chabazite, erionite, mordenite and clinoptilolite have wider pores and show the normal hydrated (lyotropic) type replacement series (BARRER, 1958; AMES, 1961).

Zeolites are used for the recovery of radioactive ions such as Cs and Sr from waste streams using clinoptilolite and mordenite, while pilot experiments have been conducted to remove the toxic ammonia from agricultural and city waste water with clinoptilolite (AMES, 1967; MERCER et al., 1969).

Adsorption. Dehydrated zeolites are excellent sorptive agents. The specific pore size may be employed to separate mixtures of compounds with different molecular size. Thus, gas mixtures may be separated e.g., oxygen and nitrogen can be produced from air with mordenite, whereas such products as branched and unbranched paraffins can be separated using the synthetic CaA sieve. Mordenite has also appeared to be suitable to remove SO_2 from polluted air; in addition, zeolites have even been used in cigarette filters. The Union Carbide Cy announced a process to remove mercury vapour (LEE, 1973). Chemical equilibria may be shifted in a desired direction by adsorptive removal of one of the products, including water (ROELOFSEN, 1972). Zeolites are widely used as desiccants of both liquids and gases e.g., natural gas. Recovery of both the zeolite and the adsorbed product is achieved by heating or by displacement with another adsorbate.

Catalysis. Zeolites show activity in a multiplicity of catalytic reactions. However, they do so only after an activation process which usually includes the incorporation of a catalytically active metal by ion exchange and calcination of the product. Although the reaction patterns are well-known in many cases, much of the actual catalysis activity remains to be elucidated (VENUTO, 1970; MINACHEV and ISAKOV, 1973).

Selective catalysis is effected by the porous structure as well as by affinity differences of the structure and thus, in combination with specific active metal ions selective dual-function catalysts can be prepared. Such products now have a widespread application as oil cracking catalysts, especially in the U.S.A.

Miscellaneous applications. A few other applications are worth mentioning. A summary of these has very recently been given by MUMPTON and SHEPPARD (1972). Like kaolinite, zeolites can be used as soft white fillers in paper. Because

of their high exchange capacity zeolites have been added to soils as conditioners while other agricultural use is found as dietary supplements for pigs and poultry, and also for adding trace elements to fertilizers. Certain types of cement supposedly benefit from zeolite addition. However, in such construction materials care should be taken that no zeolite types are used with lattices which either contract and/or expand as a result of changes in water content.

Thusfar, no comments have been made on where the expensive synthetic zeolites should be used or where perhaps the relatively cheap natural analogues could serve the purpose. Obviously, it is necessary to consider the advantages and disadvantages of both for each particular case. Purity and price will, in most cases, be the decisive factors. In case of organic synthesis high purity is of great importance since non-inert impurities such as other zeolite species will reduce the specificity of the process. If inert impurities are allowed then it must be considered what 'thermal price' has to be paid with each recovery cycle. If the zeolite bed has to be renewed after a comparatively few cycles because of rapid deterioration, whatever the cause may be, then such impurities are less important than when the zeolite life extends over a large number of cycles (DEFFEYES, 1967). Natural zeolites are to be preferred for use in purifying wastewaters, as desiccants, as fillers and for agricultural purposes, while other uses may be discovered in the future.

2. THE DEHYDRATION OF ZEOLITES A CRITICAL REVIEW

2.1. INTRODUCTION

The remarkable property of zeolites to dehydrate reversibly upon heating has led to an extensive study of this phenomenon using a large variety of methods and techniques. However, from both the controversial results of the published work and the results obtained with heating experiments by the present author, it is considered that apart from some exceptions, many of the methods and techniques in the literature have been unreliable, inadequate or both. AUMENTO (1965), working on stilbite and analcite, stated that the prime motive of his work was the unsystematical and incomplete approach of the subject. It is, therefore, unexpected that during the past 5 or 6 years there has been a distinct decline in the number of publications on the thermal behaviour of zeolites. Such self-sufficiency cannot be justified by the results of previous research and the many problems still remaining. This applies for instance to the lattice deformations and phase transformations that almost invariably accompany dehydration. The importance of this cannot easily be over-estimated from both the mineralogical and the technological point of view since the sorptive properties depend on the cell dimensions of the zeolites. A specimen not suitable for a required specific sieve action may be rendered suitable by either raising the temperature or by dehydration to a predetermined metaphase (BARRER, 1947). The activation of zeolites by heat treatment inevitably points to the determination of stability boundaries of the phases formed during this treatment. One reason why this has not yet been done systematically may be that most commercial molecular sieves used up to now are the so-called 'stable' species, i.e., zeolites whose lattices do not show any appreciable change upon heating. However, from the results obtained in the current study, it appears that only mordenite is such a genuine stable zeolite showing no other change than thermal expansion. Such thermally 'stable' minerals as analcite, clinoptiiolite, brewsterite, chabazite, erionite, offretite and even faujasite do show discernable lattice deformations as reflected for instance by the usually reversible shifting of X-ray reflections upon heating. Even if these changes could be regarded as of minor importance, which may be so in many cases, then still the neglect of zeolites showing more pronounced changes upon heating is by no means excused. It is possible to anticipate and visualize that either an appreciable lattice deformation or a phase transformation considerably changes the specific properties of the zeolite. The knowledge of all the phases that can be induced by heating zeolites, together with the characteristics of the corresponding reactions, could elucidate possible structural relations and so could lead to an extension of the present number of technical applications. It is not likely that all natural zeolites have such potential practical applications, but even if only a

limited number proved to have promising aspects, then such research would be justified.

These considerations and the development of more sophisticated techniques have led to a systematical investigation of the thermal behaviour of natural zeolites which in part is reported here.

A synopsis of earlier work is given first, restricted to what is considered most relevant in the present context.

2.2. DTA AND TG

Both differential thermal and thermogravimetric analysis (DTA and TG), the most common methods of thermal analysis, have extensively been used in the study of zeolites (HEY, 1932, '33, '34, '35, '36; MILLIGAN and WEISER, 1937; KOIZUMI, 1953, 1958; PENG, 1955; BARRER and LANGLEY, 1958; Hoss and ROY, 1960; Mrs. PÉCSI-DONÁTH, 1962, '65, '66, '68; AUMENTO, 1965, 1966). Interpretation and comparison of the results of such studies are hampered to some extent by the use of a wide variety of instruments and experimental conditions, to which thermal analysis in particular is very sensitive. This is aggravated by the general use of peak temperatures in DTA to indicate reaction temperatures rather than the more realistic and better reproducible 'characteristic temperature'or 'extrapolated onset temperature'[1] (WEBER and ROY, 1965; MC ADIE, 1971).

The older TG curves have invariably been obtained with the static heating or isothermal method, in which the samples are heated to, and equilibrated for, a shorter or longer period at predetermined temperatures which are raised with intervals to yield points through which a dehydration curve is drawn (e.g., HEY, 1932; MILLIGAN and WEISER, 1937; KOIZUMI, 1953; PENG, 1955; Hoss and ROY, 1960). It is now generally acknowledged that non-isothermal or dynamic TG has some distinct advantages over the isothermal method (FREEMAN and CARROLL, 1958; JACOBS, 1958; HOROWITZ and METZGER, 1963; CARROLL and MANCHE, 1972) and the more recent work includes dynamic TG curves (BARRER and LANGLEY, 1958; AUMENTO, 1966; PÉCSI-DONÁTH, 1966, 1968; VAN REEUWIJK, 1971).

Dynamic TG only gives a representative curve comparable with the one obtained by static heating if the dehydration reaction is not slow but proceeds rapidly i.e., there should be no significant overshoot of the equilibrium temperature. Contradictory to the opinion of MILLIGAN and WEISER (1937) there is now sufficient evidence that this is the case with zeolite dehydration (HEY, 1932; AUMENTO, 1966; SIMONOT-GRANGE et al., 1968; this work, chapter 3).

No agreement exists on the exact nature of water in zeolites. PÉCSI-DONÁTH (1966a, 1968) suggests that three types of water may be recognized viz.,

[1] The 'extrapolated onset temperature' or 'onset temperature' for short, is defined as the temperature where the tangent at the point of maximum slope of the DTA curve intersects the base-line. The 'characteristic temperature' is an abandoned term for the same.

a. water with crystal-water-like bonds
b. water bound to the lattice by OH-bonds
c. typical zeolite water.

The term typical zeolite water is generally used (not only in connection with zeolites) to indicate water that can 'freely' move into and out of the lattice without disrupting it.

Sharp DTA endothermic peaks are taken to indicate crystal water whereas broad peaks result from zeolite water. It should be realized, however, that these two types of reaction may well be very closely related. The latter type can be visualized to be composed of a series of the first type of reactions if the crystal lattice is able to adjust itself to water loss by narrowing its channels or cages in steps. This is indicated by continuous-heating X-ray photographs and computer-resolved DTA curves (see chapter 3). This is, of course, not in contradiction with the observation that water is bound at different levels of energy depending on the location in the lattice and the type of cation with which it is coordinated. This is reflected by the various endothermic DTA peaks and the corresponding dehydration steps in the TG curve, be they discrete or overlapping. Thus, water in zeolites may be divided into 'sets' of water molecules, not excluding their occurrence in one single set, as for example, in natrolite.

Next to this 'mobile' water a more obscure type of water must be present in zeolites as can be inferred from TG curves and X-ray analysis. After collapse of the structure due to thermal treatment, some (but not all) zeolites show a continuing irreversible weight loss upon further heating. The exact nature of this water is as yet unknown but may perhaps be described as residual OH attached to lattice relics. PUTZER (1969) found evidence that such OH-groups may be formed during dehydration. BREGER et al. (1970) state that the problem of how to label water in certain minerals is perennial and that, in the case of zeolites, there is a history of ambiguous usage of such adjectives as 'zeolitic', 'structural', 'loosely held' and 'tightly bound'. These authors indicate the need for methods other than the conventional to characterize water in zeolites.

2.3. HIGH TEMPERATURE X-RAY ANALYSIS

As expected, in many cases where zeolites have been thermally analysed, attempts were made to follow the reaction or identify the reaction products by means of X-ray diffraction (e.g., HEY, 1932a and b, 1933, 1936; MILLIGAN and WEISER, 1937; KOIZUMI, 1953; BARRER and LANGLEY, 1958; HOSS and ROY, 1960; AUMENTO, 1966; PÉCSI-DONÁTH, 1966).

In general, the results have been disappointing or not exploited to their fullest extent and this is a cause of the poor knowledge of the thermal behaviour of the zeolite structures.

With one exception (AIELLO et al., 1970) all the methods used produced non-continuous pictures of the lattice changes (X-ray photos or diffractograms) i.e., they are simple photographs taken at temperature-intervals rather than a con-

tinuous picture taken over the whole temperature range. The character of the transformations is not obtained in this way, and the transformation temperatures have to be estimated by interpolation. Three different techniques have been applied of which only two can be considered useful, viz., heating in furnaces attached to the diffractometer (HOSS and ROY, 1960; AUMENTO, 1966), and heating in capillaries which are sealed prior to cooling and analysis to prevent rehydration (MILLIGAN and WEISER, 1938; AUMENTO, 1966). Partial rehydration (and thus phase transformation) in the sealed capillary which still contains some water, is feasible since very small amounts of water can be sufficient for this to occur (VAN REEUWIJK, 1971).

The third technique involves cooling in air after heating the sample to a predetermined temperature (e.g. PÉCSI-DONÁTH, 1966). This allows the zeolite to rehydrate, at least in part, and metaphases cannot be expected to persist. Attempts to improve this by quickly sealing off the material in capillaries after cooling (KOIZUMI and KIRIYAMA, 1953; BARRER and LANGLEY, 1958) will fail, because upon cooling, at room temperature the initial phase has invariably reappeared. This third technique is therefore only suitable to identify irreversibly formed high-temperature phases.

With the advent of the versatile Guinier-Lenné cameras[1] all these problems have been overcome, and now it is possible to prepare continuous X-ray heating photographs of powdered material up to 1200 °C at ambient and subambient pressures and in different atmospheres. To date, however, to obtain satisfactory reflection intensities, no heating rates beyond 1 °/min. can be used with commercially available film material.

2.4. VAPOUR PRESSURE

Dehydration of zeolites resembles the evaporation of liquid water in that it involves volatilization with a corresponding 'boiling point' for each set of water molecules. This implies that the state of hydration of a zeolite is not only dependent on the temperature but also on the water vapour pressure. Therefore, considering its reversible character, the dehydration reaction can be expected to satisfy the conditions of an equilibrium reaction. Thus, thermal dehydration of zeolites under atmospheric conditions (as is usually done in experiments) is in fact isobaric dehydration at ambient water vapour pressure. Lowering this pressure, e.g., by evacuation, results in partial dehydration of those zeolites that contain water molecules requiring a relatively small amount of energy to escape, e.g., the first set in gismondite (VAN REEUWIJK, 1971).

It is not clear whether this water has to be distinguished from the so-called 'loosely held' water as described by BREGER et al. (1970) to occur in heulandite and clinoptilolite. The matter is further complicated by the contention of

[1] Manufactured by Enraf-Nonius, Delft, The Netherlands.

FOSTER (1965) that all water coming off zeolites below 150 °C is externally adsorbed water[1] and so she suggests that it be routinely determined by heating to 110 °C. However, this contention is refuted by our observation that during thermal dehydration up to 110 °C several zeolites undergo crystallographic deformation, e.g., edingtonite, chabazite and wairakite, or even phase transformation, e.g., gonnardite, laumontite, phillipsite and gismondite.

To date few workers have carried out thermal experiments on zeolites at other than ambient water vapour pressures[2] and this was some 40 years ago (HEY, 1932, 1933; TISELIUS and BROHULT, 1934; TISELIUS, 1936). By static heating, HEY obtained isohydric curves (i.e., curves connecting vapour pressure with temperature at constant zeolite composition or constant state of hydration) from which he derived isothermal dehydration curves, phase transition curves, as well as heats of hydration using the integrated form of the Clapeyron equation $\ln P = -\Delta H / RT + A$. It is strange that this method of investigation, possibly in a somewhat less laborious manner, has not been continued. TISELIUS and BROHULT (1934) and TISELIUS (1936) prepared adsorption isotherms from which they, too, calculated heats of adsorption using the same equation. Recently, SIMONOT-GRANGE et al. (1968) carried out similar experiments on heulandite and reported that the heat of hydration resembled that of 'physically adsorbed' water.

2.5. THE REACTION MECHANISM

The reaction enthalpy of dehydration of zeolites as it can be measured by DTA or DSC (differential scanning calorimetry) is the sum of the energies required by the number of processes involved, such as volatilization of water (breaking bonds with cations, with the lattice and with other water molecules), diffusion of water through the channels, and re-arrangement of the lattice. Obviously, the assessment of the contribution of each of these sub-reactions is difficult, even if it is assumed that no others are involved.

BARRER and IBBITSON (1944) found that from the kinetic approach molecules sorbed by activated zeolites can be divided into three groups:

a. molecules occluded extremely rapidly
b. molecules occluded slowly at room temperature
c. molecules excluded from the zeolite lattice.

Group *c* comprises compounds with molecular dimensions exceeding the pore diameter. Group *b* comprises molecules with cross-sectional diameters near that of the effective aperture and sorption follows the common sorption laws in that expected isotherms are found with the usual influence of temperature and vapour pressure and degree of hydration of the zeolite. Group *a* is the

[1] Often designated as H_2O- in contrast to H_2O+, the water that is an intrinsic part of the structure.

[2] Excluding the hydrothermal work on the synthesis of zeolites.

most important in the present context since the extremely rapid sorption generally occurs with small-size molecules, e.g., O_2, H_2, N_2, CH_4 and C_2H_6 and also H_2O with an effective diameter of about 2.9 Å obviously belongs to this group (MARCILLY, 1969). Thus, water transport within the lattice must tend to a free diffusion.

However, TISELIUS (1936) using an elegant optical method to observe diffusion in heulandite, noticed that the diffusion laws were only obeyed for small concentration intervals. At higher gradients Fick's law was still valid but the diffusion constant became strongly dependent on the concentration. In this experiment relatively large crystals must have been used and the effect will be much smaller with finely grained particles.

2.6. REHYDRATION

Rehydration experiments to establish the regeneration capabilities of zeolites and their metaphases have been included in thermogravimetric work of MOURANT (1933), PÉCSI-DONÁTH (1965, '66, '68), AUMENTO (1966) and VAN REEUWIJK (1971). In many cases there appears to be a distinct hysteresis effect and, depending on the zeolite species and the temperature reached, it may take a considerable time before rehydration reaches a maximum. Complete rehydration usually occurs when heating has not exceeded moderate temperatures, e.g., 250°C; higher temperatures may cause reduced rehydration capability as reported by PÉCSI-DONÁTH (1968). This explains why no direct measurement of heat of hydration is possible.

On the other hand, PÉCSI-DONÁTH found that moderate heating sometimes causes such an activation of the zeolite that more than the original water content is taken up. When rehydration time is not stated, literature data should be treated with care; AUMENTO (1966) reports that stilbite, heated to 600°C, rehydrates in air to about one third of its original water content within two days, but is fully rehydrated after a few months. Incomplete rehydration is usually attributed to decreased flexibility or even partial breakdown of the lattice. In addition, however, the nature of the rehydration reaction has to be considered. The general sequence of events during dehydration is volatilization and escape of water molecules followed by structural rearrangement. With rehydration this sequence is reversed in that structural rearrangement by necessity precedes the uptake of water. This will only take place when a minimum amount of water combines with the lattice to a thermodynamically stable structure. This will be at a lower level of kinetic energy of water molecules than at the point of completion of dehydration, hence hysteresis. By consequence, hysteresis will be much smaller in cases where no drastic lattice transformations are involved (see section 3.4).

3. THE COMPLEXITY OF THE DEHYDRATION PROCESS

3.1. TYPES OF DEHYDRATION

Examination of DTA curves of zeolites indicates that the course of the dehydration process is often far from simple. A great variety in the shape of endothermic deflections is encountered resulting both from different sizes and shapes of the individual 'peaks', and from the different ways of interaction i.e., the relative place or temperature at which they occur.

For a better understanding it may be useful to analyse this complex character, to elaborate on earlier contentions and to examplify different types before undertaking a systematic thermal investigation.

For the present, three basic types of dehydration may be considered:

1. Dehydration occurs as an apparently discrete reaction over a relatively short temperature range accompanied by a single and sharp DTA endothermic peak and a relatively steep weight loss in the TG curve. Crystallographically, this reaction is instantly followed by either a phase transformation or at least by a marked change in the unit-cell dimensions.
2. Dehydration occurs in a number of smaller consecutive steps over a relatively longer temperature range because the lattice adapts stepwise to the water loss. These adaptations involve changes in intracrystalline molecular distances and consequently in binding forces. This results in the formation of new 'sets' of water molecules, where originally only one set may have been present. Hence, the DTA endothermic peak is a broad composite one in which the composing peaks may be discernable by bulges in the overall endotherm. The corresponding weight loss is gradual usually with barely visible steps.
3. Dehydration occurs gradually, i.e., not step-wise, over a relatively wide temperature range.

In this case, it cannot be decided whether water molecules occupy equivalent positions and become bound with increasing tightness as dehydration sets in and proceeds, or whether they occupy positions with a continuous range of increasing hydration energy.

Two mechanisms may be distinguished:

a. During dehydration, the lattice gradually adapts.
b. The lattice is so rigid that no adaptation to dehydration occurs.

SMITH (1968) suggests that in wide-pore zeolites water can be stored in several layers on the internal surface. Towards the pore centre the lattice-water binding forces decrease and the water molecules occupy increasingly ill-defined positions. RESING and THOMPSON (1970), using NMR techniques, report that adsorbed water in the faujasite type zeolite 13-X is a truly intracrystalline fluid. A discussion relating to the nature of water in zeolites is given in chapter 5.

The basic types of dehydration caused by the thermal behaviour of zeolites

which are suggested above do not necessarily appear in their ideal form. Intermediate forms and also overlapping of types may occur, which can either be perceptible or not.

3.2. Examples

The thermal analyses of four different zeolite species have been selected to illustrate the variety in dehydration behaviour. Further examples can be found in chapter 4.

Experimental. Hand-picked crystals were ground in petroleum ether in an agate mortar and the powder (< 0.05 mm) was stored at 51 % relative humidity in a desiccator over a saturated $Ca(NO_3)_2$ solution in a constant temperature room (25 °C) where the relative humidity was also kept at 51 %. The thermal analyses were done on a DuPont 900/950 and later on a 990/950 assembly. For DTA both the intermediate 850° DTA cell as well as the DSC cell were employed. Unless it is stated otherwhise, thermogravimetric analysis (TG) was done in an air stream of ca. 0.2 l/min. All analyses were done in the constant temperature room. DTA curves were computer resolved on a DuPont 350 Curve Resolver. Continuous-heating X-ray diffraction powder patterns were recorded using a Guinier-Lenné camera with an average heating rate of ca. 0.3 °/min. and a filmspeed of 2 mm/hr. Cu-Kα radiation was used. With this camera the sample is situated in an oven with a water-cooled mantle and therefore the initial relative humidity must be over 51 %. Henceforth, these photographs will be referred to as G.L. X-ray photos for short.

Application of the Curve Resolver. The validity of resolving composite dehydration peaks into gaussian peaks has been questioned by Garn and Anthony (1967). Kissinger (1957) has discussed the relation between the order of reaction n and the shape of corresponding peak. He proposed this relation to be $n = 1.26\ S^{1/2}$ in which S, the 'shape index' is defined as the absolute value of the ratio of the slopes of tangents to the curve at the inflection points. Thus, in case of a symmetrical (gaussian) peak this ratio is unit and the order of reaction $n = 1.26$. It would indeed be very fortuitous if a composite peak consists of reactions all with $n = 1.26$. In section 2.4., zeolite dehydration has been compared with evaporation of liquid water. This reaction is of zero order ($n = 0$) and the DTA peak occurs when the material is exhausted. Zeolite dehydration is not an ideal well-defined single reaction since several side reactions and consecutive reactions may be involved e.g., diffusion, lattice rearrangements, cation rearrangements, rearrangements of remaining H_2O molucules, etc. Kinetically, the result is an apparently *fractional order of reaction*, which is strongly influenced by experimental factors, such as heating rate, sample packing, grain size and water vapour pressure. This is illustrated by the wide variety in shape of the various zeolite dehydration peaks.

It has not been questioned that multiple peaks can be considered to result from superposition of single peaks (MACKENZIE et al., 1972). Resolution of such peaks with the DuPont Curve Resolver is not restricted to a simple summation of gaussian peaks. On the contrary, although for convenience the initial setting of the apparatus may consist of gaussian peaks, almost any change of peak shape suiting the purpose can be introduced. Thus, virtually any composite peak may be resolved. It cannot be claimed that such a reconstruction is always correct in detail, but it can have a highly informative value.

Type 1. The dehydration of *gismondite* is taken as an example of type 1. Figure 3.1. shows that the DTA curve of gismondite consists of at least four sharp peaks together with some rounded peaks, with considerable overlap in many cases.

The same figure also shows the corresponding TG curve which exhibits predominantly steep weight losses corresponding with the sharp peaks.

The G.L. X-ray photo (fig. 3.2.) shows that most of the peaks, particularly the sharper ones, are accompanied by crystallographic transformations with a sudden break and shift of reflections.

If gismondite is not heated beyond 275°C where formation of Ca-feldspar is initiated, these transformations are completely reversible, and so on cooling in air, due to the presence of water vapour, each phase reappears in reverse sequence. When any rehydration is prevented by heating a sample in a glass capillary and sealing it before cooling, the meta-phase obtained is preserved. This is revealed by X-ray diffraction.

Hysteresis of rehydration, discussed earlier (2.6.), is exhibited by the rehydration TG curve in which some less pronounced steps are visible. It was found that when cooled in air to about 70°C the original gismondite phase reappeared. This was confirmed with G.L. X-ray photos. The mineral was however rehydrated to only 20% of its capacity. In a 'dry' N_2 gas stream (containing 5 v.p.m. H_2O) the same occurred at only 10% of its capacity. It is inferred that for the existence of any phase, a complete population with H_2O is not necessary.

Other zeolites showing this type of dehydration are, for instance, natrolite, phillipsite, gmelinite, heulandite, stilbite.

Type 2. This type may be represented by the dehydration of *edingtonite.* Both the DTA as well as the TG curve (fig. 3.1.) show two broad dehydration reactions followed by a sharper one. However, the resolved DTA curve indicates a number of consecutive and overlapping reactions accompanied by a series of smooth lattice adaptations which can be seen on the G.L. X-ray photo (fig. 3.2.). A special feature is the exothermic peak which instantly follows the final dehydration step. This results from an oxidation reaction accompanying the transformation of dehydrated edingtonite to celsian and will be discussed further in chapter 4. The resolved curve clearly shows the interaction between adjacent endothermic and exothermic peaks.

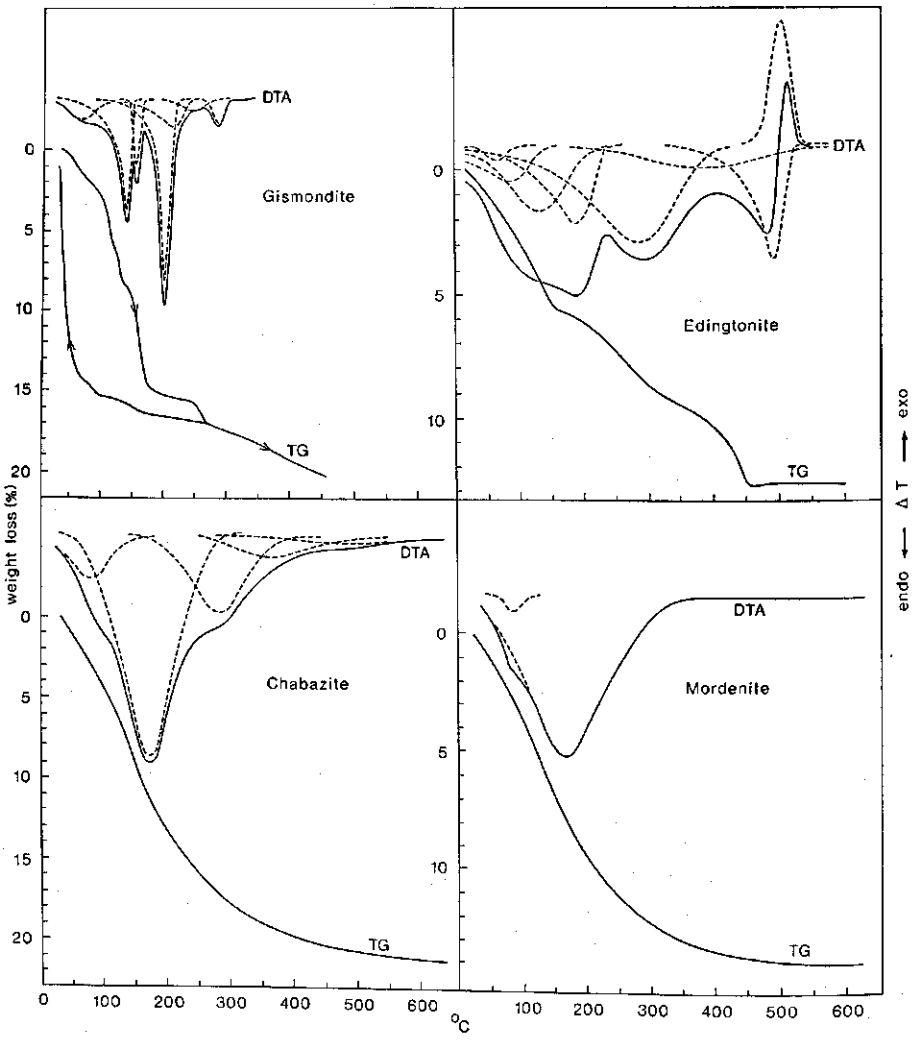

FIG. 3.1. DTA and TG curves of zeolites exhibiting different types of dehydration. Type 1: gismondite, type 2: edingtonite, type 3a: chabazite, type 3b: mordenite. Dashed peaks form resolved DTA curves. $P_{H_2O} \approx 0.03$ atm.

Examples of other zeolites showing type 2 dehydration reactions are levynite, gonnardite, laumontite.

Type 3a. The dehydration of *chabazite* falls into type 3. The DTA curve consists of one major peak with at least four smaller ones. The ratio of the magnitude of the major peak and the one next to it at a higher temperature seems to be dependent on the alkali content of this Ca-zeolite; a high ratio, as in this case, indicates a low alkali content (PASSAGLIA, 1970).

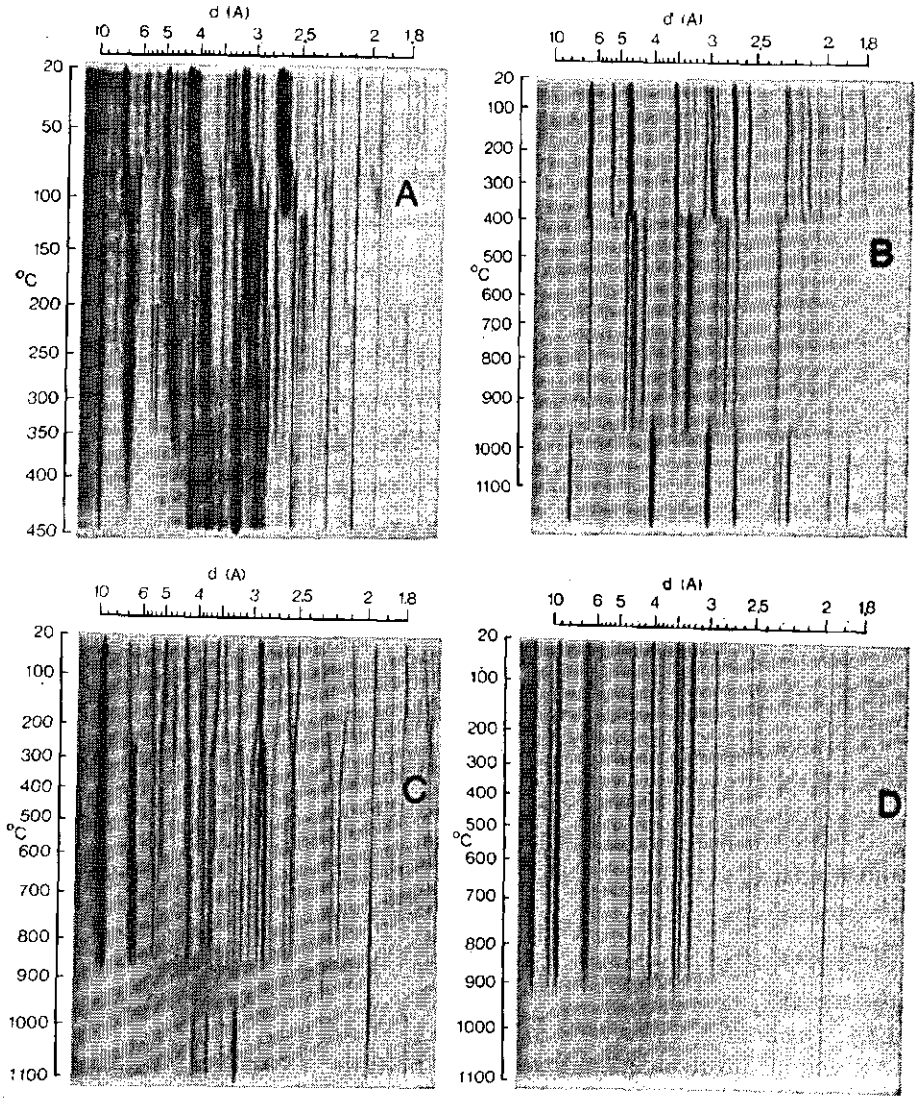

FIG. 3.2. Continuous-heating Guinier-Lenné X-ray photographs of zeolites exhibiting different types of dehydration. Type 1: gismondite (A), type 2: edingtonite (B), type 3a: chabazite (C), type 3b: mordenite (D). The continuous reflections from top to bottom of the photographs are due to the Pt sample grid.

The G.L. X-ray photo shows a prolonged, smooth adaptation of the lattice apparently following the major dehydration reaction. Considering the indices of the various reflections it can be concluded that the rhombohedral cell (SMITH, 1962; SMITH, RINALDI and DENT GLASSER, 1963) expands along the *c* axis (reflections with relatively high *c* index shift to the left i.e., to higher

TABLE 3.1. Refined unit-cell parameters of chabazite and metachabazite.

	Chabazite	Metachabazite
a (Å)	13.78	13.37
c (Å)	14.99	15.75
α	94° 33′	91° 48′
Vol. (Å^3)	9465.6	2437.7

d-values) and contracts along the other axes (reflections with relatively high *a* or *b* indices shift to the right i.e., to lower *d*-values).

This approximate but rapid interpretation is confirmed by computer refinement of the unit cell parameters (table 3.1.).

From these data it appears that the lengthening and narrowing of the chabazite cage, together with the change in angle α, occurs to such an extent that the total volume changes very little, contrary to the 8-membered ring apertures of which the effective diameter has decreased considerably by the thermal deformation (SMITH, 1962; his fig. 9).

Other zeolites with type 3 dehydration characteristics are: offretite, erionite, yugawaralite, brewsterite, analcite, wairakite.

Type 3b. Mordenite is the only natural zeolite with a lattice rigid enough to withstand any deformation upon dehydration (fig. 3.2.), while faujasite and clinoptilolite undergo very limited deformation. The mordenite DTA curve (fig. 3.1.) shows a virtually symmetrical gaussian peak superimposed by a small low-temperature peak due to very loosely held water often wrongly taken to be externally adsorbed water (see section 3.4.). Likewise, the TG curve is smooth and regular.

3.3. EFFECT OF PRESSURE ON DEHYDRATION

3.3.1. *Qualitative aspect*

Reactions involving gases are influenced by the pressure or partial pressure of the gases taking part. It is known that the equilibrium of thermal decomposition reactions may be shifted by varying the pressure, e.g., the CO_2 (partial) pressure in the $CaCO_3$ decomposition. The pressure effects in thermal reactions are extensively discussed, amongst others, by GARN (1965).

For a reversible reaction, which is usually the case with zeolite dehydration, the pressure-temperature relation may be expressed by the familiar Clausius-Clapeyron equation:

$$\frac{\mathrm{d}\log P}{\mathrm{d}(1/T)} = \frac{-\Delta H_r}{19.15} + C'$$

in which P = pressure of gas involved, T = absolute temperature of reaction,

ΔH_r = heat of hydration (in J/mole), and C' = constant of integration.

A detailed justification of the validity of this equation for zeolite dehydration is set out in chapter 5. Here, we will only illustrate the pressure effect as such.

A problem with atmosphere control is that water vapour is a gas that cannot be supplied from a pressure cylinder like nitrogen or carbondioxide. Therefore, the most simple method is that of a self-generated atmosphere by inhibited diffusion. The principle is that during dehydration sufficient water vapour is evolved to expell all other gases, the pressure thereby not exceeding the ambient pressure effected by non-sealed closing of the sample holder.

Experimental. Both the DSC cell and the intermediate 850 cell have been applied. They differ in two aspects. The sample holder for the DSC cell is a flat 12 mg aluminium pan with 6.7 mm Ø and edges of 1.4 mm high, and for the DTA cell a quartz tube with 4 mm Ø and 35 mm long (fig. 3.3.). Temperature measurement in the first case is effected by a thermocouple attached to an elevated area which is slightly smaller than the sample pan, in a constantan thermoelectric disc on which the sample pan is placed. (The DuPont DSC cell is, in fact, not a real DSC cell but rather a special kind of DTA cell because a differential temperature due to evolved heat is measured and not the energy required to maintain equal temperature in sample and reference.) Gas exchange between the sample and the ambient atmosphere can be inhibited with the DSC sample by closing the pan with an exactly fitting lid. Irregularities in the edges allow diffusion, and puncturing the lid proved to be unnecessary. Inhibited diffusion with the DTA sample is effected by the long and narrow pathway between sample and ambient atmosphere. Subatmosphere pressures have been used by evacuating the system with a water-jet pump using a wide-scale manometer together with an adjustable air-inlet valve to control the pressure.

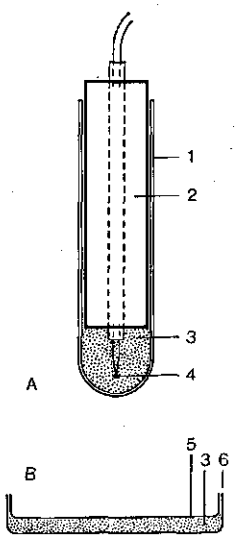

FIG. 3.3. Sample holders of DuPont DTA 850 cell (*A*) and DSC cell (*B*). 1. Quartz tube, 2. ceramic rod, 3. sample, 4. thermocouple, 5. lid, 6. pan.

Fig. 3.4. shows the pressure effect on the dehydration of natrolite using the DSC cell. Mutually comparable are curves *a* and *b*, and curves *c* and *d*. The latter two have been run at a high heating rate to ascertain sufficient water vapour production (see next section 3.3.2.). There appears to be a marked pres-

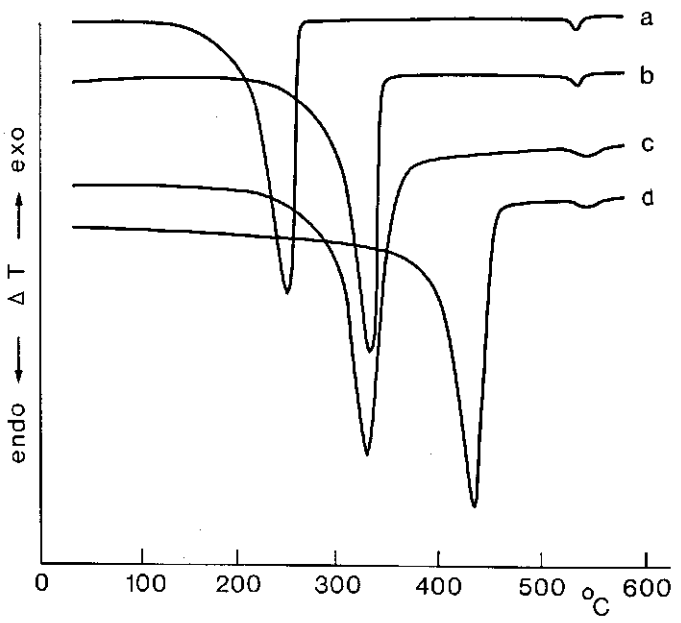

FIG. 3.4. DTA curves of natrolite obtained with DuPont DSC cell.
a. open sample pan, heating rate 10°/min, $P_{total} = 0.035$ atm, $P_{H_2O} \approx 0.0016$ atm
b. ditto, $P_{total} = 1.0$ atm, $P_{H_2O} \approx 0.032$ atm
c. closed sample pan, heating rate 50°/min, $P_{total} = 0.035$ atm, $P_{H_2O} \approx 0.035$ atm
d. ditto, $P_{total} = 1.0$ atm, $P_{H_2O} \approx 1.0$ atm
The water vapour pressures were estimated from figure 3.5.

sure influence so that the natrolite dehydration onset temperature is shifted up from 0.033 to 1.0 atm by more than 100 °C (curves *c* and *d*). Comparison of curves *b* and *c* indicates that using an open sample pan at the usual heating rate of 10°/min. corresponds with a run at a vapour pressure of about 0.03 atm. The position of the α-metanatrolite → β-metanatrolite transition (see chapter 4), a change which does not involve water vapour, is not influenced by the pressure differences used here (cf. small endothermic peaks in curves *a* and *b* or *c* and *d*). The higher heating rate causes the onset temperature of this peak to shift by only 2 °C whereas the peak temperature rises not less than 11 °C. With the 850 DTA cell an increase in heating rate has no effect at all on the onset temperature of this reaction most probably due to the more direct contact of the thermocouple with the sample. Noteworthy is the comparison between curve *b*, the ordinary DSC run, which has an onset temperature of the dehydration peak of 305 °C, with the onset temperature of 411 °C found with the ordinary DTA run (table 3.2.). These observations clearly indicate that the widely varying DTA results published by different workers are, to a large extent, due to pressure effects.

TABLE 3.2. Results of DTA of wet quartz powder and natrolite with inhibited diffusion at 1 atm. (onset temperature of dehydration peak, °C).

	Qu + H_2O	Natrolite
850 DTA, 10°/min.	100	411
850 DTA, 30°/min.	100	411
850 DTA, 50°/min.	100	411
DSC, 10°/min.	99	396
DSC, 30°/min.	101	407
DSC, 50°/min.	102	412

3.3.2. *Quantitative aspect – Calibration of pressure*

MORIE, POWERS and GLOVER (1972) have successfully applied several thermal analysis instruments, including the DuPont 850 cell for the inhibited diffusion method in determining the vapour pressure of organic liquids. It was thought that, in principle, the method described above should work quantitatively for zeolite dehydration. After establishing the pressure effect as such, there are two prerequisites for success. Dehydration equilibrium should be established rapidly enough, so that water diffusion out of the structure would not be a limiting factor (for ordinary hydrates such as $BaCl_2 . 2H_2O$ this equilibrium is usually exceeded in DTA) and sufficient water vapour should be evolved in order that air is expelled quantitatively so that $P_{H_2O} = P_{total}$. The following simple calculation shows that this condition is easily met: A 10 mg sample with 10% H_2O contains 1 mg H_2O producing 1240 mm^3 water vapour. The volume of the slightly compressed sample averages 10 mm^3 of which the solid phase makes out (using $D = 2$) 5 mm^3 leaving a free space of 5 mm^3 to be filled with vapour. For this, $5/1240 \approx 0.4\%$ of the available water is required. According to the TG curves this amount is evolved very quickly after heating is started. The dynamic procedure takes care of a continuous, although not constant, production of water vapour and thus prevents air molecules from re-entering the sample before dehydration has ended.

The most suitable procedure was selected by a few trial runs with slightly moistened quartz powder and natrolite, the results of which are presented in table 3.2. Of the two cells, the 850 DTA cell is shown to be preferred. In accordance with MORIE et al. (1972) the heating rate of 30°/min. is chosen for the standard procedure to allow for conditions when small dehydration steps are encountered which could yield insufficient water vapour at a low heating rate. Experience has indicated that the DSC cell, using a heating rate of 50°/min., can still be useful in some cases as it may give a somewhat better resolution of adjacent peaks.

The conclusive test was done using a range of sub-ambient pressures to 1 atm. This yielded a number of P—T data presented in figure 3.5. as log P vs. $1/T$, ideally resulting in straight lines i.e., if the reaction enthalpy ΔH_r does not change. This appears for both reactions to be the case. For water, the drawn

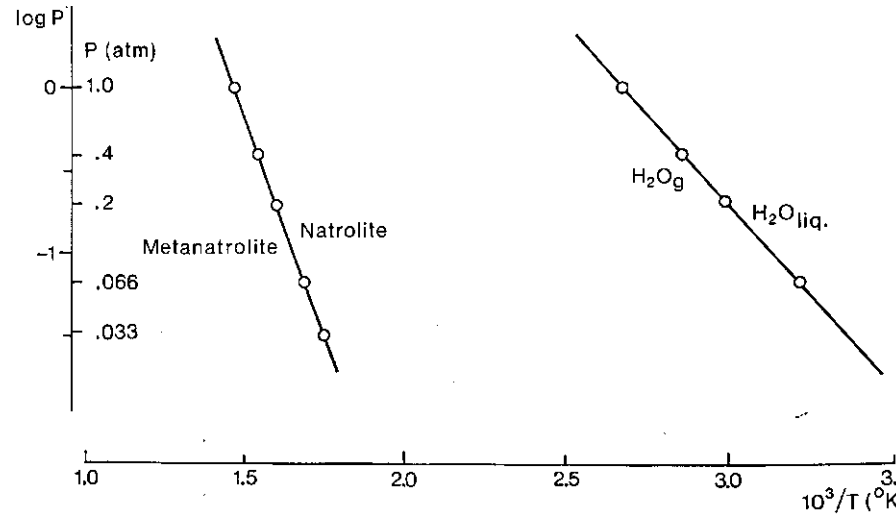

FIG. 3.5. Dehydration of natrolite and evaporation of water as determined with the DTA inhibited diffusion method and plotted as log P_{H_2O} vs. $1/T$.

line is the one using vapour pressure data from the Handbook of Chemistry and Physics (44th ed., 1962–'63) and it appears that all experimental values fall on this line. Using the Clausius-Clapeyron equation, $\Delta H_r = 19.15 \times$ slope of straight lines in figure 3.5. This yields for water 43.5 kJ/mole (Garrels and Christ, appendix 2, give 44.0 kJ/mole). For natrolite 102.9 kJ/mole is found, agreeing well with the approx. 105 kJ/mole reported by Hey (1932b). Hey's method allowed sufficient time for dehydration equilibrium, which may indicate that in our method diffusion is not a limiting factor. In addition it was found that a possible grain size effect within the size range used (< 0.05 mm) was negligible. Further applications are discussed in chapter 5.

3.4. DEHYDRATION EQUILIBRIUM AND HYSTERESIS

Although the above result would suggest that the dehydration equilibrium condition is met, and other evidence (chapter 2) indicates that zeolite dehydration proceeds rapidly, direct proof still remains to be given. To this end, a rehydration experiment using the TG equipment was conducted. Two zeolites, representing the extreme dehydration types 1 and 3, were chosen for this, viz. natrolite and chabazite respectively.

Chabazite was heated slowly (2°/min.) to ca. 290°C where heating was switched over to cooling (at the same rate). The resulting dehydration and rehydration curves are represented in figure 3.6. Cooling appears to be instantly followed by rehydration due to the air stream containing H_2O, with only slight hysteresis, indicating a situation of true equilibrium. When the same is done for

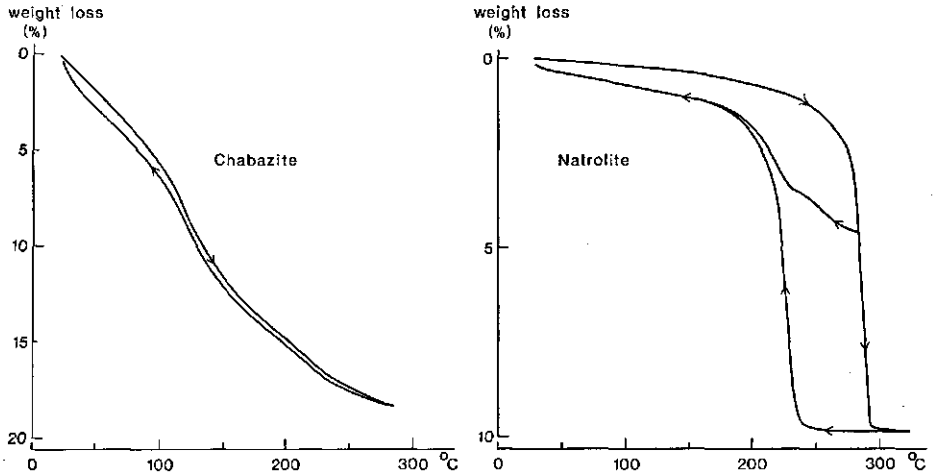

FIG. 3.6. TG dehydration-rehydration curves of natrolite and chabazite. Heating/cooling rate 2°/min. $P_{H_2O} \approx 0.025$ atm.

natrolite and cooling is set in after complete dehydration (ca. 320°C, fig. 3.6.) a strong hysteresis effect occurs and rehydration is initiated not until about 50°C below the end-point of dehydration, possibly suggesting that equilibrium was exceeded. When, however, heating is switched over to cooling at an earlier stage, somewhere halfway along the dehydration range, a different picture is obtained. Although still a strong hysteresis effect is noticed, rehydration is initiated instantly as is shown by the upward course of the rehydration curve. This is indicative of equilibrium because otherwise the curve would have either moved further downward or run horizontally as in the first case.

This process can be explained as follows. Dehydration of natrolite results in a phase transformation to α-metanatrolite (see chapter 4) which has a density near to that of the feldspars, indicating a virtually complete 'collapse' of the structural channels (this is not to be confused with complete collapse of the structure to an amorphous state). Instant rehydration is only possible as long as these channels are intact i.e., as long as they have not come too close to complete depletion. When heating is reversed to cooling somewhere halfway along the dehydration curve, part of the channels have been partially dehydrated and can take up water immediately, whereas the other part has collapsed already and will rehydrate only with the strong hysteresis effect as is indicated by the pronounced step in the rehydration curve.

This mechanism conforms to UBBELOHDE's (1957) suggestion about thermal transformations in general, that hysteresis is not necessarily in contradiction with equilibrium. When a system shows hysteresis, true equilibrium is exhibited in certain respects, but not in others. In the present case, dehydration exhibits equilibrium, whereas lattice adaptation does not.

Since the effect of heating rate variation proved to be negligible, the low heating rate used here is not detrimental to the suggested DTA method.

The small, low-temperature, endothermic peaks shown in figure 3.1. do not occur when the samples are dried prior to DTA. It makes no difference whether this is done in an oven at 110°C (and cooled without allowing to rehydrate) or in a dry atmosphere at room temperature e.g., over silica gel or dry N_2 gas.

The frequently asked question is whether this so-called 'loosely held' water is merely externally adsorbed water or is it internally adsorbed, in the structural channels or cavities?

A first clue may be the observation that a number of zeolites normally do not show this low-temperature peak, e.g., natrolite, mesolite, analcite. Figure 3.7. shows the DTA curves for chabazite and natrolite kept at three different levels of relative humidity at 25°C for 24 hours in a desiccator. The natrolite curve only shows a slight reaction after equilibration at 85%. This, however, is not restricted to natrolite since powdered 'inert' materials such as corundum and quartz also show this feature which in this case is undoubtedly adsorption on the surface.

In addition, water adsorption isotherms have been constructed for a number of zeolites and other minerals by equilibrating finely powdered samples at different levels of relative humidity in desiccators for 24 hrs. at 25°C. They are presented in figure 3.8.

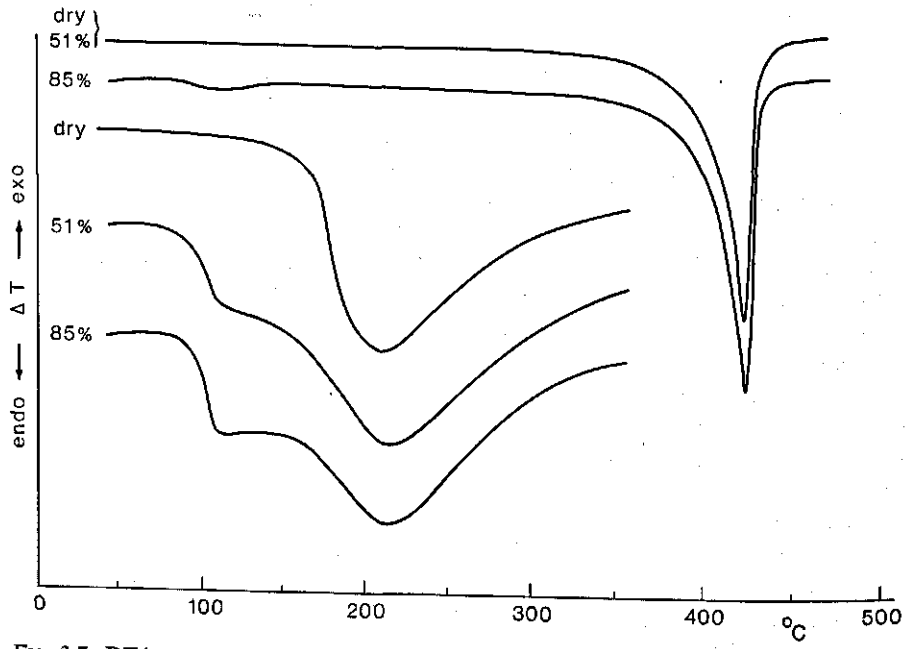

FIG. 3.7. DTA curves of natrolite (upper two curves) and chabazite (lower three curves) which were stored at three different levels of relative humidity (dry, 51% and 85% respectively). DTA 850 cell, heating rate 30°/min. $P_{H_2O} \approx 1.0$ atm.

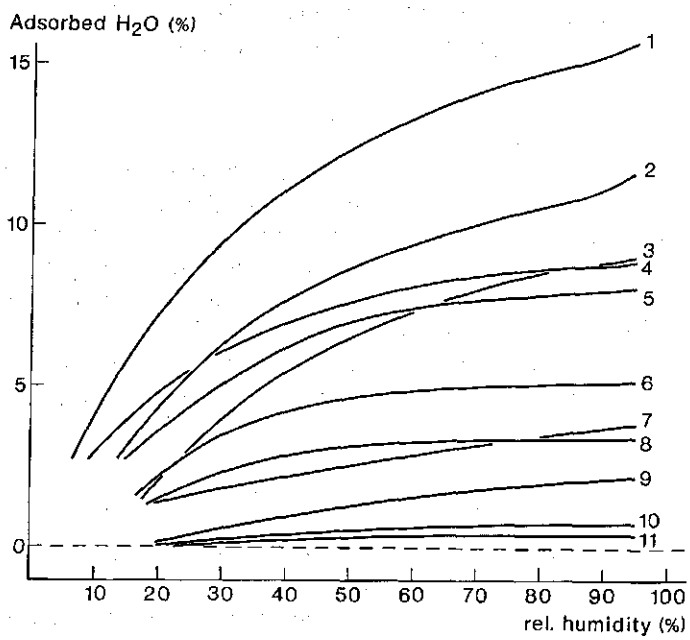

FIG. 3.8. Water adsorption isotherms of a number of zeolites and other minerals. 1. Bentonite, 2. erionite, 3. clinoptilolite, 4. mordenite, 5. chabazite, 6. heulandite, 7. kaolinite, 8. stilbite, 9. illite, 10. natrolite and mesolite, 11. analcite, feldspar and quartz.

There appears to be a wide range in adsorption capacity among the zeolites. Relatively high adsorption is exhibited by chabazite, erionite and clinoptilolite. Intermediate positions are taken by heulandite and stilbite whereas natrolite, mesolite and analcite, like powdered quartz and feldspar, show very little adsorption. The clays included for comparison acted as expected. Bentonite has swelling properties and a high surface area covered by cations; kaolinite and illite have a much lower surface area and no swelling properties. No correction is made for possible grain size differences in the zeolites, but the powdering procedure has been the same for all and the effect can be considered small.

The evidence clearly indicates that water retained by zeolites but which disappears with ordinary drying methods, is adsorbed internally in the structure and not on the surface. Consistent with this are the phase transformations sometimes accompanying the loss of this water.

4. DEHYDRATION OF ZEOLITES OF THE NATROLITE GROUP[1]

The thermal properties of few natural zeolites have been studied as extensively as those of members of the natrolite group. This applies particularly to the species natrolite, mesolite and scolecite and to a lesser extent thomsonite, whereas gonnardite and edingtonite have received little attention.

In view of the earlier discussed limitations of previous research which showed the need for a systematic thermal investigation (see chapter 2), an account will be given in this chapter of the thermal behaviour of all members of the natrolite group as obtained by a combination of the dynamic methods of thermal analysis.

4.1. Materials and Procedures

A representative specimen of each member was selected from our collection under study to illustrate the characteristic properties. Because of the similarity of the X-ray diffraction patterns, identification is sometimes difficult. Therefore, side-by-side Guinier-De Wolff X-ray photographs (Co-Kα radiation) are given in figure 4.1. Chemical analyses were obtained with X-ray fluorescence; the results, together with the calculated chemical formulae, are given in table 4.1.

In the preceding chapter it was shown that the main cause for the variation in temperature of reaction is the water vapour pressure at which the reaction occurs. Therefore, in all experiments a statement about the (partial) pressure of the gas phase involved is indispensable and will henceforth be given here.

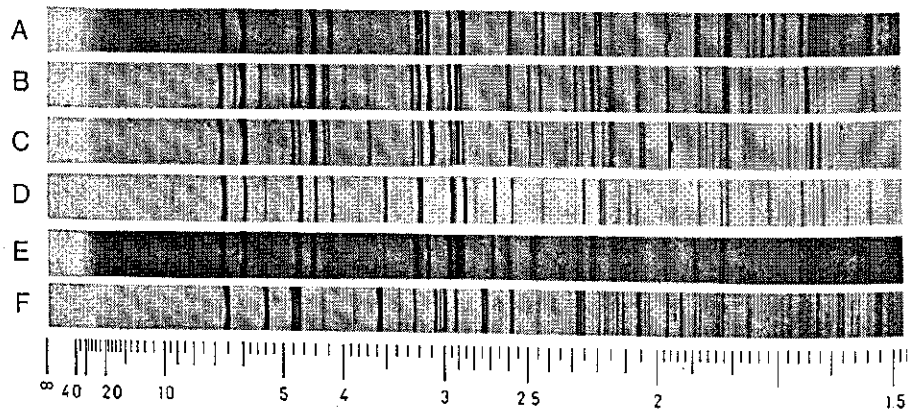

FIG. 4.1. Guinier-De Wolff X-ray photographs of zeolites of the natrolite group. A. natrolite, B. mesolite, C. scolecite, D. thomsonite, E. gonnardite, F. edingtonite.

[1] Preliminary results of the work contained in this chapter have been published earlier (VAN REEUWIJK, 1972).

TABLE 4.1. Chemical analyses of minerals of the natrolite group.

	A	B	C	D	E	F
SiO_2	47.06	46.21	45.97	38.62	42.83	35.14
Al_2O_3	26.66	26.02	25.69	31.04	28.79	20.12
Na_2O	15.36	5.08	0.26	4.26	8.02	–
CaO	0.27	10.40	14.21	12.81	7.56	–
BaO	–	–	–	–	–	31.18
H_2O	9.76	13.34	14.44	13.48	13.78	13.16
Total	99.06	101.05	100.57	100.21	100.98	99.60

A. *Natrolite*, $Na_{15.23}Ca_{0.15}Al_{16.09}Si_{24.08}O_{80} \cdot 16.58\ H_2O$, (Auvergne, France)
B. *Mesolite*, 3 ($Na_{5.09}Ca_{5.76}Si_{23.95}Al_{15.86}O_{80} \cdot 24.04\ H_2O$), (Oregon, U.S.A.)
C. *Scolecite*, $Na_{0.26}Ca_{7.96}Si_{24.09}Al_{15.84}O_{80} \cdot 25.22\ H_2O$, (Teigarhorn, Iceland)
D. *Thomsonite*, $Na_{4.40}Ca_{7.31}Si_{20.62}Al_{19.50}O_{80} \cdot 23.99\ H_2O$, (Kilpatrick, Scotland)
E. *Gonnardite*, $Na_{8.15}Ca_{3.15}Si_{22.49}Al_{17.79}O_{80} \cdot 24.12\ H_2O$, (Auvergne, France)
F. *Edingtonite*, $Ba_{8.27}Si_{23.82}Al_{16.05}O_{80} \cdot 29.74\ H_2O$, (Böhlet, Sweden)

DTA and TG were done in a conditioned room as described in section 3.2. For DTA the DSC cell was used; samples of ca. 10 mg were analysed in open cups at a heating rate of 10°/min. and $P_{H_2O} \approx 0.03$ atm. For TG, 10–20 mg samples were analysed at a heating rate of 10°/min. in an airstream of ca. 0.2 l/min. probably reducing the effective P_{H_2O} to about 0.025 atm. The DTA curves were computer resolved on the DuPont 350 Curve Resolver. G.L. X-ray photos were taken as described in section 3.2., from the prevailing relative humidity, P_{H_2O} is estimated at 0.01 atm. The X-ray diffraction powder data are listed in appendix 1. Determination of phase boundaries and heats of hydration are given in chapter 5.

4.2. RESULTS AND DISCUSSION

The DTA and TG curves are represented in figure 4.2. and the C.L. X-ray photographs in figure 4.3.

The question arises how to indicate reaction temperatures in this discussion. It has been common practice to use the peak temperature or peak maximum for this although the onset temperature is definitely closer to the true reaction temperature. The disadvantage of the onset temperature is that it is often not suitable for instant reading from the curve, especially with broad peaks. For this reason, and for the need to compare with previous work, peak maxima will in general be used to indicate reactions, whereas onset temperatures will only be used where necessary.

4.2.1. *Natrolite*

The DTA and TG curves of natrolite are the simplest of the group. Dehydration occurs in a type-1 single step with a peak maximum at 350°C. This is in accordance with the structure proposed by TAYLOR et al. (1933) and MEIER

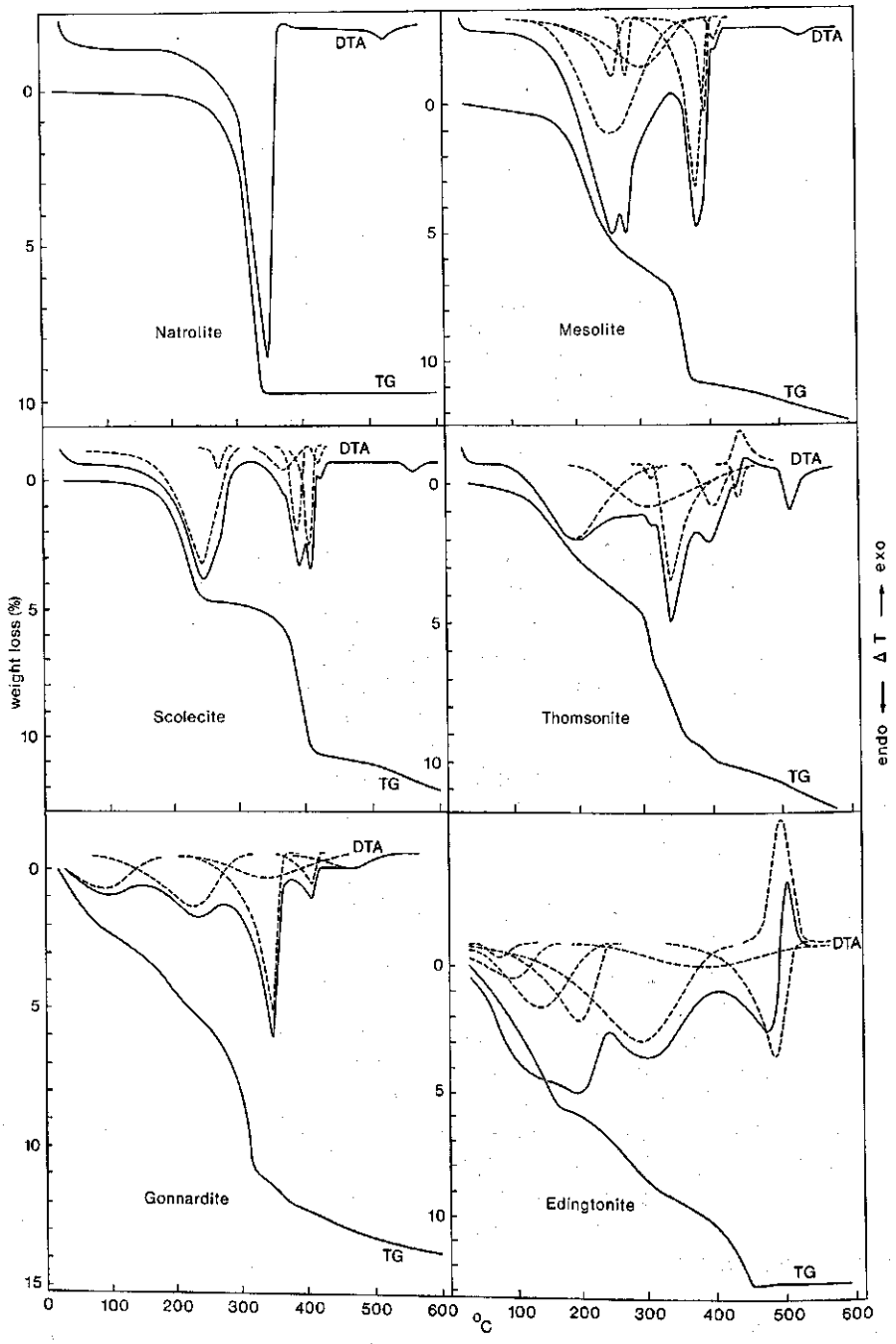

FIG. 4.2. DTA and TG curves of zeolites of the natrolite group. Dashed peaks form resolved DTA curves. $P_{H_2O} \approx 0.03$ atm.

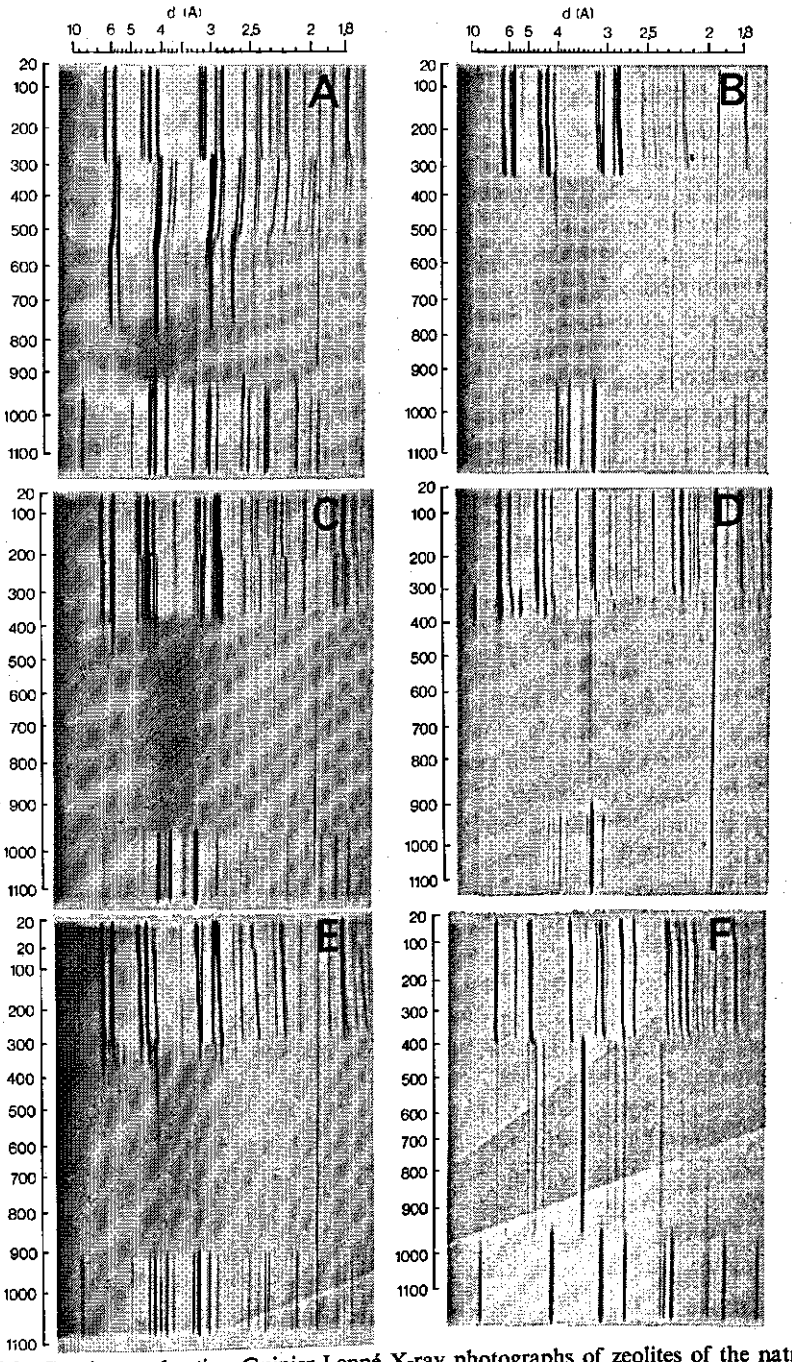

FIG. 4.3. Continuous-heating Guinier-Lenné X-ray photographs of zeolites of the natrolite group. A. natrolite, B. mesolite, C. scolecite, D. thomsonite, E. gonnardite, F. edingtonite. The continuous reflections from top to bottom of the photographs are due to the Pt sample grid.

(1960) in which all H_2O molecules occupy equivalent positions. The TG curve indicates that no residual water is left after the reaction. The G.L. X-ray photo (fig. 4.3A.) shows the corresponding transformation to metanatrolite to take place at 285°C. If the phase boundary, determined by onset temperatures of the dehydration reaction at different pressures (see figure 3.4. and 5.4.) is extrapolated to $P_{H_2O} = 0.01$ atm., the water vapour pressure prevailing in the G.L. camera, then an onset temperature of about 275°C is found. This is somewhat lower than the temperature where the phase transition occurs and supports the contention made earlier that the structural channels only collapse after, or close to the end of, the dehydration reaction and not concurrently.

Peak temperatures reported by other workers are from 50° to 100°C higher than the 350°C found here which is suggestive of higher experimental water vapour pressures. This is supported by corresponding isothermally obtained TG curves which have their steep section even at a slightly lower temperature than the present one (KOIZUMI, 1953; PENG, 1955; PÉCSI-DONÁTH, 1962).

After indexing the reflections on the G.L. X-ray photograph using JCPDS card 19–1185, it was observed that the phase transition to metanatrolite is preceded by a lattice contraction along the *a* and *b* axes, together with a slight expansion along the *c* axis. The G.L. X-ray photo reveals that in contrast to what was hitherto believed, metanatrolite consists of two distinct phases, the second being initiated at about 510°C accompanied by a small endothermic peak in the DTA due to heat of transition alone, since no dehydration is involved.

Metanatrolite as a single phase was first described by HEY (1932) and more recently by FANG (1963) and PEACOR (1973) all using single crystal techniques. With an iteration computer program for finding the unit cell from powder data (VISSER, 1969) it was possible to calculate the cell parameters of metanatrolite from the G.L. X-ray photo. These, together with the values published to date, which are those for α-metanatrolite (the lower metaphase), are given in table 4.2.

The main difference with FANG's results concerns the *c* parameter, which he found to be virtually unchanged whereas in our case it has definitely decreased. The space group was proposed by FANG to be monoclinic F_2 whereas our data

TABLE 4.2. Unit-cell parameters of natrolite and α-metanatrolite.

	Natrolite		α-Metanatrolite		
	JCPDS-card 19–1185	This study (Auvergne)	FANG	PEACOR	This study
a (Å)	18.28	18.26	16.34	16.20	16.32
b	18.62	18.57	17.09	17.02	17.10
c	6.59	6.56	6.60	–	6.44
γ (°)	90	90	90	–	
V (Å³)	2243.1	2225.9	1843.1	–	1797.2

fitted the orthorhombic *Fmmm*, but did not exclude F_2. In any case, γ does not deviate from 90°.

Contrary to dehydrated chabazite (cf. table 3.1.) whose cell volume is little different from that of the hydrated form, metanatrolite has a nearly 20% smaller cell volume than natrolite. Calculation of the specific density yields 2.53 g/cm³ which is quite near that of albite indicating the almost complete collapse of the structural channels.

The structure of β-metanatrolite appears to be somewhat simpler than that of the α-form and has a larger cell volume. Sofar, however, attempts to determine cell parameters for β-metanatrolite as well as those for the metaphases of the other members, have been unsuccessful.

Rehydration is possible to the stage that the structure becomes X-amorphous at about 775°C.

At 900°C α-carnegieite is formed. This phase appears to exist only over a short temperature range because gradual transformation to nepheline is initiated at 910°C and completed at 970°C. According to the known phase relations, the formation of nepheline from carnegieite by heating is an unusual sequence (SMITH and TUTTLE, 1957; LEVIN et al., 1969).

From the reaction equation

$$\underset{\text{natrolite}}{Na_{16}Al_{16}Si_{24} \cdot 16H_2O} \rightarrow \underset{\text{nepheline}}{16NaAlSiO_4} + 8SiO_2 + 16H_2O$$

it appears that about 17% of the material at high temperature consists of silica. However, up to 1150°C (maximum temperature of the camera) no crystalline silica phase can be detected. The occurrence of albite as a heating product of natrolite (PÉCSI-DONÁTH, 1968) has not been observed in any of the samples.

4.2.2. *Mesolite*

The dehydration of mesolite appears to occur in two main steps, the first of which is a composite reaction with peak maxima in the unresolved DTA trace at 255°C and 275°C (fig. 4.2.). During this reaction 12 molecules of H_2O are lost (per 80 oxygens). The heating G.L. X-ray photo (fig. 4.3B.) shows that the transition to metamesolite is initiated at ca. 175°C and entails a contraction of the framework along the *a* and *b* axes bringing about a narrowing of the main channels which run parallel to the *c* axis. The (111) and (511) reflections at 6.13 and 5.42 Å disappear above 200°C but reappear upon rehydration.

The second main step, when 7 H_2O are given off, occurs over a shorter temperature range than the first and is also a composite reaction. The magnitude of the small peak at 410°C in the DTA trace, varies from specimen to specimen and may even not be apparent.

The G.L. X-ray photo (fig. 4.3B.) shows that the metastructure is largely destroyed after final dehydration at 320°C, and subsequently only some diffuse reflections are discernable. Rehydration beyond this transition is not possible. From the TG curve it can be seen that not all the water in this mineral is revers-

ibly removable, the remaining water which is probably lattice relic-OH, is gradually given off during further heating. The disappearance of the remaining reflections at 490 °C is accompanied by a weak endothermic peak at 540 °C in the DTA, which indicates a total collapse of the structure remnants.

PENG (1955) has described the dehydration of natrolite, mesolite and scolecite in some detail. He could largely explain the DTA and TG traces in terms of strengths with which the H_2O molecules are held, based on the structure analyses of PAULING (1930) and TAYLOR et al. (1933). However, in detail his reasoning appears to be too simple. Resolving the DTA curve (see fig. 4.2.) indicates that the true mechanism is considerably more complicated than the direct DTA curve would suggest. This applies particularly to the first main reaction which appears to consist of no fewer than four subreactions. Because the peaks are relatively broad, the most probable mechanism is that of the changing environment of the H_2O molecules during dehydration. This is complicated because two types of cation (Na and Ca) are present. The dehydration type is an intermediate between types 1 and 2. The narrow sharp peak at 275 °C is probably associated with the lattice change to metamesolite.

The second main reaction, during which 7 H_2O are lost, appears to consist of two sharp type-1 peaks associated with two well-defined sets of probably 5 and 2 water molecules, respectively. The small peak at 410 °C is taken to result from the structure degradation. Indicative for this is the absence of this peak in the derivative thermogravimetric analysis curve (not shown here) suggesting that in this reaction no water loss is involved. This peak should be distinguished from the total-collapse peak at 540 °C.

At 910 °C a high-temperature feldspar phase is formed, which, when compared with a set of X-ray photographs of members of the albite-anorthite series, shows close resemblance to bytownite ($Ab_{20}An_{80}$).

Not all available material can be incorporated in this phase and from 975 °C onwards a nepheline phase can also be observed.

If all Na and Ca is incorporated in $Ab_{20}An_{80}$ and nepheline, then silica remains as in the case of natrolite:

$$\underset{\text{mesolite}}{Na_{5.3}Ca_{5.3}Al_{16}Si_{24}O_{80} \cdot 24H_2O} \rightarrow 2.3\ \underset{\text{ca. } Ab_{20}An_{80}}{Na_{0.3}Ca_{2.3}Al_5Si_7O_{24}} + 4.6\ \underset{\text{nepheline}}{NaAlSiO_4} + 3.2\ SiO_2 + 24\ H_2O$$

Here again no crystalline form of silica could be detected.

4.2.3. *Scolecite*

The dehydration of scolectite is very similar to that of mesolite and also occurs in two main steps. Unlike mesolite, here the first step, during which 8 H_2O are removed, is a single reaction as shown by resolving the curve and is in accordance with the monocationic (Ca) nature of the mineral. The small peak at 275 °C is due to the lattice contraction as in the case of mesolite (see fig. 4.3C.).

Qualitatively, the composition of the second main reaction is almost identical to that of mesolite indicating that the two well-defined sets of water molecules do not arise from coordination with two different cations as could be inferred in case of mesolite.

The lattice breakdown pattern and loss of relic-OH upon further heating is also very similar to that of mesolite.

At 950 °C high temperature anorthite is formed without any apparent accompanying phase, although again according to the stoichiometry silica remains:

$$\underset{\text{scolecite}}{Ca_8Al_{16}Si_{24}O_{80} \cdot 24\,H_2O} \rightarrow 8\,\underset{\text{anorthite}}{CaAl_2Si_2O_8} + 8\,SiO_2 + 24\,H_2O$$

In addition to differences in temperatures of reaction, a diagnostic difference between mesolite and scolecite is the course of both the DTA and TG curves between the two main dehydration steps. For mesolite this part is sloping, whereas for scolecite it is virtually horizontal.

4.2.4. *Thomsonite*

The dehydration of thomsonite appears to follow a pattern different from the previous members. The first part, when 8 H_2O are lost, is a type-3a dehydration consisting of a slight but definite contraction along the *a* axis and an even smaller expansion along the *c* axis (fig. 4.3D.). As the G.L. X-ray photo shows, this ends in a phase transition, which is also reflected by the small endotherm at 320 °C. This is followed by a rather sharp peak indicative of the loss of a set of 8 H_2O molecules occupying equivalent positions. According to the G.L. X-ray photo this step also induces a marked lattice rearrangement although no thermal effect is apparent. During the subsequent final step another 2 H_2O are removed. The TG trace shows (fig. 4.2.) that as with mesolite and scolecite, some residual OH appears to be present when the framework irreversibly degrades to a phase still giving the same reflections as the previous phase but very much weaker. Like with mesolite and scolecite this transition is accompanied by an endothermic peak instantly followed however by an exothermic recrystallization reaction. Noteworthy is the peak-size reducing effect of such an interference.

Just below 900 °C a bytownite/anorthite phase is formed (about $Ab_{10}An_{90}$) followed by nepheline at 910 °C. No crystalline SiO_2 phase could be detected although according to the reaction here again silica remains:

$$\underset{\text{thomsonite}}{Na_{4.4}Ca_{7.3}Al_{19.5}Si_{20.6}O_{80} \cdot 24\,H_2O} \rightarrow 2.6\,\underset{\text{ca. } Ab_{10}An_{90}}{Na_{0.2}Ca_{2.8}Al_{5.7}Si_{6.1}O_{24}} +$$

$$+ 3.9\,\underset{\text{nepheline}}{NaAlSiO_4} + 2.2\,SiO_2 + 24\,H_2O$$

4.2.5. *Gonnardite*

No detailed study of the structure of gonnardite has been made but it is believed to be similar to that of thomsonite (SMITH, 1963). This relation is expressed by the thermal behaviour. The most important difference is the occur-

rence of an early dehydration step below 100 °C (fig. 4.2E.) when 5 H_2O are given off. This water loss induces a marked contraction of the lattice along the *a* and *b* axes as shown by figure 4.3E. This shift, resulting in a merging of reflections, occurs just above room temperature and could only be shown clearly when the heating was started somewhat later than the film transport. The subsequent dehydration steps, where 5, 9, and 2 molecules H_2O are lost respectively, are very similar to those of thomsonite. A gonnardite sample from Mazé, Japan (sample described by HARADA et al., 1967) exhibited a sharper peak for the first dehydration step (not shown here) but no marked contraction of the lattice. The room temperature phase of this sample is identical to the second phase of the gonnardite from Auvergne.

Unlike thomsonite, gonnardite does not show a lattice transformation after the broad reaction and preceding the large sharp peak. Also, the exotherm following the final dehydration step in thomsonite is not apparent here, and the lattice collapse is of a more gradual nature (see fig. 4.2E.).

The subsequent high-temperature phases are the same as those for mesolite. As in the previous cases, according to the stoichiometry silica is left over but does not appear as a crystalline phase.

Like natrolite, the Mazé sample yielded α-carnegieite as an additional high temperature phase which is in accordance with its higher sodium content compared with that of the Auvergne sample.

4.2.6. *Edingtonite*

At present two type locations of edingtonite are known viz., Böhlet, Sweden and Kilpatrick, Scotland. New X-ray data of both specimens are given in appendix 1. For the thermal investigation only of the Böhlet specimen sufficient material was available.

A DTA curve of the Böhlet edingtonite has been reported by PÉCSI-DONÁTH (1962) and differs from ours only in temperature measurement. It shows two rather broad and one sharper endothermic peaks at ca. 170°, 280°, and 465 °C, respectively (fig. 4.2.). The corresponding steps in the dehydration curve indicate water losses of 12, 10, and 7 molecules respectively. The TG curve indicates that no more water is available so that edingtonite contains 29 H_2O per 80 oxygen atoms. HEY (1934) reports that edingtonite contains 32 H_2O per 80 oxygen atoms on the basis that air-dry material takes up additional water when the water vapour pressure is raised. As this feature is by no means restricted to this mineral, the argument is questionable but underlines the necessity of stating the history of a zeolite sample, including the last moments, prior to analysis (see also section 3.5.).

As with the other members of the group, dehydration of edingtonite effects a lattice contraction along the *a* and *b* axes together with an expansion along the *c* axis (fig. 4.3F.) resulting in a merging of a number of reflections. These shifts are completely reversible.

The resolved DTA curve has already been discussed in section 3.2. Because of its prominence, a special feature needs mentioning. The final dehydration

peak is instantly followed by a relatively large exothermic peak. A similar succession but with smaller peaks was also found for thomsonite. However, in this case the exothermic reaction is of a different nature. Unlike the case of thomsonite, the reaction is accompanied by a small weight increase (see fig. 4.2.). It does not occur in a nitrogen gas atmosphere and is retarded at reduced pressures. It is inferred that an oxidation reaction must take place. The G.L. X-ray photo shows that the reaction does not entail a collapse of the lattice as suggested by PÉCSI-DONÁTH (1962) but the irreversible formation of celsian and an, as yet, unidentified phase. Because of this, the nature of the oxidation reaction is unknown. This unidentified phase gives the following X-ray reflections: (d in Å, at room temperature) 5.60 (w), 4.74 (vs), 4.48 (s), 4.22 (vs), 3.58 (w), 3.55 (w), 2.68 (s), 2.30 (w). A close relation between celsian and the unidentified phase is indicated by their simultaneous disappearance at the transformation to hexacelsian at 930°C.

The transformation of edingtonite to hexacelsian is represented by the equation:

$$\underset{\text{edingtonite}}{Ba_8Al_{16}Si_{24}O_{80} \cdot 29\ H_2O} \rightarrow 8\ \underset{\text{hexacelsian}}{BaAl_2Si_2O_8} + 8\ SiO_2 + 29\ H_2O$$

and here again silica remains. Unlike the reactions shown by other members of the group, this silica crystallizes as β-cristobalite at ca. 1050°C, as indicated by some weak reflections on the original G.L. X-ray photo (fig. 4.3F.). The coexistence of hexacelsian and β-cristobalite at such a relatively low temperature is not represented in the $BaAl_2Si_2O_8$-SiO_2 phase diagram of FOSTER and LIN (1969).

4.3. CONCLUSIONS

Upon dehydration, all members of the natrolite group react by a contraction of the lattice along the a and b axes and often an expansion along the c axis. This is in accordance with the general structure of these minerals which consists of parallel chains of (Al, Si)O_4 tetrahedra in the z direction, less prominently linked together in x and y directions.

Although natrolite, mesolite, and scolecite are isotypes, the structural behaviour of natrolite appears to deviate significantly from that of mesolite and scolecite which show a good mutual resemblance. Thomsonite and gonnardite, which are also supposed to be isotypes, are similar in thermal behaviour and show, moreover, properties of both natrolite (350°C endothermic peak) and mesolite/scolecite (ca. 200° and 400°C endothermic peaks, not all the water reversibly removable).

Apart from thermal expansion of the crystal lattice, the structural relationship of edingtonite with the group is not expressed by its thermal behaviour. Unlike the behaviour of the other members, after dehydration further heating produces an irreversible crystallographic transformation without going through an apparent X-amorphous phase. In all cases, resolution of the DTA curves gave a much clearer understanding of the actual thermal reactions.

5. PRESSURE-TEMPERATURE RELATIONS

In chapter 3 it was demonstrated that pressure-temperature relations of zeolite dehydration as obtained with the inhibited diffusion DTA method yielded promising results. Plotting $P-T$ data according to the Clausius-Clapeyron equation resulted in a straight line and, because equilibrium was reached, calculation of the reaction enthalpy ΔH_r from the slope seemed to be permitted.

In the present chapter theoretical aspects of this method will be discussed. In addition, applications such as the determination of (meta)phase boundaries and a discussion of the nature of water in zeolites will be given.

5.1. The Clausius-Clapeyron equation

Consider the general zeolite dehydration reaction:

$$\underset{\text{zeolite}}{A} \rightarrow \underset{\text{metazeolite}}{B} + \underset{\text{gas}}{H_2O}$$

In case of equilibrium, the relation between temperature and pressure is given by the Clapeyron equation:

$$\frac{dP}{dT} = \frac{\Delta H_r}{T\Delta V_r} \tag{5.1}$$

in which ΔH_r = molar reaction enthalpy or molar heat of dehydration

ΔV_r = molar volume change of reaction.

For this reaction the molar volume change is:

$$\Delta V_r = \Delta V_{solids} + V_{H_2O_{gas}}$$

The volume term for the solids in this equation is only a very small contribution and may be neglected in comparison with the volume contribution of the gas (Krauskopf, 1967; E-an Zen, pers. comm.). Only at pressures above two or three hundred atmospheres the term may become of significance (Orville and Greenwood, 1965, see below).

If perfect gas behaviour is assumed, the gas law gives:

$$V_{H_2O} = RT/P \quad \text{(for one mole)}$$

Substitution of $\Delta V_r = RT/P$ in (5.1) yields:

$$\frac{dP}{dT} = \frac{\Delta H_r \,.\, P}{RT^2}$$

or

$$\frac{d\ln P}{dT} = \frac{\Delta H_r}{RT^2} \tag{5.2}$$

This is the familiar Clausius-Clapeyron equation.[1] For numerical calculations it is convenient to restate equation (5.2) in integrated form: Assuming ΔH_r constant (discussed below):

$$\int d\ln P = \frac{\Delta H_r}{RT} \int \frac{dT}{T^2}$$

or

$$\ln P = \frac{-\Delta H_r}{RT} + C \quad (C = \text{constant of integration})$$

Substituting $R = 8.315$ J/mole/deg and going to decimal logarithms:

$$\log P = \frac{-\Delta H_r}{19.15} \cdot \frac{1}{T} + C' \tag{5.3}$$

This is the equation of a straight line with slope $-\Delta H_r/19.15$ if $\log P$ and $1/T$ are plotted as variables.

The most important restrictions applying to the use of the Clausius-Clapeyron equation in the present case are:

1. Reversible reaction (equilibrium)
2. Pressure-volume work only
3. Ideal gas for the gas phase
4. ΔH_r constant

Of these conditions, only the latter two may need discussion.

Ad 3. In the present experiments, the water vapour pressures range from ca. 0.01 to 5 atm. (see next section). Ideal gas behaviour can generally be assumed up to at least 1 atm. For water vapour pressures of a few atmospheres the fugacity is still very close to unity because of the high critical pressure of water vapour (see universal gas activity coefficient chart, GARRELS and CHRIST, 1965, p. 25).

Ad 4. According to the pressure correction equation of ORVILLE and GREENWOOD (1965): $\Delta H_r(P) = \Delta H_r(1 \text{ atm.}) + (P-1)\, V_{solids}$, only at pressures significantly higher than 1 atm. i.e., above a few hundred atmospheres, correction will be needed.

The change of ΔH_r with temperature, i.e., the change in heat capacity $\Delta C_P = (\delta \Delta H_r/\delta T)_P$ of reactants to products, is negligible within a few tenths of degrees, and even for a few hundred degrees usually amounts to only a few per cent (KRAUSKOPF, 1967, p. 211).

Because insufficient heat capacity data for zeolites are available some uncertainty exists, but evidence indicates that no serious error is introduced (see

[1] Note that P in this equation is identical to the equilibrium constant: $K = [B]\,[H_2O]/[A]$ hence, $K = [H_2O]$ in which $[H_2O] = P_{H_2O}/P^0_{H_2O}$. Thus, if $P^0_{H_2O}$ is taken to be 1 atm, as is done here for convenience, then P in equation (5.2) has the numerical value of the pressure in atm. but is dimensionless. It is, however, fundamentally immaterial what pressure unit is chosen.

section 5.4.2.) and the assumption that ΔH_r is constant in the present working range seems justified.

It should be noted that pressure-temperature equilibrium combinations ($P-T$ pairs) can only be expected to fit the line of equation (5.3) if in each case the same reaction is involved i.e., in each case the zeolite should have the same degree of hydration. In practice, this condition can be met by taking fresh material from the same bulk sample for each determination.

Because ΔC_P can be taken constant in the present temperature range, like ΔH°_r, ΔS°_r does not change significantly with temperature either (except at phase changes) and therefore the change in ΔG°_r with temperature is a constant one (WEISBROD, 1968; ZEN, 1971):

$$\Delta G^\circ_r(T, 1) = \Delta H^\circ_r(298, 1) - T\Delta S^\circ_r(298, 1)^1 \tag{5.4}$$

In addition, because $(\delta S/\delta T)_P = C_P/T$ and $(\delta H/\delta T)_P = C_P$, changes in ΔH°_r and ΔS°_r, caused by changes in heat capacities of the reactants and products, with changes in temperature, tend to counterbalance one another in equation (5.4) (GARRELS and CHRIST, 1965, p. 323).

The earlier discussed constancy of ΔH_r in the present pressure range implies that the (near) constancy of ΔC_P with temperature is also valid over this pressure range (that is, the index P which stands for constant pressure, in practice indicates a limited pressure range). Hence, the linear change of ΔG°_r with temperature is not significantly influenced by pressure in the present range. Thus, we may write:

$$\Delta G^\circ_r(T, 1) = -RT\ln P \tag{5.5}$$

in which P and T can be substituted by experimental $P-T$ pairs[2] which yield values for the change in standard Gibbs free energy of reaction at different temperatures and thus, by a straight line, at 298.15°K.

Because of the relation

$$\frac{\delta \Delta G^\circ_r}{\delta T} = -\Delta S^\circ_r$$

[1] The reference states of ΔH°_f and ΔG°_f of the compounds involved in the reactions are the composing elements in their standard state at one atm. and the stated temperature. The standard state for the condensed elements are the most stable form at one atm. and the stated temperature. For gaseous elements the standard state is the ideal gas at one atm. pressure (see ROBIE and WALDBAUM, 1968).

Wherever the reference state is not specified it is taken to be 298.15°K and one atm. pressure. In equation (5.4) the specification (298, 1) is added for clarity since on the right and left hand side the reference state is not the same. Note that specification of the reference state of ΔH°_r and ΔS°_r is also superfluous because they are practically constant in the present working range (see text).

[2] In equation (5.5) P is again identical to the equilibrium constant (see footnote p. 41).

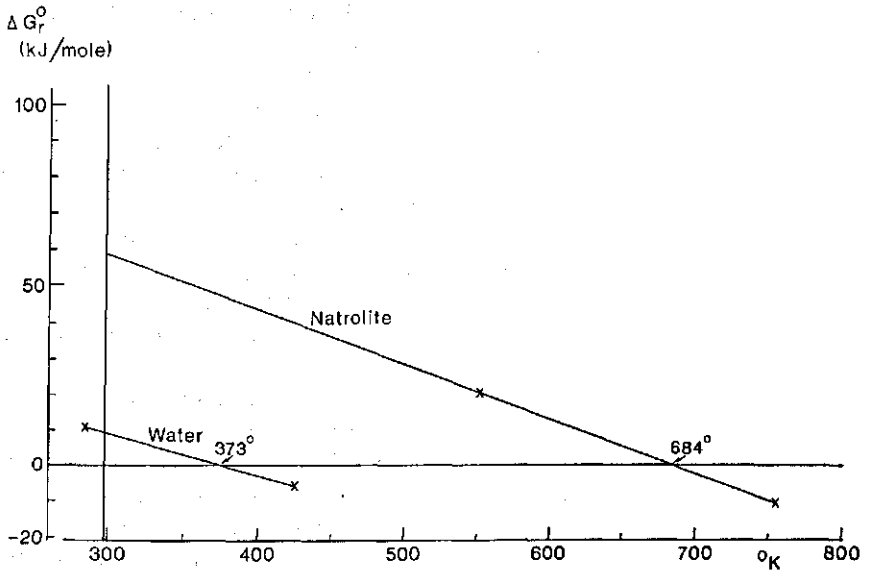

FIG. 5.1. Graphical determination of ΔG°_r (298, 1) and ΔS°_r (298, 1) of the dehydration of natrolite and the evaporation of water. The value of ΔG°_r is read directly from the figure; the value of ΔS°_r is the slope of the line.

the numerical value of ΔS°_r is the slope of this line (see section 5.2. and fig. 5.1.).

If a larger number (e.g., $\geqslant 10$) of data are available, a more appropriate method is the following:

Substituting (5.5) in (5.4) gives:

$$RT\ln P = -\Delta H^\circ_r + T\Delta S^\circ_r$$

which expressed in decimal logarithms and divided by 19.15 T, gives:

$$\log P = \frac{-\Delta H^\circ_r}{19.15} \cdot \frac{1}{T} + \frac{\Delta S^\circ_r}{19.15} \tag{5.6}$$

Equation (5.6) is equivalent to equation (5.3) and it appears that the constant of integration in the latter contains the value of ΔS°_r. The straight line defined by equation (5.6) can be obtained from the P—T data using the least squares fit and yields values for ΔH°_r and ΔS°_r.

5.2. EXPERIMENTAL

Pressure-temperature relations were obtained according to the DTA method described in section 3.3.2. For two reasons it was considered advantageous to extend the pressure range to pressures somewhat higher than 1 atm. Firstly, to

verify the linearity of the Clausius-Clapeyron relation over a longer range, and secondly to possibly improve the accuracy of the method.

To this end, a pressure jar was developed that fitted the cell base of the Du-Pont apparatus (see appendix 2). Pressure was supplied from a nitrogen gas cylinder. Thus, a pressure range from 0.01–5 atm. could be effected with relatively simple means.[1] To reduce possible systematic errors, the equipment was calibrated over the full pressure range with liquid water using powdered quartz as filling material. The $P-T$ pairs are formed by the extrapolated onset temperature of the DTA peak and the corresponding pre-adjusted pressure. Initially, for each reaction eight $P-T$ pairs were determined viz., at 0.013, 0.033, 0.066, 0.20, 0.40, 1.0, 2.0 and 5.0 atm. Duplicate runs indicated a reproducibility usually well within $\pm$ 3 °C, except sometimes for the 5 atm. runs where determination of the onset temperature was not always satisfactory.

For reactions occurring below ca. 50 °C, it was difficult to produce a satisfactory pre-reaction base-line. The measuring cell was then cooled with liquid nitrogen. In most cases more than one specimen was used for measurement or was at least checked at a few $P-T$ pairs. No significant deviations were encountered and therefore the results can be considered representative for the mineral in question.

Experience with the method and the results indicated that for a successful application the number of $P-T$ pairs per reaction could be limited to 10–12 per reaction, including some duplicates, and that the use of pressures above 1 atmosphere is not essential (for errors, see section 5.4.1.). An approximate but rapid estimation of the course of the straight line can be obtained by determining two duplicate runs at 0.05 and 1.0 atm. respectively. The value for $\Delta H°_r$ can then be obtained directly from the slope of this line i.e., not using the least-square fitting. In this case, the value of $\Delta S°_r$ can be obtained using equation (5.5) and the type of graph shown for the evaporation of water and the dehydration of natrolite in figure 5.1.

The extrapolated onset temperature can be considered representative for the whole reaction only if the peak is not too broad. For such reactions (e.g., dehydration type 3, chapter 3) this temperature only represents the first part of the reaction.

This aspect becomes even more serious if a low-temperature dehydration reaction, as discussed in chapter 3, preceeds a major dehydration reaction. This is a general problem and a possible source of error whenever closely adjacent or overlapping peaks occur, especially when the extent of overlapping alters with changing pressure. This feature was illustrated with $BaCl_2 . 2H_2O$ by GARN (1965; p. 262).

A method was found to overcome this problem. It appeared that if a DTA run was stopped somewhere during such a broad dehydration reaction (type 2

[1] The lower limit of a water-jet pump is ca. 0.02 atm., and for lower pressures an electrical vacuum pump should be used.

and 3), and the run was restarted immediately after forced cooling to a predetermined but arbitrary temperature (preferably well above room temperature) the dehydration reaction would continue from where it was halted and, in effect, a 'new' peak with a corresponding new onset temperature (see figure 5.2., chabazite) was obtained. In this way it appeared possible to subdivide the reaction in steps or, rather, to 'penetrate' the zeolite to any desired extent, and determine the $P-T$ relations there in exactly the same way as described above and with the same reproducibility.

This feature is not restricted to broad peaks since the same is exhibited by zeolites with type-1 dehydration (sharp peaks) as is shown for gismondite in figure 5.2. Such a zeolite can also be dehydrated step by step or rather peak by peak, and even so-called double peaks may be dealt with individually.

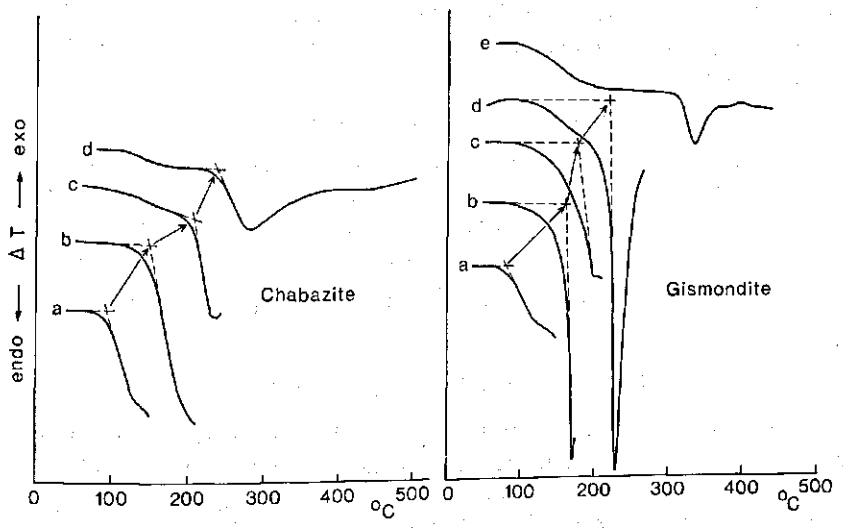

FIG. 5.2. DTA curves of chabazite and gismondite obtained with the 'penetration method' (see text). The arrows indicate the onset temperatures obtained successively from *a* to *d* and *e* respectively. Compare these DTA curves with the original ones in figure 3.1.

5.3. METHOD BY FISHER AND ZEN

FISHER and ZEN (1971) and ZEN (1971) have proposed a method for calculating thermodynamic parameters of minerals based on the use of 'hydrothermal point data (actually, bracket data) for individual T, P values' and argued that this is to be preferred to methods using derivatives (slopes) of such data as employed by ORVILLE and GREENWOOD (1965) and WEISBROD (1968). Since the present method is closely related to the latter two methods, a comparison needs to be made.

5.3.1. *Preparation for use*

FISHER and ZEN consider the simple univariant[1] dehydration reaction

$$A \rightleftarrows B + H_2O.$$

For equilibrium they write (their equation 4 B)[2]:

$$\Delta G_r(T_E, P_E) = \Delta G^0_{f,\,B}(298, 1) - \Delta G^0_{f,\,A}(298, 1) + \Delta G^0_{f,\,H_2O}(298, 1) - \\ - \int_{298}^{T_E} \Delta S_{f,\,s}(T)dT - \int_{298}^{T_E} S_{f,\,H_2O}(T)dT + \int_{1}^{P_E} \Delta V_s(P)dP + \\ \int_{1}^{P_E} V_{H_2O}(P)\ dP = 0 \qquad (5.7)$$

(T_E, P_E indicating equilibrium temperature and pressure; f = formation; s = solids)

in which:

$$\int_{298}^{T_E} \Delta S_{f,\,s}(T)dT = \Delta S^0_{f,\,s}(T_E - 298) \text{ (by approximation)}$$

S_f for each solid is a very slowly varying function of T, and the difference between S_f of products and reactants is an even more stable quantity ($\Delta C_P = 0$, the constant entropy method),

and: $\int_{1}^{P_E} \Delta V_s(P)dP = \Delta V_s(P_E - 1)$, (by approximation)

The volume change, ΔV_s is largely independent of temperature and pressure and, as indicated earlier, may be neglected compared to the $V_{H_2O_g}$ integral.

The two integrals pertaining to H_2O in equation (5.7) may be expressed as functions of the Gibbs free energy as follows:

$$\int_{298}^{T_E} S_{f,\,H_2O_g}(T)dT = \Delta G^0_{f,\,H_2O_g}(T_E, 1) - \Delta G^0_{f,\,H_2O_g}(298, 1)$$

and

$$\int_{1}^{P_E} V_{H_2O_g}(P)dP = G_{H_2O_g}(T_E, P_E) - G_{H_2O_g}(T_E, 1)$$

(using the tables by BURNHAM, HOLLOWAY and DAVIS, 1969; which employ the triple point of water as standard state. The 'G_{H_2O}' terms are actually ΔG_{H_2O} values, as a difference is taken, this is of no consequence.)

Equation (5.7) then becomes (neglecting the ΔV_s term):

$$0 = \Delta G^0_{f,\,B}(298, 1) - \Delta G^0_{f,\,A}(298, 1) - \Delta S^0_{f,\,s}(T_E - 298) + \\ + \Delta G^0_{f,\,H_2O}(T_E, 1) + G_{H_2O_g}(T_E, P_E) - G_{H_2O}(T_E, 1) \qquad (5.8)$$

Defining:

$$G^*_{H_2O_g}(T_E, P_E) = \Delta G^0_{f,\,H_2O_g}(T_E, 1) + G_{H_2O_g}(T_E, P_E) - G_{H_2O_g}(T_E, 1) \qquad (5.9)$$

[1] It could be argued that zeolite dehydration is a bivariant reaction rather than a univariant one since the phase boundary need not be sharp and the two phases may coexist (GRANGE, 1964; SIMONOT-GRANGE et al., 1968). However, in the present case it is not unrealistic to visualize such a reaction as the sum of very small, univariant, dehydration steps. Thus, in the above equations, B represents a slightly less hydrated phase than A rather than the fully dehydrated and hydrated phase, respectively. This agrees with the results of the earlier described penetration method (section 5.2.) and supports the contention that the standard entropy change of reaction can by approximation be taken to be the entropy of water in zeolites (see section 5.4.).

[2] In the method by FISHER and ZEN the standard state pressure is defined as one bar. Since 1 atm. = 1.013 bar, the ultimate results can be directly compared.

this in (5.8):

$$\Delta G^0_{f,\,B}(298,1) - \Delta G^0_{f,\,A}(298,1) - \Delta S^0_{f,\,s}(T_E - 298) + \\ + G^*_{H_2O_g}(T_E, P_E) = 0 \qquad (5.10)$$

Now, substituting two P–T pairs gives a solution for $\Delta S^0_{f,\,s}$:

$$(T_1, P_1): \; 0 = \Delta G^0_{f,\,s}(298,1) - \Delta S^0_{f,\,s}(T_1 - 298) + G^*_{H_2O_g}(T_1, P_1)$$
$$(T_2, P_2): \; 0 = \Delta G^0_{f,\,s}(298,1) - \Delta S^0_{f,\,s}(T_2 - 298) + G^*_{H_2O_g}(T_2, P_2)$$

Subtraction:

$$\Delta S^0_{f,\,s} = \frac{G^*_{H_2O_g}(T_2, P_2) - G^*_{H_2O_g}(T_1, P_1)}{T_2 - T_1} \qquad (5.11)$$

To calculate the standard entropy change of reaction ΔS^0_r, the change in standard entropy of formation from the elements of the solids is converted to absolute entropies as follows:

Defining:

$$\Delta S^0_{f,\,s} \equiv S^0_{f,\,B} - S^0_{f,\,A}$$
$$= S^0_B - S^0_{elements} - S^0_A - S^0_{elements} - S^0_{H_2} - {}^1/_2\, S^0_{O_2}$$
$$= S^0_B - S^0_A + 233.1 \text{ J/mole/deg}$$

or:

$$S^0_B - S^0_A = \Delta S^0_{f,\,s} - 233.1 \text{ J/mole/deg}$$

Also:

$$\Delta S^0_r = S^0_{H_2O_g} + S^0_B - S^0_A \text{ (i.e., evaporation of water from A)} \qquad (5.12)$$

and thus:

$$\Delta S^0_r = 188.7 + \Delta S^0_{f,\,s} - 233.1 \text{ J/mole/deg}$$

or

$$\Delta S^0_r = \Delta S^0_{f,\,s} - 44.4 \text{ J/mole/deg} \qquad (5.13)$$

Although equation (5.13) is needed for the calculation, equation (5.12) is of more informative importance because it contains the term $(S^0_A - S^0_B)$ which is the loss of entropy by A when it loses water, i.e., the entropy contribution of water in the hydrous phase, including a water-framework interaction term.

ZEN (1971) proposed a method to calculate the standard enthalpy of reaction $\Delta H^0_r(298,1)$ from the value $\Delta S^0_{f,\,s}$ as calculated from equation (5.11):

$$\Delta H^0_r(298,1) = \Delta H^0_{f,\,B}(298,1) - \Delta H^0_{f,\,A}(298,1) + \\ + \Delta H^0_{f,\,H_2O_g}(298,1) \qquad (5.14)$$

Then write:

$$\Delta H^0_f(298,1) = \Delta G^0_f(298,1) + 298 \times \Delta S^0_f(298,1) \qquad (5.15)$$

Substituting (5.15) for each term in (5.14) gives:

$$\Delta H^0_r(298,1) = \Delta G^0_{f,\,B}(298,1) - \Delta G^0_{f,\,A}(298,1) + \\ + 298 \times \Delta S^0_{f,\,s}(298,1) + \Delta H^0_{f,\,H_2O_g}(298,1) \qquad (5.16)$$

To eliminate the unknown ΔG^0_f terms subtract equation (5.10) from (5.16), then:

$$\Delta H^0_r(298,1) = \Delta H^0_{f,\,H_2O_g}(298,1) - G^*_{H_2O_g}(T_E, P_E) + T_E \times \Delta S^0_{f,\,s}$$

FISHER and ZEN (1971) presented tables for G^* in the pressure range 100–10,000 bars and temperature range 100–1000°C. Pressure-temperature work of the present study falls outside these ranges, and values for G^* have to be calculated by finding the three individual terms in equation (5.9) using different tables:

Values of $\Delta G^0_{f,\,H_2O_g}$ (T_E, 1) are derived from ROBIE and WALDBAUM (1968), conversion of one atmosphere to one bar is done by addition of $0.013 \times T$(°K) to the given ΔG^0_f value. Conversion of calories to Joules is done by multiplication by 4.184.

Values of G_{H_2O} (T_E, P_E) are calculated from *The Steam Tables* (BAIN, 1964) using $\bar{g} = \bar{h} - T.\bar{s}$ in which $\bar{h}$ = specific enthalpy and $\bar{s}$ = specific entropy. (These values are given in J/gram and J/gram/deg respectively, and have to be converted to J/mole and J/mole/deg by multiplication by 18.)

Values of $G_{H_2O_g}$ (T_E, 1) can be taken directly from table 2b of BURNHAM, HOLLOWAY and DAVIS (1969), but have to be converted from calories to Joules.

Results of application of this method to our own data and comparison with results of the proposed graphical method are given next.

5.3.2. *Comparison of results*

For three arbitrarily chosen zeolite dehydration reactions values for ΔH^0_r and ΔS^0_r have been calculated according to the method by FISHER and ZEN (1971) and the present graphical method, in both cases using the same P—T data obtained by the earlier described DTA method.

The input for the FISHER and ZEN method consisted of two points (P—T pairs) on the log$P$ vs. $10^3/T$ line at pressures of 1.0 and 0.033 atm. For the present method, the input was this line itself (slope).

The results, given in table 5.1., indicate that the two methods are highly consistent with each other and that, provided the experimental data are correct, neither can be given preference.

Rectilinear best-fitting of data over a P—T range should give statistically more reliable results than using two individual brackets. Furthermore, in the present case, the graphical method is to be preferred because the method by FISHER and ZEN is much more laborious as long as tables for G^* are not available for lower P and T values (FISHER and ZEN, 1971, their table 1).

TABLE 5.1. Some thermodynamic data of zeolite thermal dehydration reactions calculated according to two different methods (ΔH^0_r: kJ/mole H_2O; ΔS^0_r: J/mole H_2O/deg).

	FISHER & ZEN method		Graphical method	
	ΔH^0_r	ΔS^0_r	ΔH^0_r	ΔS^0_r
Natrolite	102.1	149.4	102.9	150.6
Phillipsite, main step	59.8	122.6	59.4	120.9
Stilbite, 1st step	73.6	151.9	73.6	152.3

5.4. Results and Discussion

Plotting $P-T$ pairs for zeolite dehydration using linear P and T scales results in the type of graph as given in figure 5.3. for natrolite dehydration. Although the phase boundaries are delineated in this way, little quantitative information can be drawn directly from this type of graph and therefore the experimental results are presented in terms of the Clausius-Clapeyron equation (equation 5.6). This is shown in figure 5.4. for zeolites of the natrolite group and in figure 5.5. for a selection of other representative zeolites.

The derived thermodynamic data of the dehydration of these together with some other zeolites are presented in table 5.2. Values for ΔH^0_r and ΔS^0_r were calculated with the least squares fit of $P-T$ pairs (equation 5.6). Instead of values for ΔS^0_r, those for S^0_{wz} are listed. These are estimates of the standard entropy of water in zeolites and calculated according to the equation:

$$S^0_{wz} = S^0_{H_2O_g} - \Delta S^0_r$$

This implies that all the entropy change of zeolite dehydration is allotted to the evaporation of water. It may be argued that this is very approximate because the aluminosilicate lattice with the cations may simultaneously undergo an entropy change, especially at phase transitions. Since insufficient heat capacity data are available, it is at present impossible to evaluate this effect quanti-

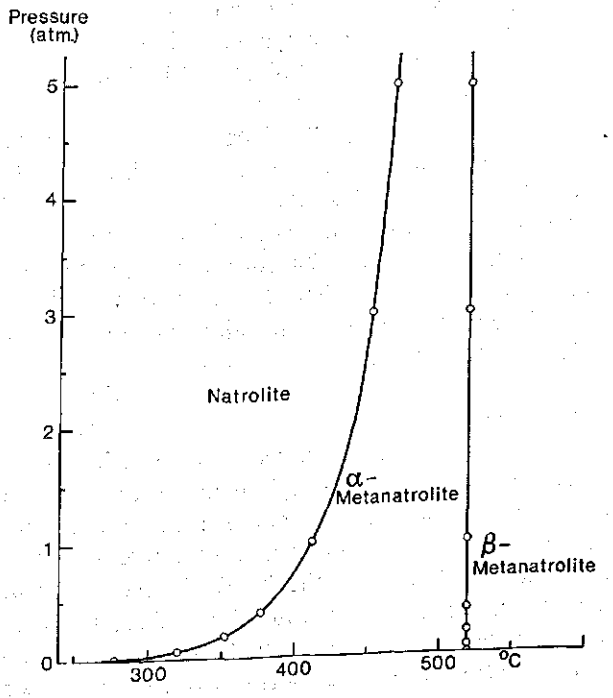

Fig. 5.3. Equilibrium dehydration curve for natrolite.

tatively. The correction method for oxide-sum entropies (LATIMER, 1951; FYFE et al., 1959) using experimental and calculated molar volumes, which are known for a few zeolites and their dehydration products e.g., natrolite and analcite, is too approximate to be of use.

However, it can also be argued that a possible entropy change of the lattice is of very limited importance in this respect since it was shown earlier (section 4.2.1.) that during dehydration, the bulk of the water usually escapes *prior* to drastic lattice deformations (dehydration type 1) and it is this bulk reaction that is used for measurements. When lattice deformation keeps pace with dehydration or when no deformation occurs (types 2 and 3), the change per water molecule can be considered small and only a few of these molecules are used for measurements, viz., those escaping at the beginning of the long-range reaction. In the following discussion of the results these contentions will be supported.

5.4.1. *Errors*

No direct statement can be made about the systematic experimental error of the method used. Circumstantial evidence has been, and will be given (table 5.3.) that the method is applicable to zeolite dehydration.

The correlation coefficient for the straight line, best-fitted with the least-square method, was greater than 0.99 for all sets of data. A certain error is implied because in most cases a limited number of $P-T$ pairs were used to calculate the line (usually 10–12). This error can be found from the standard deviation of the calculation. Two examples are given.

For natrolite, 28 $P-T$ pairs were available yielding a line with equation: $y = -5.37x + 7.88$. From this, $\Delta H^0_r = 102.9 \pm 2.1$ kJ/mole and $\Delta S^0_r = 150.6 \pm 0.8$ J/mole/deg (P = 0.05) were calculated.

For gmelinite (3rd reaction), 12 $P-T$ pairs gave a line with equation: $y = -3.82x + 6.51$. From this, $\Delta H^0_r = 73.2 \pm 2.5$ kJ/mole and $\Delta S^0_r = 124.7 \pm 1.7$ J/mole/deg (P = 0.05) were calculated.

In no case did the standard deviation for ΔH^0_r exceed 4.0 and for ΔS^0_r exceed 3.4. It can therefore be stated that for general convenience the standard reaction enthalpy values ΔH^0_r as determined by this method are accurate within $\pm$ 4 kJ/mole and the standard reaction entropy values ΔS^0_r within $\pm$ 3.5 J/mole/deg (see table 5.2.).

5.4.2. *Phase boundaries*

The solid lines in figures 5.4. and 5.5. delineate phase boundaries of zeolites, their metaphases and possibly other high-temperature phases up to 600 °C. Dashed lines indicate dehydration reactions (DTA peaks) not accompanied by distinct phase transformations or deformations whereas dotted lines do not indicate specific reactions but depict the $P-T$ relation for zeolite water molecules as found by the penetration method. Since these phase boundaries are based on DTA onset temperatures, there will probably be a small discrepancy with the actual phase transition which was shown to occur at a slightly higher temperature.

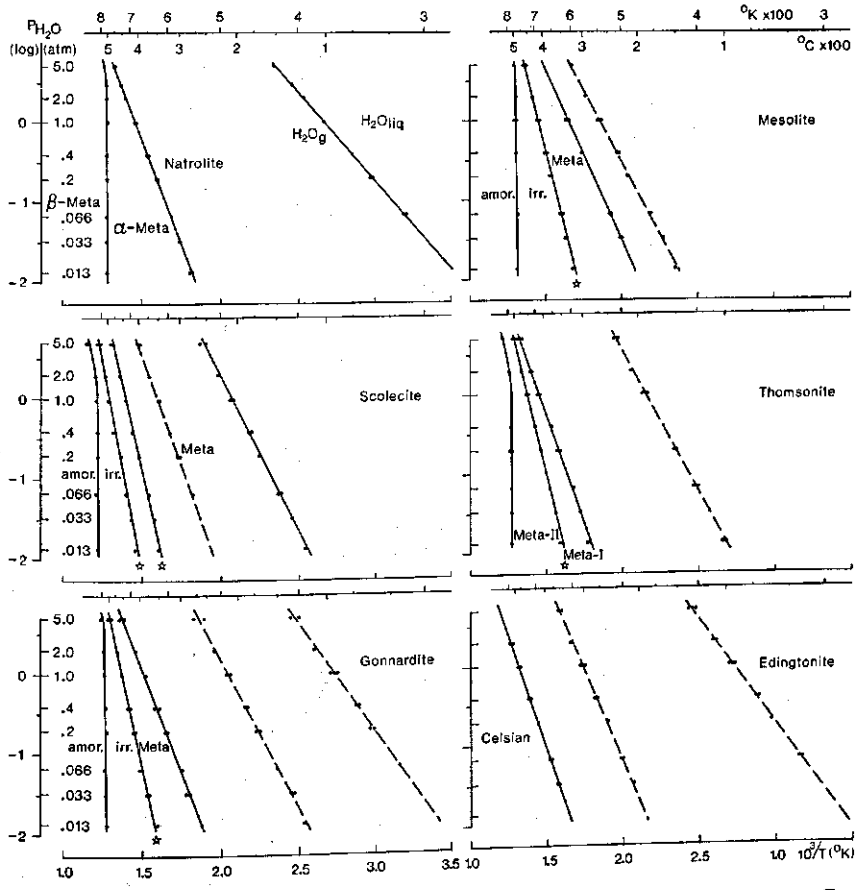

FIG. 5.4. Log P_{H_2O} vs. $1/T$ of dehydration equilibria of zeolites of the natrolite group. Continuous lines delineate approximate phase boundaries; dashed lines indicate dehydration reactions not accompanied by a phase transition. Lines not representing equilibrium are marked with an asterisk. Irr. = irreversible; amor. = X-amorphous.

Boundaries pertaining to reactions not involving water, such as $\alpha \rightarrow \beta$ metanatrolite, the direct formation of high-temperature feldspars (phillipsite group) and the various structure-collapse reactions, run parallel to the pressure axis (at least in the pressure range used here). Since these reactions depend on the final dehydration step they will give way at higher pressures when this final step reaches these non pressure-dependent reactions. In practice, the phase boundaries will then coincide e.g., natrolite will eventually change directly to β-metanatrolite (although the momentary existence of α-metanatrolite as an intermediate step cannot be ruled out).

5.4.3. *Heat of dehydration*

The most striking feature of the ΔH^0_r values in table 5.2. is that none are

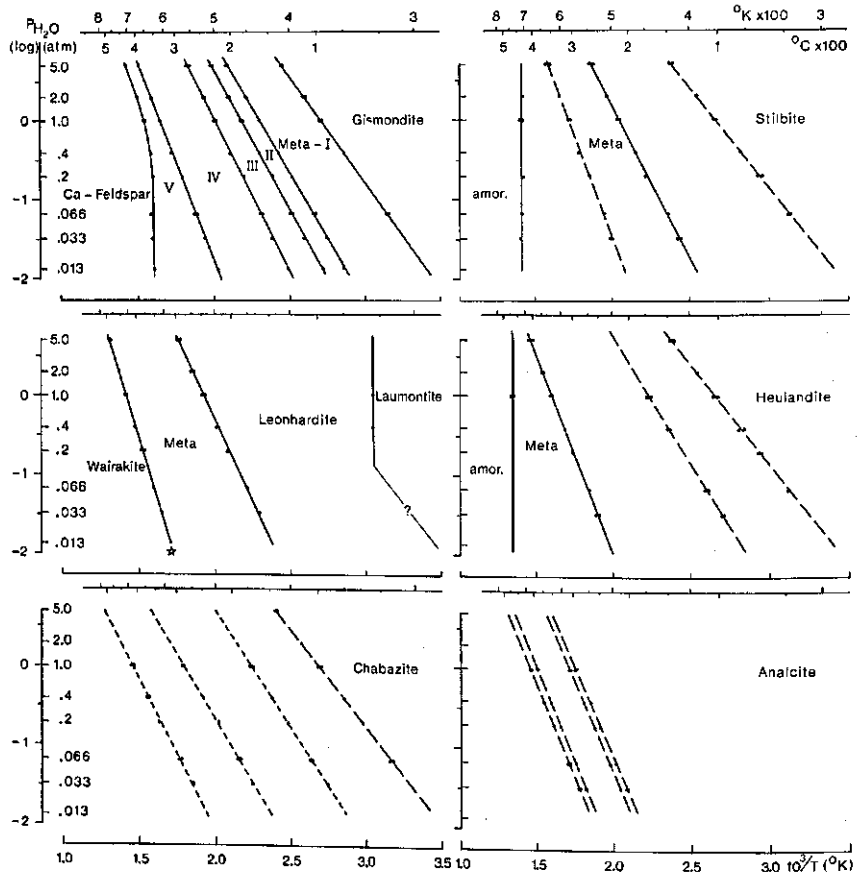

FIG. 5.5. Log P_{H_2O} vs. $1/T$ of dehydration equilibria of some zeolites. Continuous lines delineate approximate phase boundaries; dashed lines indicate dehydration reactions not accompanied by a phase transition; dotted lines indicate dehydration not appearing as a discrete reaction but obtained with the penetration method (see text). Lines not representing equilibrium are marked with an asterisk. Amor. = X-amorphous.

below the heat of evaporation of pure water i.e., 43.5 kJ/mole (10.4 kcal/mole). The lowest values are those for the so-called 'loosely held' water and range consistently between 47 and 49 kJ/mole (11.3 and 11.7 kcal/mole). SIMONOT-GRANGE et al. (1968) state that physically adsorbed water in general has a vaporization enthalpy ranging from 48–58 kJ/mole (10.5 to 14 kcal/mole). If this is true, then the first-step water of thomsonite, gonnardite and gismondite, having a ΔH^0_r value of about 52 kJ/mole, would also belong to this group. It was shown earlier (section 3.4) that such loosely held water is internally adsorbed in the zeolite structure rather than on the external surface. In terms of hydration energy, however, there appears to be no difference.

The results show that in successive dehydration steps a higher enthalpy is

TABLE 5.2. Thermodynamic data of dehydration reactions of some natural zeolites.[1]
(onset temperature t: °C at P_{H_2O} = 1 atm.; ΔH^0_r: kJ/mole H_2O ± 4; S^0_{wz}: J/mole H_2O/deg ± 3.5.)

Mineral	t	ΔH^0_r	S^0_{wz}	t	ΔH^0_r	S^0_{wz}	t	ΔH^0_r	S^0_{wz}	t	ΔH^0_r	S^0_{wz}	t	ΔH^0_r	S^0_{wz}
Water	100	43.5	69.8												
Natrolite				411	102.9	38.1									
Mesolite				266	69.5	60.7	333*	82.8	53.6	417	152.3	–40.0			
Scolecite				240	81.2	38.9	347	92.5	40.6	447	161.5	–34.3	504	201.7	–55.2
Thomsonite				191	68.2	41.0	417	105.0	37.7	455	157.7	–24.7			
Gonnardite				100	52.3	46.0	216	70.7	46.0	390	100.0	38.5	457	174.9	–54.8
Edingtonite				100	51.9	47.6	308	87.0	37.7	491	110.5	43.9			
Gismondite				100	52.3	46.4	160	63.6	43.1	184	67.4	42.7	224	74.5	39.7
													333	97.1	30.1
Stilbite	100	49.1	58.6	212	73.6	36.4	305	100.8	15.0						
Heulandite	100	48.5	59.0	179*	62.8	45.6	345	94.6	37.7						
Laumontite[2]	100	48.1	59.8	243	80.3	33.1	426	130.5	1.7						
Phillipsite	100	48.9	58.7	157*	54.4	62.3	225	59.4	67.8						
Gmelinite	100	47.7	62.3	164*	57.3	59.0	315	73.2	64.0	412	105.9	35.2			
Chabazite	100	47.3	62.4	175*	36.5	63.6	326*	64.9	69.5	418*	77.4	71.9			
Erionite	100	48.1	60.7	167*	56.9	59.4									
Clinoptilolite	100	48.2	62.3	242*	63.2	66.5	331*	70.3	71.1						
Mordenite	100	48.1	60.2	181*	59.0	38.6									
Faujasite	100	47.6	61.1	184*	54.4	67.0									
Analcite				296*	83.7	38.2	387*	86.6	59.7						

[1] The first column gives data for 'loosely bound' water only. [2] actually: Leonhardite. * Obtained with penetration method (see section 5.2.).

always involved (even if this does not occur in discrete steps, such as in chabazite). This is due to the fact that water being removed at higher temperature (at the same pressure) is more strongly bound.

Considering the earlier contention that the measured energies pertain either mainly or only to the evaporation of water, rather than including any accompanying or subsequent lattice energy changes, together with the inference that diffusion does not play an important role (instant equilibrium), it may be concluded that the ΔH^0_r values found constitute a good estimate of the actual heat of hydration per mole of water held in zeolites. This is supported by the observation that the enthalpy of evaporation of 'loosely held' water is only slightly higher than that of liquid water. Thus, even if there would be no difference in terms of energy with liquid water, the contribution by other factors would be in the order of only 4 kJ/mole.

It is interesting to compare ΔH^0_r values of table 5.2. with the few published by other workers (or derived from their data) and with values obtained by the present writer using the DuPont DSC cell (see table 5.3.).

In general the results of the present method agree well with those obtained by others. By contrast and unexpectedly, many of the DSC results do not compare favourably. Although the good agreement between the other results is no proof of their correctness, some of the DSC results are at least suspect i.e., those less than 43.5 kJ/mole, whereas others must be definitely in error, i.e., in case of gismondite where values of successive dehydration steps do not increase. These errors may, to a large extent, be caused by baseline errors (especially for broad peaks) and calibration errors, but considering the magnitude of some of the deviations, other but as yet obscure, factors may be involved.

TABLE 5.3. Comparison of heats of hydration (ΔH in kJ/mole H_2O) of some zeolites as obtained by different authors using different methods.

Mineral	Present method	DuPont DSC[1]	Other methods[2]
Natrolite	102.9	89.1	≈ 105
Mesolite	69.5–82.8	73.2	62–80
Scolecite	72.4–92.5	81.6	89.5
Thomsonite	68.2	54.8	≈ 67
	105.0	64.6	≈ 88
Edingtonite	51.9	30.1	46–59
	110.5	39.7	≈ 140
Gismondite	63.6	41.8	–
	67.4	26.8	–
	74.5	57.7	–
	97.1	24.7	–
Heulandite	48.5	–	48.5
	59.4	–	≈ 63
	94.6	–	≈ 92

[1] VAN REEUWIJK (1971, 1972).
[2] Natrolite minerals: HEY (1932a & b, 1933, 1934, 1936)
Heulandite: SIMONOT-GRANGE et al. (1968).

5.4.4. *Water in zeolites*

The values of S^0_{wz} in table 5.2., taken to be an estimate of the entropy of water in zeolites, show a most interesting picture. Taking the errors into account they can be divided into three categories: *a.* values from 58–72 J/mole/deg (14–17 cal/mole/deg), *b.* values from 30–47 J/mole/deg (7–11 cal/mole/deg) and *c.* values below 30 J/mole/deg (7 cal/mole/deg). The values of the latter category are clearly too low and, by definition, negative values cannot exist. In these cases the DTA method failed because the equilibrium condition could not be met. This is inferred from the observation that such values are never found for a first step in the dehydration but invariably after a phase transformation or drastic lattice deformation e.g., mesolite, scolecite, thomsonite, gonnardite, stilbite, laumontite and gmelinite (see G.L. X-ray photographs figs. 4.2. and 5.6.). These changes apparently put up a physical barrier or trap preventing free movement of the water molecules by narrowing of structural channels and apertures, and blocking by cations. Drastic lattice changes do not necessarily bring about such blocking. This is demonstrated by gismondite where none of the metaphases seems to put up a significant hindrance, although there appears to be a tendency to increasingly lower entropy values.

The significance of the other two categories is that entropy values in the range of 58–72 J/mole/deg suggest a degree of disorder of H_2O molecules near to that of liquid water (69.8 J/mole/deg or 16.7 cal/mole/deg), whereas values ranging from 30–47 J/mole/deg are near to that of ice (= 38.1 at 273 °K and 41.4 J/mole/deg at 298 °K according to FYFE et al., (1959) and 44.8 J/mole/deg according to ROBIE and WALDBAUM (1968) or $\sim$ 10 cal/mole/deg) and virtually coincides with the range of entropy increments per mole of water accompanying hydration of some 24 salt hydrates listed by FYFE et al. (1959, p. 117). From this, the important conclusion can be drawn that, in addition to the so-called 'loosely held' water (table 5.2., 1st column), two types of constitutional water may occur in zeolites, viz. 'crystal water' and 'zeolitic water', both in the traditional sense. Furthermore, from the present results it can be concluded that the entropy of the 'zeolitic water' does not exceed that of liquid water as was recently suggested by ZEN (1972).

The consistency with which the S^0_{wz} values fall within the rather narrow ranges of crystal water and zeolitic water supports the earlier assumption that ΔS^0_r as used here is not significantly influenced by lattice entropy-change contributions. Had such an influence been present then the S^0_{wz} values would have been systematically lower, probably to varying extents. It is probable that such results would not have been examined closely and so their significance not realized in case of the relatively high values for zeolitic water, but in the case of crystal water attention would have been drawn to the consistently and impossibly low values which would then have been found.

The relation between the type of water and the crystal structure of the zeolite seems to be a clear one. As a general rule it can be said that the relatively compact zeolites (approximately those with $D > 2.15$; see table 5.4.) contain crystal water, whereas the more open species contain zeolitic water. From an

TABLE 5.4. Correlation of entropy of water in zeolites with specific density (D) and cation position (lo = low-entropy or crystal water; hi = high-entropy or zeolitic water).

Mineral	Water entropy	D (aver.)	Cations at fixed position
Natrolite	lo	2.23	yes (1, 2)
Mesolite	hi/lo	2.26	yes (1)
Scolecite	lo	2.27	yes (1)
Thomsonite	lo	2.25	yes (1)
Gonnardite	lo	2.30	yes ?
Edingtonite	lo	2.75	yes (3)
Gismondite	lo	2.28	yes (4, 5)
Stilbite	lo	2.16	yes (6, 7)
Heulandite	lo	2.20	yes (8, 9)
Laumontite	lo	2.28	yes (10, 11, 12)
Phillipsite	hi	2.19	yes/no (13, 14)
Gmelinite	hi/lo	2.07	yes/no (15)
Chabazite	hi	2.08	no (16)
Erionite	hi	2.02	no (17)
Clinoptilolite	hi	2.11	?
Mordenite	hi	2.14	no (18)
Faujasite	hi	1.92	no (19, 20)
Analcite	lo/hi	2.26	yes (21)

1 TAYLOR et al. (1933)
2 MEIER (1960)
3 TAYLOR & JACKSON (1933)
4 FISCHER (1963)
5 FISCHER & SCHRAMM (1970)
6 SLAUGHTER (1970)
7 GALLI (1971)
8 MERKLE & SLAUGHTER (1968)
9 ALBERTI (1972)
10 SCHRAMM & FISCHER (1970)
11 SCHRAMM (1973)
12 BARTL (1970)
13 STEINFINK (1962)
14 RINALDI et al. (1973)
15 AIELLO et al. (1970)
16 SMITH et al. (1963)
17 GARD & TAIT (1973)
18 MEIER (1961)
19 BERGERHOFF et al. (1958)
20 BAUR (1964)
21 TAYLOR (1930, 1938)

examination of the structural analysis of the various zeolites studied, it appears that low entropy (crystal water) generally results from coordination with cations occupying fixed positions in the channels and cavities, whereas high entropy results from coordination of the water molecules with cations that cannot be located at specific fixed positions (see table 5.4.).

Although in many cases of low-entropy water both the cations and the coordinated water molecules are bonded to framework oxygens, this seems not to be a prerequisite. In heulandite, for instance, only the cations are bonded to the framework, whereas the water molecules are bonded only to the cations. In stilbite the opposite is found, the Ca ions are bonded only to the water molecules which are themselves bonded to the framework.

Comparison of the structures of liquid water and ice reveals that both have essentially the same structure in which each H_2O molecule is tetrahedrally coordinated with four other H_2O molecules. In liquid water this structure is only pseudocrystalline, differing from ice in that the hydrogen bonds are continually

broken and remade and that molecules are being interchanged as a result of thermal motion. Thus, the average number of other molecules with which each water molecule is bonded, at any instant, will be lower than four. The relatively higher entropy of liquid water results from this higher degree of disorder. The comparison between water and ice can be extended to intracrystalline H_2O. It is known that in crystals the H_2O molecules also show a tendency to tetrahedral coordination. This may either be with other H_2O molecules or with cations and framework oxygens. In figure 5.6. some of these possibilities are schematically drawn, which does not necessarily mean that all these occur in zeolites. The low entropy arises when the water molecules are so bonded that their position is fixed and no spontaneous 'jump-overs' occur. This is the case when they are coordinated with cations in fixed position or directly with framework oxygens or both. That such different 'structures' of H_2O molecules all result in about the same entropy is consistent with the fact that of ice many polymorphs are known, all with entropies roughly in the same range as found here for low-entropy water (derived from EISENBERG and KAUZMANN, 1969, their table 3.6.).

High entropy arises when no fixed position can be assigned to the H_2O molecules and the possibility of breaking and remaking bonds is created. This does not imply that such molecules are exclusively coordinated with other H_2O molecules, on the contrary, cations and framework oxygens will be taken up in this large system of coordination because ice and water are, in reality, one large continuous molecule of oxygens bonded by hydrogens. Thus, such a system will have properties similar to those of an electrolytic solution rather than to those of ice.

Upon dehydration, the situation may be drastically altered since the original distribution of bonds and forces is changed. One possibility would suggest that

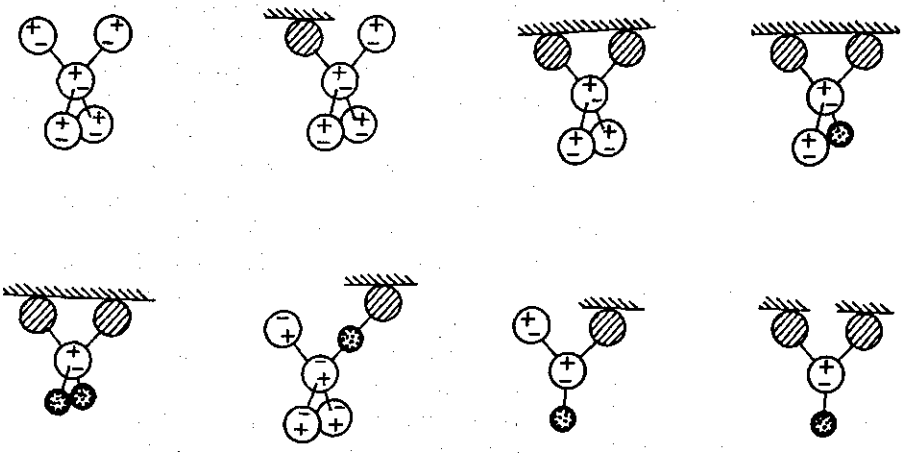

FIG. 5.6. Schematic representation of some possible environments of water molecules in zeolites. Open circles: H_2O molecules; hatched circles: framework oxygens; dotted circles: cations.

upon dehydration the remaining water molecules are bonded with increasing tightness and with an increasing tendency to occupy fixed positions. The former appears to be true, the latter generally not (e.g., chabazite, see below).

The position of the so-called 'loosely bound' water can be explained as follows. This water can usually be adsorbed by zeolites containing unoccupied H_2O positions in the structure. This means that there is space for such H_2O molecules to be coordinated, but between occupancy and non-occupancy there is sufficiently little enthalpy change (see table 5.2.) for it to be governed by the relative humidity of the air at room temperature. This implies a free exchange with 'outside' water molecules, hence the high entropy. In DTA it shows up as a low-temperature peak, i.e., with an onset temperature of ca. 100 °C at $P_{H_2O} = 1$ atm.

5.4.5. *Special features*

Finally, some special features observed will be discussed.

Mesolite. All water in zeolites of the natrolite group belongs to the low-entropy type. An exception appears to be water escaping during the first step of mesolite dehydration (the second step remains uncertain because of the negative entropy). Because this step consists of a composite peak in the DTA curve, it was thought that mutual influence perhaps led to a misinterpretation. However, when the final part of the composite peak was treated with the penetration method, a relatively high value was still found (see table 5.2.). The reason for this is not apparent. Although the environment of cations and water molecules in mesolite has as yet not been established by detailed crystal structure determination, considering the close structural relationship with the other members of the group, it is unlikely that this environment deviates much from that in the others.

Heulandite and clinoptilolite. These minerals are very closely related but have entirely different thermal properties. A discussion relating to this problem has been going on for a long time and still continues (HEY and BANNISTER, 1934; MUMPTON, 1960; SHEPARD and STARKEY, 1964; BREGER et al., 1970; BOLES, 1972; GOTTARDI et al., 1973).

Typical heulandites contain mainly bivalent cations (Ca), whereas clinoptilolites contain monovalent cations (Na > K). In addition, clinoptilolites are richer in silica and thermally considerably more stable. The thermal properties appeared to be more dependent on the type of cation than on the silica content: the higher the ionic potential of the cation, the less stable the mineral is (GOTTARDI et al., 1973).

The present results indicate low-entropy water in heulandite and high-entropy water in clinoptilolite suggesting that bivalent cations occupy fixed positions in the structure whereas monovalent cations do not. The former is confirmed by the detailed structure determination but for clinoptilolite no such analysis has been reported yet.

Laumontite - leonhardite. It is well known that laumontite readily dehydrates to leonhardite, at the loss of 1/8 of its water; usually just with air-drying (COOMBS, 1952). The nine different 'laumontite' specimens in our collection all turned out to be leonhardite, only in one case coexisting with laumontite. Soaking the material in water immediately reverses the reaction. The transition could only be shown on the G.L. X-ray photo if the sample was slightly moistened before heating was started (see fig. 5.7.E). A DTA curve of such powdered wet material indicated that the reaction takes place at 57 °C (1 atm. pressure). When sufficient H_2O molecules are released below the boiling point of water, formation of liquid water occurs. Dehydration of some salt hydrates leads to the same situation e.g., the first dehydration steps of $CuSO_4 . 5H_2O$ and $BaCl_2 . 2H_2O$ (WENDLANDT, 1970). The result is the occurrence of a quadruple point in the laumontite system i.e., four phases may co-exist viz., laumontite, leonhardite, H_2O (l) and H_2O (g).

Because of the occurrence of liquid water, changes in pressure had no significant effect on the reaction temperature because the fugacity of liquid water is highly insensitive to pressure changes. Thus, determination of $P-T$ relations of the laumontite-leonhardite transition can only be done at pressures below 0.017 atm., the pressure at which water boils at 57 °C. Therefore, to obtain $P-T$ pairs sufficiently far apart, cooling of the measuring cell is necessary.

Chabazite. Dehydration reactions of the types 2 and 3 (chapter 3) can only be approached with the penetration method. For chabazite this has been done to nearly the end of the dehydration. A high entropy for water was consistently found. This would indicate that the entropy of the water molecules is truly independent of the enthalpy of hydration (bonding forces) i.e., the degree of disorder is not reduced when the water content decreases; the results even indicate a tendency of the opposite.

Gmelinite. The interesting feature of gmelinite is that it contains all three types of water distinguished in this study. This is in excellent agreement with the structure which consists of two basic elements viz., the gmelinite cage and the hexagonal prism (BARRER and KERR, 1959). The situation in the gmelinite cage can be assumed to be similar to that in the somewhat larger chabazite cage (no fixed cation positions). In analogy to offretite (AIELLO et al., 1970) part of the Na ions may occupy the narrow hexagonal prisms in fixed position thus accounting for the low-entropy water. As with clinoptilolite, the detailed crystal structure determination has to be awaited for confirmation.

Analcite. The behaviour of analcite, a mineral that is not always classified as a true zeolite (DEER et al., 1963), is unlike that of any of the other zeolites investigated. Because this mineral exhibits dehydration type 3b, the penetration method has to be used. It appears that both the low and the high-entropy types of water are present in this mineral, the former escaping prior to the latter.

In the structure of analcite all the cations (Na) are believed to occupy specific sites and to be bonded to framework oxygens (TAYLOR, 1930, 1938). However,

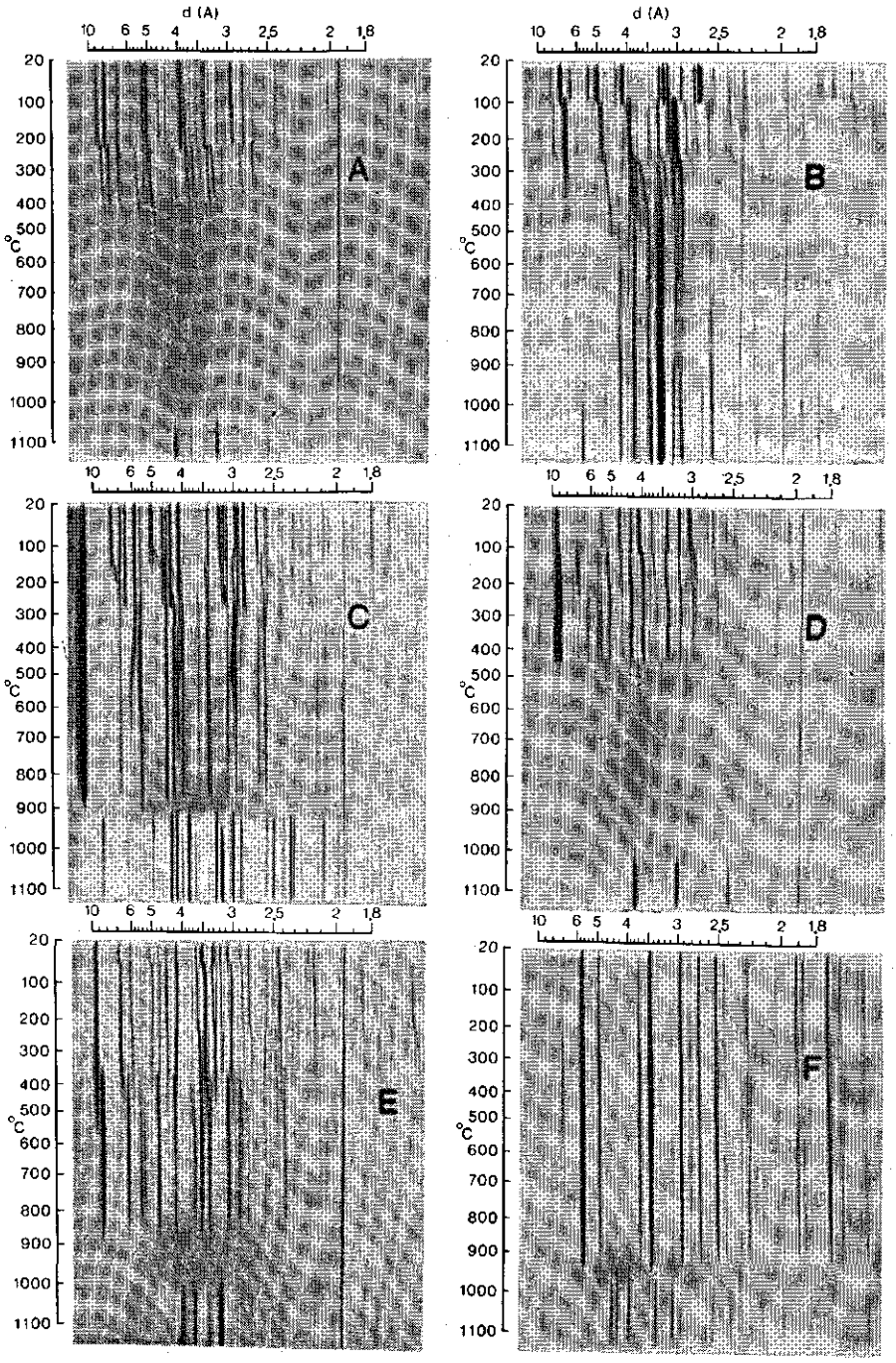

FIG. 5.7. Continuous-heating Guinier-Lenné X-ray photographs of some zeolites. A. heulandite, B. phillipsite, C. gmelinite, D. stilbite, E. laumontite, F. analcite. The continuous reflections from top to bottom of the photographs are due to the Pt sample grid.

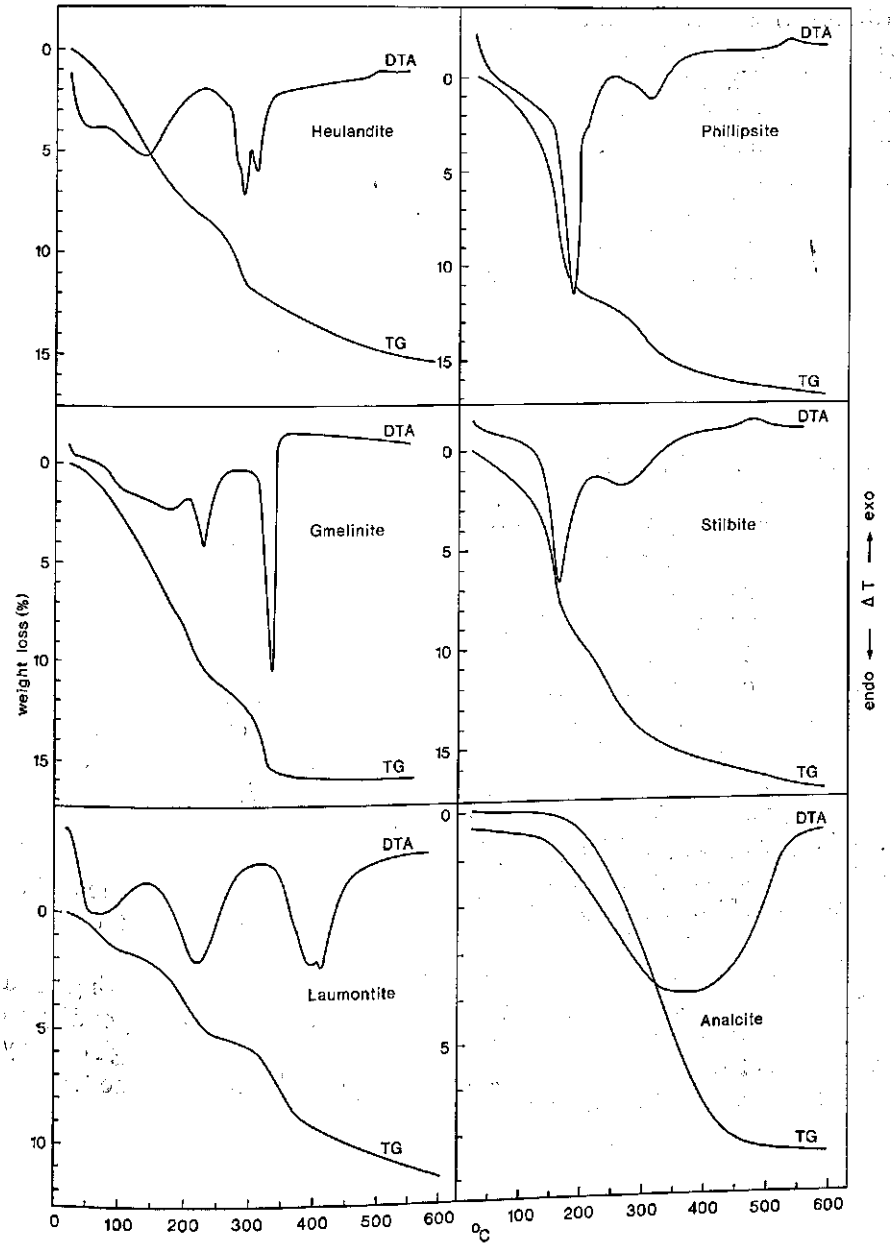

FIG. 5.8. DTA and TG curves of the zeolites given in figure 5.7. $P_{H2O} \approx 0.05$ atm.

because of the complexity of the structural aspects and the variation in composition, no detailed crystal structure determination has been reported yet (BEATTIE, 1954; SAHA, 1959).

An important feature of the dehydration is shown by the G.L. X-ray photo

(fig. 5.7F.) which shows a splitting-up of many reflections at ca. 200 °C. This coincides with the break between low-entropy and high-entropy water shown in figure 5.5. (G.L. photo taken at $P_{H_2O} \approx 0.01$ atm.) and corresponds with a slight discontinuity in the otherwise smooth DTA curve (fig. 5.8.). This break, which was earlier reported by KOIZUMI (1953) and recently by BALGORD and ROY (1973), may indicate a change from cubic or pseudo-cubic to tetragonal symmetry and may be accompanied by a change in cation and water environment. It is to be noted that upon completion of the dehydration, the framework has returned to its original structure.

5.5. CONCLUSIONS

Because of the ease with which water can escape zeolite structures, the inhibited diffusion DTA method proved to give satisfactory results in determining pressure-temperature relations of zeolite dehydration reactions. The results, when plotted according to the Clausius-Clapeyron equation facilitate calculation of the standard enthalpy of reaction (which was taken to be the heat of hydration), as well as the standard entropy change of reaction. The latter value, when substracted from the standard entropy of water vapour, was taken to be a measure of the standard entropy contribution of water in zeolites.

It appeared that in zeolites at least three types of water may be present: 1. crystal water or low-entropy water with a standard entropy value in the range of 30–47 J/mole/deg (7–11 cal/mole/deg); 2. zeolitic or high-entropy water with a standard entropy in the range of 58–72 J/mole/deg (14–17 cal/mole/deg); 3. so-called 'loosely bound' water with a high standard entropy of 58–63 J/mole/deg (14–15 cal/mole/deg). The difference between the two high-entropy water categories becomes apparent in the temperature at which they are released. The loosely bound type will have disappeared above the boiling point of liquid water, the zeolitic type not.

Generally, low entropy arises when H_2O molecules are occupying fixed positions in the zeolite cages and channels because of hydrogen bonding to framework oxygens or to cations bonded to framework oxygens. High entropy arises when the molecules possess a higher degree of disorder because they are not coordinated in fixed positions.

SUMMARY

The zeolites constitute a group of minerals of much interest from geological, mineralogical and technological points of view. Structurally, they are tectosilicates with an 'open' framework containing channels and cavities which accommodate cations and water molecules. Generally, these cations are exchangeable and the water molecules can be removed or replaced reversibly without disrupting the framework.

Because of the widespread occurrence of zeolites in various environments, they offer a fruitful field of investigation to geologists and this has led to the recognition of the so-called zeolite facies.

Technologically, no mineral group is as versatile in its application possibilities as the zeolites. This is due to their high physical stability and specific sorptive properties. For this reason, zeolites are synthesized on a large scale and then appropriately named molecular sieves. In recent years large and relatively pure deposits of useful zeolites have been discovered. Since these can be made available at relatively low cost, the interest in natural zeolites is rapidly reviving.

For many applications, zeolites have to be activated by heating. This involves dehydration of the minerals and consequently often causes drastic, but usually reversible, changes in the structure and unit-cell dimensions. Hence, the thermal properties of zeolites have been studied for many years. A brief review of this work is given in chapter 2. Because of the unsystematic approach in which inadequate techniques were often employed, the results have frequently been both inaccurate and controversial.

In chapter 3, the dehydration process which is a composite reaction, is analysed. Zeolite dehydration appears to occur according to one or more of three basic types. Type 1 is a discrete reaction over a relatively short temperature range accompanied by a sharp peak in the DTA curve and a marked crystallographic transformation. Type 2 consists of a sequence of small dehydration steps resulting in a broad, often somewhat irregular DTA peak accompanied by small stepwise lattice adaptations. With type 3, dehydration occurs gradually without any apparent break, also resulting in a broad and smooth DTA peak. The lattice may either adapt gradually or remain virtually unaltered.

Water vapour pressure strongly influences the reaction temperature and the dehydration process appears to occur so rapidly that equilibrium is instantly reached. The dehydration-rehydration hysteresis effect occurring in several zeolites is not caused by possible non-equilibrium conditions of the dehydration reaction but by the lattice transformation.

The so-called 'loosely held' water, denoted in chemical analyses as H_2O-, appeared to be adsorbed internally in the structure instead of on the external surface.

In chapter 4 a systematic thermal investigation of the zeolites belonging to the natrolite group, using dynamic methods of thermal analysis, is given. Upon

heating and dehydration all members of this group react by a contraction of the lattice along the *a* and *b* axes and often an expansion along the *c* axis, in accordance with the general fibrous structure.

Natrolite shows the highest thermal stability of the group and has a low (α) and a high (β) metaphase. Its isotypes mesolite and scolecite show a mutually resembling thermal behaviour which is very different from that of natrolite. The isotypes thomsonite and gonnardite also show a mutual resemblance with certain aspects of both natrolite and mesolite/scolecite. The relationship of edingtonite with the other members was not reflected by its thermal behaviour. X-ray data of all meta-phases were collected.

With the aid of the DTA inhibited diffusion method pressure-temperature relations of zeolite dehydration reactions have been studied in chapter 5. The Clausius-Clapeyron equation appeared to be applicable and facilitated calculation of thermodynamic parameters of the reactions. For 18 zeolites more than 50 values for the heat of hydration have been calculated of which only a few had to be rejected because of non-equilibrium experimental conditions. From the reaction entropy change, values for the entropy of water in zeolites were calculated. These indicated that at least three types of water can be present in zeolites: 1. crystal water or low-entropy water with a standard entropy of 30–47 J/mole/deg (7–11 cal/mole/deg); 2. zeolitic water or high-entropy water with a standard entropy in the range of 58–72 J/mole/deg (14–17 cal/mole/deg); 3. so-called 'loosely bound' water with a high standard entropy of 58–63 J/mole/deg (14–15 cal/mole/deg).

Low entropy appears to be associated with water molecules occupying 'fixed positions' in the structure whereas high entropy is associated with molecules possessing a higher degree of disorder because they are not coordinated in fixed positions.

SAMENVATTING

Zeolieten vormen een groep mineralen die vanuit geologisch, mineralogisch en technologisch oogpunt van groot belang zijn. Structureel behoren ze tot de tektosilikaten en hebben een z.g. 'open' rooster waarin zich kanalen en holten bevinden die kationen en watermolekulen bevatten. Deze kationen zijn in het algemeen uitwisselbaar terwijl de watermolekulen reversibel kunnen worden verwijderd of vervangen door bepaalde andere molekulen zonder dat het kristalrooster wordt aangetast.

Omdat zeolieten verbreid voorkomen en onder diverse omstandigheden worden gevormd, hebben zij sterk de aandacht getrokken van geologen hetgeen heeft geleid tot de herkenning van de zogenaamde zeolietfacies.

In technologisch opzicht heeft geen mineraalgroep zulke uitgebreide toepassingsmogelijkheden als die der zeolieten. Dit is het gevolg van hun grote fysische stabiliteit en hun specifieke adsorptie eigenschappen. Om deze reden worden zeolieten op grote schaal gesynthetiseerd en dan meestal 'molekulaire zeven' genoemd. In de afgelopen jaren zijn grote en relatief zuivere afzettingen van waardevolle zeolieten ontdekt. Aangezien deze kunnen worden gewonnen voor een fractie van de prijs van synthetische analogen, neemt de belangstelling voor natuurlijke zeolieten snel toe.

Voor veel toepassingen moeten de zeolieten worden geactiveerd door middel van verhitting. Dit heeft dehydratatie tot gevolg wat gepaard kan gaan met ingrijpende, doch in het algemeen reversibele veranderingen in de structuur en afmetingen van de eenheidscel. Het thermisch gedrag van zeolieten is daarom reeds geruime tijd onderwerp van studie. Een kort overzicht hiervan wordt gegeven in hoofdstuk 2. De aanpak blijkt fragmentarisch te zijn geweest waarbij bovendien vaak ondoelmatige methoden werden toegepast. Hierdoor waren de resultaten dikwijls onjuist en/of met elkaar in tegenspraak.

In hoofdstuk 3 wordt het complexe karakter van het dehydratatie proces geanalyseerd. De reactie blijkt volgens één of meer van drie basistypen te verlopen. Type 1 is een duidelijke reactie over een relatief kort temperatuurtraject en gaat gepaard met scherpe piek in de DTA curve en een duidelijke kristallografische transformatie. Type 2 bestaat uit een opeenvolging van kleine dehydratatiestappen wat leidt tot een brede, soms iets onregelmatige DTA piek en zich kristallografisch uit in kleine, stapsgewijze aanpassingen van het rooster. Dehydratatie volgens type 3 geschiedt geleidelijk, zonder enige aanwijsbare onregelmatigheid wat resulteert in een brede regelmatige DTA piek. Het kristalrooster past zich eveneens geleidelijk aan of blijft nagenoeg onveranderd.

De waterdampspanning heeft grote invloed op het dehydratatie evenwicht en dus op de reactietemperatuur. Het blijkt dat het dehydratatieproces zich zo snel kan voltrekken dat de evenwichtstoestand onmiddellijk wordt bereikt. Bij een aantal zeolieten treedt een sterke dehydratatie-rehydratatie hysterese op. Deze is echter niet het gevolg van het niet bereiken van dehydratatie evenwicht, maar van hysterese in de roosterveranderingen.

Het zg. 'loosely held' water dat in chemische analyses wel als H_2O- wordt aangeduid, blijkt niet te zijn geadsorbeerd aan het externe oppervlak van zeolieten, doch in de structurele holten en kanalen.

In hoofdstuk 4 wordt een systematisch thermisch onderzoek van zeolieten behorend tot de natrolietgroep beschreven. Bij verhitting en dehydratatie reageren alle mineralen van deze groep door een samentrekking van het rooster langs de *a* en *b* as en dikwijls een uitrekking langs de *c* as. Dit is in overeenstemming met de vezelstruktuur van deze groep.

Natroliet heeft de grootste thermische stabiliteit en vertoont een lage (α) en hoge (β) metafase. Mesoliet en scoleciet zijn isotypen van natroliet maar hebben een heel ander thermisch gedrag dat onderling wel sterk overeenkomt. De isotypen thomsoniet en gonnardiet vertonen onderling eveneens grote overeenkomst met kenmerken van zowel natroliet als mesoliet/scoleciet. Edingtoniet vertoont een geheel afwijkend thermisch gedrag. Van alle fasen werden de röntgenografische gegevens verzameld.

In hoofdstuk 5 is met behulp van de 'inhibited diffusion' DTA methode de druk-temperatuur relatie van zeoliet-dehydratatiereacties bepaald. Met behulp van de Clausius-Clapeyron vergelijking zijn aan 18 zeolieten de thermodynamische parameters van ruim 50 dehydratatiereacties berekend. Slechts een klein aantal reacties bleek ongeschikt voor deze bepaling omdat geen evenwichtstoestand kon worden bereikt.

Naast berekening van hydratatie-energieën, werden via de reactie-entropieverandering waarden berekend voor de entropie van water in zeolieten. Hieruit bleek, dat tenminste drie soorten water in zeolieten aanwezig kunnen zijn: 1. kristalwater met een lage standaard entropie in de orde van 30–47 J/mol/graad (7–11 cal/mol/graad); 2. zeolitisch water met een hoge standaard entropie in de orde van 58–72 J/mol/graad (14–17 cal/mol/graad); 3. het zg. 'loosely bound' water met een hoge standaard entropie van 58–63 J/mol/graad (14–15 cal/mol/graad).

Een lage entropie van het water blijkt samen te hangen met het innemen van een 'vaste plaats' in het kristalrooster, terwijl een hoge entropie samenhangt met het feit dat watermolekulen niet een vaste plaats in het rooster innemen en daardoor een hogere graad van wanorde bezitten.

APPENDIX 1

X-RAY DATA OF ROOM TEMPERATURE PHASES AND METAPHASES OF ZEOLITES OF THE NATROLITE GROUP

The room temperature phases were measured on Guinier-De Wolff X-ray photographs, whereas the metaphases were measured on Guinier-Lenné X-ray photographs. All room-temperature phase data were computer refined and the cell parameters calculated.

As for the metaphases, thusfar, determination of cell parameters was only successful for α-metanatrolite. This is probably due to a somewhat inferior standardization of the G.L. X-ray photographs which caused errors in 2Θ measurements in the order of 0.05°. The temperature indications are accurate within $\pm$ 5°C; $P_{H_2O} \approx 0.01$ atm.

The specimens are those represented in table 1.1. except for the Kilpatrick edingtonite sample. The two edingtonite specimens are represented in the form of JCPDS cards as they have been submitted to the Joint Committee on Powder Diffraction Standards in this form.

NATROLITE (at 20°C)

Orthorhombic, *Fdd2*, $a = 18.259$, $b = 18.574$, $c = 6.563$

d_{obs}	d_{calc}	*hkl*	*I*	d_{obs}	d_{calc}	*hkl*	*I*
6.53	6.51	220	8	2.271	2.282	800	3
5.89	5.86	111	10		2.281	371	
4.65	4.64	040	6	2.248	2.252	062	5
4.57	4.56	400	5		2.250	280	
4.38	4.37	131	10	2.230	2.231	602	4
4.34	4.34	311	10	2.218	2.216	820	1
4.14	4.14	240	6	2.187	2.186	262	8
4.10	4.10	420	5	2.174	2.170	660	8
3.62	3.62	331	1		2.169	622	
3.25	3.25	440	2	2.041	2.048	840	4
3.18	3.18	151	9	2.036	2.046	313	4
3.14	3.14	511	9		2.040	571	
3.092	3.094	022	10		2.030	750	
3.088	3.088	202	10	1.957	1.957	191	5
2.927	2.931	222	10		1.954	333	
		260		1.929	1.928	911	1
2.882	2.892	620	2	1.879	1.875	153	5
2.851	2.855	351	9		1.873	391	
2.829	2.837	531	9	1.868	1.867	513	5
2.563	2.562	460	4	1.838	1.837	860	1
	2.561	422			1.836	822	
2.552	2.545	640	5	1.819	1.820	2.10.0	2
2.429	2.438	171	6	1.803	1.800	353	5
2.396	2.403	711	6	1.796	1.796	533	4
2.314	2.322	080	2	1.789	1.789	771	4
2.305	2.311	442	5				

Sample: Auvergne, France. Camera: Guinier-De Wolff. Co-Kα rad. $\lambda = 1.7902$ *I*: visual

α-METANATROLITE (at 350°C)

Orthorhombic *Fmmm*, or monoclinic *F2*, $a = 16.320$, $b = 17.098$, $c = 6.445$, $\gamma = 90°$

d_{obs}	d_{calc}	*hkl*	*I*	d_{obs}	d_{calc}	*hkl*	*I*
5.89	5.90	220	10	2.297	2.295	640	1
5.65	5.66	111	9	2.262	2.262	171	3
4.28	4.27	040	3	2.181	2.176	442	4
4.13	4.13	131	7		2.175	711	
4.04	4.04	311	8	2.094	–	n.i.	2
3.78	3.79	240	3	2.019	2.019	622	2
3.68	3.68	420	3	1.996	1.995	133	1
3.36	3.36	331	2	1.985	1.985	313	2
3.02	3.02	022	10		1.984	820	
3.01	3.00	202	10	1.893	1.893	480	1
2.97	2.97	151	4		1.891	264	
2.87	2.87	511	5	1.866	1.871	571	1
2.83	2.83	222	4		1.869	642	
2.72	2.72	600	5	1.807	1.811	191	2
2.69	2.69	260	4		1.808	153	
2.64	2.64	351	6	1.785	1.785	513	2
2.595	2.593	531	6		1.781	082	
	2.592	620		1.711	1.712	533	<1
2.529	2.528	402	<1		1.710	0.10.0	
2.454	2.454	242	4	1.682	1.681	680	1
2.427	2.425	422	3		1.679	662	
2.329	2.336	460	<1				

β-METANATROLITE (at 600°C)

d_{obs}	*I*	d_{obs}	*I*	d_{obs}	*I*
6.16	7	3.08	1	2.32	1
5.66	7	3.04	3	2.30	1
4.39	1	3.01	6	2.22	1
4.09	10	2.85	2	1.99	< 1
3.92	1	2.72	4	1.84	1
3.46	< 1	2.48	2	1.81	< 1
3.11	1				

Sample: Auvergne, France. Camera: Guinier-Lenné. Cu-Kα rad. $\lambda = 1.5405$ *I*: visual

MESOLITE (at 20°C)

Monoclinic $C2$, $a = 56.70$, $b = 6.54$, $c = 18.44$, $\beta = 90°$

d_{obs}	d_{calc}	hkl	I	d_{obs}	d_{calc}	hkl	I
7.78	7.73	402	1	3.07	3.07	006	2
6.60	6.60	602	9		3.06	222	
6.13	6.13	111	4	3.02	3.01	422	1
5.86	5.86	311	10	2.982	2.986	715	2
5.42	5.42	511	4	2.934	2.930	622	10
4.91	4.91	711	1	2.920	2.923	606	2
4.73	4.73	12.0.0	9	2.890	2.883	123	9
4.61	4.61	004	8		2.884	15.1.3	
4.46	4.47	113	1	2.859	2.862	915	10
4.41	4.40	911	9	2.831	2.831	20.0.0	1
	4.39	404			2.823	10.2.1	
4.35	4.36	313	9	2.725	2.724	11.1.5	1
4.21	4.21	12.0.2	6	2.687	2.681	19.1.1	<1
4.16	4.17	513	2	2.674	2.671	17.1.3	<1
4.14	4.14	604	2	2.619	2.620	424	<1
3.95	3.95	11.1.1	1	2.584	2.584	13.1.5	4
3.92	3.92	713	1		2.576	12.0.6	
3.65	3.65	913	3	2.568	2.561	624	4
3.58	3.58	10.0.4	1	2.498	2.491	824	1
3.50	3.50	614	<1	2.473	2.473	21.1.1	5
3.44	–	n.i.	1	2.422	2.423	317	5
3.30	3.31	16.0.2	1	2.362	–	n.i.	1
	3.30	12.0.4		2.323	–	n.i.	2
3.29	–	n.i.	1	2.312	2.314	17.1.5	2
3.23	3.22	15.1.1	9	2.270	2.275	408	5
	3.21	115			2.269	18.2.0	
3.19	3.19	420	1	2.253	–	n.i.	1
3.17	3.17	315	9	2.240	2.239	026	2
3.09	3.09	515	10			608	
		620		2.204	2.200	18.0.6	5
				2.180	2.179	626	5

Sample: Oregon, U.S.A. Camera: Guinier-De Wolff. Co-Kα rad. $\lambda = 1.7902$ I: visual.

METAMESOLITE (at 250°C)

d_{obs}	I	d_{obs}	I	d_{obs}	I
6.43	8	2.93	8	1.796	3
5.82	10	2.85	7	1.778	2
4.62	5	2.82	7	1.747	1
4.49	3	2.57	2	1.729	1
4.31	9	2.55	2	1.719	1
4.31	9	2.44	3	1.689	1
4.12	3	2.39	3	1.673	1
4.06	2	2.22	1	1.642	3
3.60	1	2.20	2	1.627	< 1
3.23	1	2.16	3	1.614	1
3.18	5	2.05	2	1.524	3
3.12	5	1.873	1	1.454	3
3.08	7	1.863	1		

Sample: Oregon, U.S.A. Camera: Guinier-Lenné. Cu-Kα rad. $\lambda = 1.5405$ I: visual.

SCOLECITE (at 20 °C)

Monoclinic[1] *Aa*, $a = 9.77$, $b = 18.95$, $c = 6.52$, $\beta = 108.88°$

d_{obs}	d_{calc}	*hkl*	*I*	d_{obs}	d_{calc}	*hkl*	*I*
6.62	6.62	120	9	2.917	2.916	222	8
5.89	5.87	011	10	2.901	2.900	151	7
5.84	5.83	11$\bar{1}$	10	2.888	2.888	25$\bar{1}$	7
4.74	4.74	040	7	2.880	2.878	231	7
4.62	4.62	200	6	2.858	2.857	33$\bar{1}$	10
4.41	4.41	031	10	2.686	2.686	14$\bar{2}$	2
4.38	4.38	111	10	2.608	2.608	260	1
4.33	4.34	21$\bar{1}$	4	2.586	2.586	042	4
4.22	4.22	140	5		2.584	340	
4.16	4.16	220	4	2.576	2.577	122	4
3.67	3.67	131	2		2.574	24$\bar{2}$	
3.64	3.64	23$\bar{1}$	6	2.554	2.553	32$\bar{2}$	2
3.31	3.31	240	1	2.479	2.479	071	5
3.23	3.23	051	8		2.477	17$\bar{1}$	
	3.22	15$\bar{1}$		2.459	2.460	251	<1
3.19	3.19	211	5	2.447	2.447	35$\bar{1}$	2
3.16	3.16	060	7	2.438	2.438	311	2
		31$\bar{1}$		2.420	2.420	41$\bar{1}$	5
3.084	3.085	002	9	2.369	2.369	080	<1
	3.083	12$\bar{2}$		2.332	2.332	142	1
3.065	3.065	20$\bar{2}$	7	2.321	2.321	171	2
2.989	2.989	160	3	2.314	2.314	27$\bar{1}$	2
2.934	2.934	022	10			34$\bar{2}$	
	2.932	320			2.312	400	
				2.295	2.295	180	2
				2.291	2.291	331	1
				2.269	2.269	16$\bar{2}$	5

Sample: Teigarhorn, Iceland. Camera: Guinier-De Wolff. Co-Kα rad. $\lambda = 1.7902$ *I*: visual.

[1] The data also fitted monoclinic *Cc* with $a = 18.50$, $b = 18.95$, $c = 6.52$, $\beta = 90.61°$. Space group *Aa* was chosen because of arguments put forward by SMITH and WALLS (1971).

METASCOLECITE (at 300 °C)

d_{obs}	I	d_{obs}	I	d_{obs}	I
6.53	10	2.66	2	2.364	1
5.88	10	2.61	2	2.355	1
5.81	6	2.57	2	2.314	< 1
4.71	9	2.56	2	2.297	1
4.61	1	2.54	2	2.288	1
4.54	8	2.48	2	2.248	2
4.43	9	2.45	2	2.222	2
4.33	10	2.42	2	2.205	1
4.31	10	2.39	4	2.181	4
4.18	7	3.08	4	2.167	2
4.09	6	2.97	1	2.155	< 1
3.64	1	2.94	7	2.146	< 1
3.61	2	2.91	1	2.094	1
3.27	2	2.90	5	2.042	3
3.24	3	2.86	6	1.998	< 1
3.19	4	2.84	3	1.961	2
3.14	6	2.82	6	1.941	< 1
3.11	3				

Sample: Teigarhorn, Iceland. Camera: Guinier-Lenné. Cu-Kα rad. $\lambda = 1.5405$ I: visual.

THOMSONITE (at 20 °C)

Orthorhombic *Pnma*, $a = 13.07$, $b = 13.09$, $c = 13.23$.

d_{obs}	d_{calc}	*hkl*	*I*	d_{obs}	d_{calc}	*hkl*	*I*
9.26	9.31	011	3	2.858	2.860	241	10
	9.30	101			2.859	412	
6.62	6.61	002	10		2.855	421	
6.54	6.55	020	8	2.795	2.796	332	5
	6.53	200		2.679	2.679	242	10
5.90	5.90	102	10		2.674	422	
5.38	5.38	112	6		2.585	134	
4.66	4.66	022	9	2.583	2.582	314	8
	4.65	202			2.579	143	
4.63	4.63	220	9		2.575	413	
4.38	4.39	122	8	2.572	2.572	051	<1
	4.38	212			2.569	341	
4.14	4.15	031	8	2.563	2.564	501	<1
	4.14	301		2.445	2.445	234	<1
3.98	3.98	113	<1		2.444	324	
3.96	3.95	131	<1		2.435	342	
3.79	3.79	222	3	2.433	2.434	250	7
3.51	3.51	132	10		2.433	432	
		312			2.431	502	
	3.50	231			2.393	251	
		321		2.389	2.390	512	<1
3.28	3.28	040	4		2.388	521	
	3.27	400		2.332	2.328	044	1
3.21	3.21	104	9	2.314	2.314	440	1
3.18	3.18	232	8	2.291	2.292	144	3
		322			2.288	414	
3.09	3.10	303	1	2.282	2.284	252	<1
	3.09	141			2.279	441	
	3.08	411				522	
2.951	2.952	024	9	2.256	2.256	334	9
	2.950	204			2.254	053	
2.938	2.937	042	3	2.223	2.221	153	1
2.925	2.930	240	4	2.204	2.204	006	1
		402		2.192	2.193	244	9
	2.924	420			2.190	424	
2.866	2.865	142	10	2.178	2.178	600	8
				2.136	2.138	235	<1
					2.137	325	

Sample: Kilpatrick, Scotland. Camera: Guinier-De Wolff. Co-Kα rad. $\lambda = 1.7902$ *I*: visual.

METATHOMSONITE-I (at 310 °C)

d_{obs}	I	d_{obs}	I	d_{obs}	I
9.21	1	3.95	1	2.42	4
6.80	5	3.92	1	2.24	4
6.65	3	3.77	1	2.21	1
6.54	5	3.49	9	2.12	1
5.84	7	3.18	8	2.07	1
5.36	5	2.93	4	1.930	1
5.33	5	2.92	2	1.916	< 1
4.61	10	2.85	3	1.870	1
4.35	8	2.66	4	1.796	2
4.14	7	2.57	2		

METATHOMSONITE-II (at 350 °C)

d_{obs}	I	d_{obs}	I	d_{obs}	I
10.0	< 1	4.65	2	2.88	1
9.72	< 1	4.56	2	2.83	1
9.21	< 1	4.40	1	2.77	< 1
9.11	8	4.33	10	2.67	6
8.18	1	4.06	7	2.65	1
6.94	3	3.91	1	2.59	1
6.70	1	3.88	1	2.51	1
6.62	8	3.76	3	2.44	1
6.50	8	3.50	7	2.42	1
6.37	7	3.16	2	2.41	1
5.75	9	3.13	3	2.37	< 1
5.35	8	3.11	7	2.35	1
5.27	5	2.90	7		

Sample: Kilpatrick, Scotland. Camera: Guinier-Lenné. $\lambda = 1.5405$ I: visual. Cu-Kα rad.

GONNARDITE (at 20 °C, preheated to 150 °C)

Orthorhombic *Pnnn*, $a = 13.06$, $b = 13.24$, $c = 6.58$

d_{obs}	d_{calc}	*hkl*	*I*	d_{obs}	d_{calc}	*hkl*	*I*
6.60	6.62	020	5	2.337	2.334	042	1
5.89	5.89	011	8	2.268	2.262	350	2
	5.88	101		2.253	2.256	332	3
5.37	5.37	111	1		2.248	530	
4.64	4.65	220	5	2.203	2.207	060	5
4.40	4.40	121	8		2.198	242	
4.37	4.37	211	1	2.189	2.192	441	2
4.18	4.18	130	2		2.188	422	
4.13	4.13	310	1	2.176	2.176	600	<1
3.78	3.80	221	<1	2.122	2.127	531	<1
3.50	3.50	311	4	2.067	2.067	620	3
3.27	3.26	400	<1		2.066	161	
3.20	3.20	231	10	1.986	1.984	223	<1
3.18	3.18	321	2	1.973	1.973	621	3
3.12	3.10	112?	9	1.965	1.965	033	<1
2.96	2.95	240	10	1.957	1.955	522	<1
		022		1.943	1.943	133	1
2.94	2.94	202	6		1.938	313	
2.88	2.88	141	9	1.890	1.886	361	4
2.86	2.86	411	5	1.881	1.881	233	2
2.68	2.68	421	5		1.879	323	
2.595	2.594	150	6	1.826	1.828	460	1
2.579	2.586	132	4	1.817	1.815	602	6
	2.575	312				162	
2.457	2.455	051	4	1.809	1.812	143	2
2.430	2.427	501	1		1.804	413	
2.386	2.388	511	1				

Sample: Auvergne, France. Camera: Guinier-De Wolff. Co-Kα rad. $\lambda = 1.7902$ *I*: visual.

METAGONNARDITE-I (at 220 °C)

d_{obs}	I	d_{obs}	I	d_{obs}	I
6.63	3	2.96	7	2.19	6
6.52	8	2.95	2	2.16	2
5.91	10	2.90	1	2.07	2
4.65	3	2.85	10	1.940	1
4.60	8	2.66	4	1.887	3
4.38	10	2.58	6	1.812	4
4.11	7	2.42	6	1.796	< 1
3.50	5	2.32	2	1.786	< 1
3.20	1	2.30	1	1.743	1
3.17	9	2.25	3	1.702	2
3.13	7				

METAGONNARDITE-II (at 340 °C)

d_{obs}	I	d_{obs}	I
6.58	10	3.49	5
6.13	2	3.16	7
5.82	5	2.96	1
5.64	3	2.92	4
5.32	3	2.91	1
4.60	8	2.85	4
4.35	7	2.83	4
4.29	5	2.65	7
4.17	6	2.56	< 1
4.13	6	2.42	3
3.76	1		

Sample: Auvergne, France. Camera: Guinier-Lenné. Cu-Kα rad. $\lambda = 1.5404$ I: visual.

METAEDINGTONITE (at 330 °C)

d_{obs}	I	d_{obs}	I	d_{obs}	I
7.26	2	2.95	4	2.016	1
6.59	10	2.73	8	1.984	< 1
5.46	1	2.72	8	1.942	5
5.41	3	2.60	8	1.885	< 1
4.76	8	2.44	< 1	1.879	< 1
4.70	9	2.34	< 1	1.830	2
4.26	< 1	2.28	4	1.819	2
3.86	< 1	2.27	4	1.792	< 1
3.61	< 1	2.24	4	1.785	< 1
3.57	10	2.18	3	1.766	< 1
3.36	2	2.17	2	1.755	< 1
3.28	2	2.13	< 1	1.678	1
3.10	6	2.116	3	1.641	4
3.01	5	2.078	2	1.624	< 1
2.99	4	2.050	2	1.586	1

Sample: Böhlet, Sweden. Camera: Guinier-Lenné. Cu-Kα rad. $\lambda = 1.5404$ I: visual.

d	6.51	4.70	3.59	6.78	$BaAl_2Si_3O_{10}\cdot 4H_2O$
I/I_1	100	70	65	6	Barium Aluminium Silicate Hydrate — Edingtonite

Rad. CoKα λ 1.7902 Filter Guinier Dia. 114.6
Cut off 50 Å I/I_1 Photometer
Ref. Technisch Physische Dienst, Delft

Sys. Orthorhombic S.G. $P2_12_12$ (18)
a_0 9.534 b_0 9.649 c_0 6.507 A 0.9881 C 0.6744
α 90.00 β 90.00 γ 90.00 Z 2 Dx 2.814
Ref. Ibid

$\epsilon\alpha$ 1.5405(Na) $n\omega\beta$ 1.5528 $\epsilon\gamma$ 1.5569 Sign -
2V 53°52' D 2.777 mp Color White, grayish
Ref. Hey, Min. Mag. 23 483 (1934)

Mineral from Böhlet
To replace 12-577

d A	I/I_1	hkl	d A	I/I_1	hkl
6.78	6	110	2.855	2	301
6.51	100	001	2.760	55	131
5.37	60	101,011	2.740	55	311
4.82	55	020	2.696	<1	022
4.77	30	200	2.687	<1	202
4.70	70	111	2.665	2	230
4.30	6	120	2.655	4	320
4.27	4	210	2.595	25	122
3.876	4	021	2.589	30	212
3.846	2	201	2.466	4	231
3.590	65	121	2.457	4	321
3.572	55	211	2.410	2	040
3.391	12	220	2.383	<1	400
3.254	10	002	2.347	2	222
3.083	20	012,102	2.287	20	032
3.048	14	130	2.275	16	302
3.019	14	310	2.260	20	330,041
3.007	10	221	2.258	<1	401
2.954	30	112	2.224	<1	132
2.883	2	031	2.212	<1	312

d					
I/I_1					

Rad. λ Filter Dia.
Cut off I/I_1
Ref.

Sys. S.G.
a_0 b_0 c_0 A C
α β γ Z Dx
Ref.

$\epsilon\alpha$ $n\omega\beta$ $\epsilon\gamma$ Sign
2V D mp Color
Ref.

d A	I/I_1	hkl	d A	I/I_1	hkl
2.201	10	141	1.845	4	341
2.180	8	411	1.837	4	431
2.168	4	003	1.828	12	223,501
2.152	6	240	1.817	2	151
2.136	16	331,420			
2.116	6	013,103			
2.067	14	113			
2.057	4	322			
2.043	2	241			
2.031	4	421			
1.979	2	023			
1.975	2	203			
1.936	8	123,042			
		213			
1.922	<1	340,402			
1.915	<1	430			
1.899	4	142			
1.886	4	412			
1.871	2	510			
1.857	<1	332			
1.850	2	051			

d	3.576	6.51	2.741	6.77	$BaAl_2Si_3O_{10}.4H_2O$
I/I_1	100	80	75	6	Barium Aluminium Silicate Hydrate — Edingtonite

Rad. CoKα λ 1.7902 Filter Guinier Dia. 114.6
Cut off 50Å I/I_1 Photometer
Ref. Technisch Physische Dienst, Delft

Sys. Orthorhombic S.G. $P2_12_12$ (18)
a_0 9.570 b_0 9.570 c_0 6.510 A 1.0000 C 0.6803
α 90.00 β 90.00 γ 90.00 Z 2 Dx 2.814
Ref. Ibid

εα nωβ εγ Sign
2V D mp Color
Ref.

Mineral from Kilpatrick
Pseudo-tetragonal (optically biaxial)

d A	I/I_1	hkl	d A	I/I_1	hkl
6.77	6	110	2.344	2	222
6.51	80	001	2.278	30	032
5.38	60	011	2.246	16	041
4.79	50	020	2.215	4	132
4.69	50	111	2.185	14	141
4.28	8	120	2.170	2	003
3.856	2	021	2.139	8	240
3.576	100	121	2.130	8	331
3.384	8	220	2.117	4	013
3.255	8	002	2.067	8	113
3.081	16	012	2.057	4	232
3.027	25	130	2.033	6	241
2.998	10	221	1.976	6	023
2.931	25	112	1.936	6	123
2.863	2	031	1.914	2	050,340
			1.890	6	142
2.741	75	131	1.877	2	150
2.651	4	230	1.852	2	332
2.589	45	122	1.836	10	051,341
2.456	4	231	1.826	8	223
2.392	2	040			

d					
I/I_1					

Rad. λ Filter Dia.
Cut off I/I_1
Ref.

Sys. S.G.
a_0 b_0 c_0 A C
α β γ Z Dx
Ref.

εα nωβ εγ Sign
2V D mp Color
Ref.

d A	I/I_1	hkl	d A	I/I_1	hkl
1.803	4	151			
1.777	2	250			
1.764	6	133			
1.714	2	251			
1.692	4	440			
1.680	2	233			
1.650	14	052,342			
1.644	2	350			
1.627	6	004,152			
1.609	2	043			
1.596	4	060			
1.584	4	145,114			
1.560	4	252			
1.524	8	243,124			
1.513	6	260			
1.502	4	442			
1.475	2	261			
1.466	2	224,352			
1.435	10	053,062			
		134,343			

APPENDIX 2

A PRESSURE JAR FOR THE DUPONT 990 DTA CELL-BASE MODULE

In order to extend the working pressure range of the ordinary DuPont 990 DTA cell-base module to pressures greater than 1 atmosphere, a special jar was designed and made.[1]

The jar was constructed from a 170 mm long brass pipe, 1.5 mm thick by 75 mm diameter. One end was sealed by soldering into it an exactly fitting 5 mm thick brass lid. The other end was fitted with an 8 mm thick soldered neck-flange of 120 mm in which a groove was made for the same rubber sealing ring used for the standard glass jars. The jar was attached to the cell base-plate (as distinct from the cell-base module) with six 5 mm brass cap screws. This base-plate was attached more firmly to the cell-base module with an additional four cap screws (see fig. 1). The original foam-rubber gasket situated between the base-plate and the cell-base module was not sufficiently pressure-proof and had to be replaced by a solid rubber gasket made from a motor-car tube. Pressure was supplied from a nitrogen gas cylinder using clamps on all tubing connections. The device was tested up to 6 atm. pressure.

[1] The skilful making of the jar by Messrs. A. E. and T. JANSEN of the Physics Department is gratefully acknowledged.

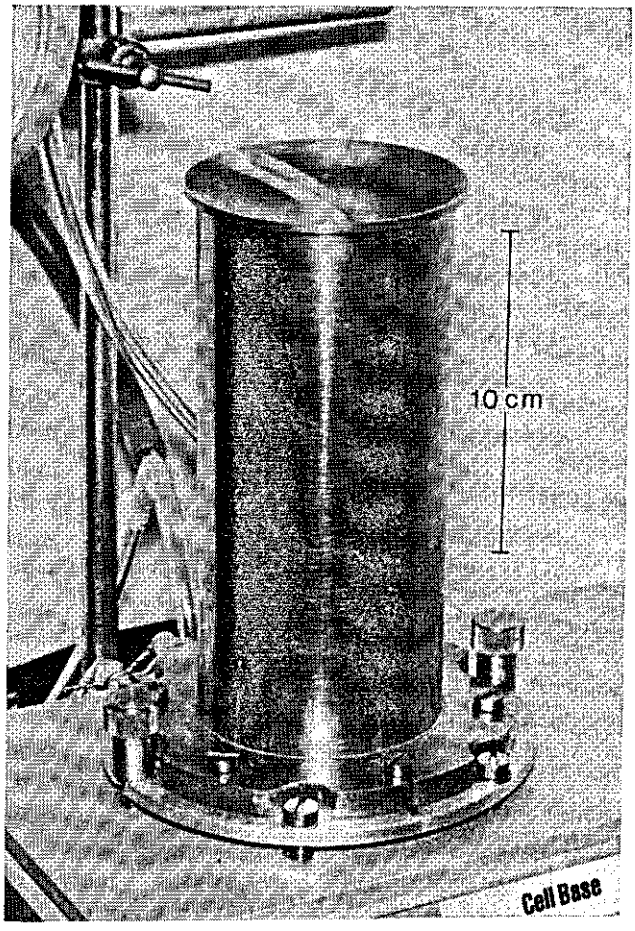

FIG. 1. Pressure jar for DuPont 990 cell-base module shown in position. Note the extra screws connecting the cell base-plate with the module.

ACKNOWLEDGEMENTS

This work was performed at the Department of Soil Science and Geology of the Agricultural University at Wageningen, The Netherlands.

Thanks are due to Dr. L. VAN DER PLAS for suggesting zeolites as a field of study and for his interest and criticism during the preparation of this thesis.

The instructive discussions with Mr. W. NORDE of the Dept. of Physical and Colloid Chemistry were much appreciated. Prof. Dr. J. LYKLEMA of the same department critically read some parts of the manuscript and provided valuable comments.

The enthousiastic assistance of the post-graduate students F. J. C. BLOK and J. P. VAN STAVEREN is gratefully acknowledged.

Special thanks are due to Mr. J. W. VISSER of Technisch Fysische Dienst and Technological University at Delft, for his willingness to make the many crystallographic computations.

The assistance of the following persons during the final stage of the preparation of the manuscript is acknowledged: Mr. C. BERRYMAN for removing most of the grammatical weeds, Mr. G. BUURMAN, Mr. O. D. JERONIMUS and Mr. P. G. M. VERSTEEG for preparing the diagrams, Mr. Z. VAN DRUUTEN for the photographical work and Miss A. BOUTER for typing and retyping the manuscript.

The author is indebted to a large number of persons and institutes who kindly donated mineral specimens used during this study: AKZO Chemie, Amsterdam; Dr. A. ALIETTI; Prof. R. M. BARRER; Prof. D. S. COOMBS; Dr. R. E. CORCORAN; Mr. J. P. COUTURIÉ; Dept. of Geology, University of Utrecht; Dr. K. HARADA; Dr. R. L. HAY; Mr. J. J. VAN KEMPEN; Dr. H. NAIRIS; Dr. O. V. PETERSEN; Dr. D. P. ROELOFSEN; Dr. Y. SEKI; Dr. E. M. TAYLOR; Mr. J. C. WHITE; Prof. W. S. WISE; Dr. P. C. ZWAAN.

The author is particularly grateful to The National Museum of Geology and Mineralogy at Leiden, for putting its entire collection of zeolites at his disposal.

REFERENCES

AIELLO, R., R. M. BARRER, J. A. DAVIES and I. S. KERR (1970) Molecule sieving in relation to cation type and position in unfaulted offretite. Trans. Farad. Soc. **66**: 1610–1617.

ALBERTI, A. (1972) On the crystal structure of the zeolite heulandite. Tschermaks Min. Petr. Mitt. **18**: 129–146.

AMES, L. L. (1961) Cation sieve properties of the open zeolites chabazite, mordenite, erionite and clinoptilolite. Amer. Miner. **46**: 1120–1131.

AMES, L. L. (1964) Some zeolite equilibria with alkali metal cations. Amer. Miner. **49**: 127–145.

AMES, L. L. (1967) Zeolitic removal of ammonium ions from agricultural and other waste waters. Proc. 13th Pacific N.W. Industr. Waste Conf. 1967; Wash. State Univ.

AUMENTO, F. (1965) Thermal transformations of selected zeolites and related hydrated silicates. Ph. D. thesis, Dept. of Geology, Dalhousie Univ. Halifax, N.S. Canada.

AUMENTO, F. (1966) Thermal transformations of stilbite. Can. J. Earth Sc. **3**: 351–366.

BAIN, R. W. (1964) The Steam Tables. Dept. Sci. Ind. Res., National Eng. Lab., London.

BALDAR, N. A. and L. D. WHITTIG (1968) Occurrence and synthesis of soil zeolites. Soil Sci. Soc. Amer. Proc. **32**: 235–238.

BALGORD, W. D. and R. ROY (1973) Crystal chemical relationships in the analcite family II. Influence of temperature and P_{H_2O} on structure. In: Molecular Sieves, Adv. in Chem. Series **121**: 189–199.

BARRER, R. M. (1947) Molecular sieve action at low temperatures. Nature **159**: 508.

BARRER, R. M. (1958) Crystalline ion exchangers. Proc. Chem. Soc. **1958**: 99–113.

BARRER, R. M. and D. A. LANGLEY (1958) Reactions and stability of chabazite-like phases. J. Chem. Soc. (London) **1958**: 3804–3825.

BARRER, R. M. (1964) Molecular sieves. Endeavour **XXIII**: 122–130.

BARRER, R. M. (1973) Suggestions for chemical nomenclature of synthetic and natural zeolites. Mimeographed report presented at Third Int. Conf. Mol. Sieve Zeolites (Zürich).

BARRER, R. M. and D. A. IBBITSON (1944) Kinetics of formation of zeolitic solid solutions. Trans. Farad. Soc. **40**: 206–216.

BARRER, R. M. and I. S. KERR (1959) Intracrystalline channels in levynite and some related zeolites. Trans. Farad. Soc. **55-II**: 1915–1923.

BARTL, H. (1970) Strukturverfeinerung von Leonhardit, $Ca(Al_2Si_4O_{12}) \cdot 3H_2O$ mittels Neutronenbeugung. Neues Jahrb. Mineral. (Monatshefte) **1967**: 298–310.

BAUR, W. H. (1964) On the cation and water positions in faujasite. Amer. Miner. **49**: 697–704.

BEATTIE, I. R. (1954) The structure of analcite and ion-exchanged forms of analcite. Acta Cryst. **7**: 357–359.

BERGERHOFF, G., W. H. BAUER and W. NOWACKI (1958) Ueber die Kristallstruktur des Faujasites. Neues Jahrb. Min. (Monatsh.) **1958**: 193–200.

BOLES, J. R. (1972) Composition, optical properties, cell dimensions and thermal stability of some heulandite group minerals. Amer. Miner. **57**: 1463–1493.

BREGER, I. A., J. C. CHANDLER and P. ZUBOVIC (1970) An infrared study of water in heulandite and clinoptilolite. Amer. Miner. **55**: 825–839.

BURNHAM, C. W., J. R. HOLLOWAY and N. F. DAVIS (1969) Thermodynamic properties of water to 1000°C and 10,000 bars. Geol. Soc. Amer. Spec. Paper **132**.

CARROLL, B. and E. P. MANCHE (1972) Kinetic analysis of chemical reactions for non-isothermal procedures. Thermochim. Acta **3**: 449–459.

COOMBS, D. S. (1952) Cell size, optical properties and chemical composition of laumontite and leonhardite. Amer. Miner. **37**: 812–830.

COOMBS, D. S. (1970) Present status of the zeolite facies. Second Int. Conf. Mol. Sieve Zeolites (Worcester) Preprints: 556–566.

COOMBS, D. S., A. J. ELLIS, W. S. FYFE and A. M. TAYLOR (1959) The zeolite facies, with comments on the interpretation of hydrothermal syntheses. Geochim. Cosmochim. Acta **17**: 53–107.

CRONSTEDT, A. F. (1756) Rön och beskrifning om en obekant barg art, som kallas zeolites. Kongl. Vetenskaps Academicus Handlingar **17**: 120–123.
DAMOUR, A. (1857) Recherches sur les propriétés hygroscopiques des mineraux de la famille des zéolites. Compt. Rend. Acad. Sci. **44**: 975–980.
DEER, W. A., R. A. HOWIE and J. ZUSSMAN (1963) Rock forming minerals, Vol. **4** Framework Silicates. Longmans, Green and Co, London.
DEFFEYES, K. S. (1959) Zeolites in sedimentary rocks. J. Sed. Pet. **29**: 602–609.
DEFFEYES, K. S. (1967) Natural zeolite deposits of potential commercial use. Uncorr. preprint Soc. Chem. Industry.
DOELTER, C. (1890) Ueber die künstliche Darstellung und die chemische Constitution einiger Zeolithe. Neues Jahrb. Min. **1**: 118–139.
EICHHORN, H. (1858) Ueber die Einwirkung verdünnter Salzlösungen auf Silikat. Poggendorffs Annalen der Physik **105**: 126–133.
EISENBERG, D. and W. KAUZMANN (1969) The structure and properties of water. Oxford Univ. Press, Ely House, London.
FANG, J. H. (1963) Cell dimensions of dehydrated natrolite. Amer. Miner. **48**: 414–417.
FISCHER, K. F. (1963) The crystal structure determination of the zeolite gismondite. Amer. Miner. **48**: 664–672.
FISCHER, K. F. and V. SCHRAMM (1970) Crystal structure of gismondite, a detailed refinement. Second Int. Conf. Mol. Sieve Zeolites (Worcester) Preprints: 508–516.
FISHER, J. R. and E-AN ZEN (1971) Thermochemical calculations from hydrothermal phase equilibrium data and the free energy of H_2O. Am. J. Sci. **270**: 297–314.
FOSTER, MARGARET D. (1965) Studies of the zeolites. U.S. Geol. Surv. Prof. Paper **504-D**, E.
FOSTER, W. R. and H. C. Lin (1969) Studies in the system BaO-Al_2O_3-SiO_2 II. The binary system celsian – silica. Amer. J. Sci. **267-A**: 134-144.
FREEMAN, E. S. and B. CARROLL (1958) The application of thermoanalytical techniques to reaction kinetics. The thermogravimetric evaluation of the kinetics of the decomposition of calcium oxalate monohydrate. J. Phys. Chem. **62**: 394–397.
FRIEDEL, G. (1896) Sur quelques propriétés nouvelles des zéolithes. Bull. Soc. franç. Min., Paris, **19**: 94–118.
FYFE, W. S., F. TURNER and J. VERHOOGEN (1959) Metamorphic reactions and metamorphic facies. Geol. Soc. Amer. Memoir **73**.
GALLI, E. (1971) Refinement of the crystal structure of stilbite. Acta Cryst. **B27**: 833–841.
GANS, R. (1915) Die Karakterisierung des Bodens nach der molekularen Zusammensetzung des durch Salzsäure zersetzlichen silikatischen Anteiles (der zeolithischen Silikaten). Jahrb. d. Preuss. Geol. Landesanstalt **35 I**, 219–255.
GARD, J. A. and H. F. W. TAYLOR (1958) An investigation of two new minerals: rhodesite and mountainite. Min. Mag. **31**: 611–623.
GARD, J. A. and J. M. TAIT (1973) Refinement of the crystal structure of erionite. Third Int. Conf. Mol. Sieve Zeolites, Paper **102** (Preprint).
GARN, P. D. (1965) Thermoanalytical methods of investigation. Acad. Press, New York, London.
GARN, P. D. and G. D. Anthony (1967) The questionable kinetics of kaolin dehydration. J. Therm. Anal. **1**: 29–33.
GARRELS, R. M. and C. L. CHRIST (1965) Solutions, minerals, and equilibria. Harper and Row, New York.
GOTTARDI, G., A. ALIETTI and L. POPPI (1973) The behaviour on heating of the zeolites with heulandite structure. Third Int. Conf. Mol. Sieve Zeolites, Paper **121** (Preprint).
GRANGE, M.-H. (1964) Critère pour l'identification d'eau zéolitique dans les hydrates en analyse thermique différentielle et en thermogravimétrie. C. R. Acad. Sc. Paris, **259** Groupe 8: 3277–3280.
HARADA, K., S. IWAMOTO and K. KIHARA (1967) Erionite, phillipsite and gonnardite in the amygdales of altered basalt from Mazé, Niigata Prefecture, Japan. Amer. Miner. **52**: 1785–1794.
HAY, R. L. (1966) Zeolites and zeolitic reactions in sedimentary rocks. Geol. Soc. Amer. Spec.

Paper 85.
HELFFERICH, F. (1964) A simple identification reaction for zeolites (molecular sieves). Amer. Miner. 49: 1752–1754.
HERSCH, C. H. (1961) Molecular sieves. Reinhold Publ. Corp., Chapman and Hall, Ltd. London.
HEY, M. H. (1932a) Studies on the zeolites. Part II. Thomsonite (including faroelite) and gonnardite. Min. Mag. 23: 51–125.
HEY, M. H. (1932b) Studies on the zeolites. Part III. Natrolite and metanatrolite. Min. Mag. 23: 243–289.
HEY, M. H. (1933) Studies on the zeolites. Part V. Mesolite. Min. Mag. 23: 421–447.
HEY, M. H. (1934) Studies on the zeolites. Part VI. Edingtonite. Min. Mag. 23: 483–494.
HEY, M. H. (1935) Studies on the zeolites. Part VIII. A theory of the vapour pressure of the zeolites, and of the diffusion of water or gases in a zeolite crystal. Min. Mag. 24: 99–130.
HEY, M. H. (1936) Studies on the zeolites. Part IX. Scolecite and metascolecite. Min. Mag. 24: 227–253.
HEY, M. H. and F. A. BANNISTER (1934) Clinoptilolite, a silica-rich variety of heulandite. Min. Mag. 23: 536–559.
HINTZE, C. (1897) Handbuch der Mineralogie, 2. Band. Verlag Von Veit & Co, Leipzig.
HOOVER, D. L. (1969) Genesis of zeolites, Nevada Test Site. Geol. Soc. Amer. Memoir 110: 275–284.
HOROWITZ, H. H. and G. METZGER (1963) A new analysis of thermogravimetric traces. Anal. Chem. 35: 1464–1468.
HOSS, H. and R. ROY (1960) Zeolite studies III: On natural phillipsite, gismondite, harmotome, chabazite and gmelinite. Beitr. Mineral. Petrogr. 7: 389–408.
IJIMA, A. and K. HARADA (1968) Authigenic zeolites in zeolitic palagonite tuffs on Oahu, Hawaii. Amer. Miner. 54: 182–197.
JACOBS, T. (1958) Kinetics of the thermal dehydration of kaolinite. Nature 182: 1086–1087.
KISSINGER, H. E. (1957) Reaction kinetics in differential thermal analysis. Anal. Chem. 29: 1702–1706.
KOIZUMI, M. (1953) The differential thermal analysis curves and the dehydration curves of zeolites. Min. J. (Japan) 1: 36–47.
KOIZUMI, M. (1958) On zeolitic water. Science Reports no. 7. Inst. Geol. Sci., Osaka University, Japan.
KOIZUMI, M. and R. KIRIYAMA (1953) Structural changes of some zeolites due to their thermal dehydrations. Scientific Rep. no. 2. Inst. Geol. Sci., North College, Osaka Univ.
KOIZUMI, M. and R. ROY (1960) Zeolite studies. I. Synthesis and stability of the calcium zeolites. J. Geol. 68: 41–53.
KOSSOWSKAYA, A. G. (1973) Genetic associations of sedimentary zeolites in the Soviet Union. Molecular Sieves, Adv. in Chem. Series 121: 200–208.
KRAUSKOPF, K. B. (1967) Introduction to geochemistry. Mc. Graw Hill Book Cy., New York.
LATIMER, W. M. (1951) Methods of estimating the entropy of solid compounds. Am. Chem. Soc. J. 73: 1480–1482.
LEE, H. (1973) Applied aspects of zeolite adsorbents. Molecular Sieves, Adv. in Chem. 121: 311–318.
LEVIN, E. M., C. R. ROBBINS and H. F. MCMURDIE (1969) Phase diagrams for ceramists (2nd ed.). The Amer. Ceram. Soc., Columbus, Ohio: 181–184.
MACKENZIE, R. C., C. J. KEATCH, D. DOLLIMORE, J. A. FORRESTER, A. A. HODGSON and J. R. REDFERN (1972) Nomenclature in thermal analysis-II. Talanta 19: 1079–1081.
MARCILLY, C. (1969) Classification et structure des zéolites. Revue de l'Inst. Franc. du Petrole et Ann. des Combust. Liq. XXIV: 657–677.
MASON, B. and L. B. SAND (1960) Clinoptilolite from Patagonia. The relationship between clinoptilolite and heulandite. Amer. Miner. 45: 341–350.
MCADIE, H. G. (1971) Thermal analysis standards. Need and realization. J. Therm. Anal. 3: 79–102.
MEIER, W. M. (1960) The crystal structure of natrolite. Zeit. Krist. 113: 430–444.

MEIER, W. M. (1961) The crystal structure of mordenite (ptilolite). Zeit. Krist. **115**: 439–450.
MEIER, W. M. (1968) Zeolite Structures. S.C.I. Monograph. Mol. Sieves: 10–27.
MERCER, B. W., L. L. AMES, C. J. TONHILL, W. J. VAN SLYKE and R. B. DEAN (1969) Ammonia removal from secondary effluents by selective ion exchange. 42nd Ann. Conf. Water Poll. Control Federation, Dallas, Oct. 5–10, 1969 (Mimeograph).
MERKLE, A. B. and M. SLAUGHTER (1968) Determination and refinement of the structure of heulandite. Amer. Miner. **53**: 1120–1138.
MILLIGAN, W. O. and H. B. WEISER (1937) The mechanism of the dehydration of zeolites. J. Phys. Chem. **41**: 1029–1040.
MINACHEV, KH. and YA. I. ISAKOV (1973) Catalytic properties of zeolites – A general review. In: Molecular Sieves, Adv. in Chem. Series **121**: 451–460.
MORIE, G. P., T. A. POWERS and C. A. GLOVER (1972) Evaluation of thermal analysis equipment for the determination of vapor pressure and heat of vaporization. Thermochim. Acta **3**: 259–269.
MOURANT, A. E. (1933) The dehydration of thomsonite. Min. Mag. **23**: 371–375.
MUMPTON, F. A. (1960) Clinoptilolite redefined. Amer. Miner. **45**: 351–369.
MUMPTON, F. A. and R. A. SHEPPARD (1972) Zeolites. Geotimes, March 1972: 16–18.
ORVILLE, P. M. and H. J. GREENWOOD (1965) Determination of ΔH of reaction from experimental pressure-temperature curves. Amer. J. Sci. **263**: 678–683.
PASSAGLIA, E. (1970) The crystal chemistry of chabazites. Amer. Miner. **55**: 1278–1301.
PAULING, L. (1930) The structure of some sodium and calcium aluminosilicates. Proc. Nat. Acad. Sci. **16**: 453–459.
PEACOR, D. R. (1973) High-temperature, single-crystal X-ray study of natrolite. Amer. Miner. **58**: 676–680.
PÉCSI-DONÁTH, É. (1962) Investigation of the thermal decomposition of zeolites by the DTA method. Acta Geol. Hung. **6**: 429–442.
PÉCSI-DONÁTH, É. (1965) On the individual properties of some Hungarian zeolites. Acta Geol. Hung. **9**: 235–257.
PÉCSI-DONÁTH, É. (1966a) On the relationship between lattice structure and 'zeolite water' in gmelinite, heulandite and scolecite. Acta Miner. Petr. **17**: 143–158.
PÉCSI-DONÁTH, É. (1966b) Extensive studies on the determination of the relation between structure and water retention in phillipsite and gonnardite. Annales, Univ. Budapest, Geol. Sect. **9**: 109–121 (in Russian).
PÉCSI-DONÁTH, É. (1968) Some contributions to the knowledge of zeolites. Acta Miner. Petr. **18**: 127–141.
PENG, C. J. (1955) Thermal analysis study of the natrolite group. Amer. Miner. **40**: 834–856.
PUTZER, D. (1969) Impulsspektrometrische Untersuchung der Protonenspinresonanz des zeolithisch gebundenen Wassers an Gismondin. Doctoral thesis Johann Wolfgang Goethe-Universität, Frankfurt am Main, BRD.
RESING, H. A. and J. K. THOMPSON (1970) NMR relaxation of water in zeolite 13-X. Second Int. Conf. Mol. Sieve Zeolites, (Worcester) Preprints: 770–775.
RINALDI, R., J. J. PLUTH and J. V. SMITH (1973) Refinement of crystal structure of natural K, Ca phillipsite. Third Int. Conf. Mol. Sieve Zeolites, Paper **103** (Preprint).
ROBIE, R. A. and D. R. WALDBAUM (1968) Thermodynamic properties of minerals and related substances at 298.15 K (25.0°C) and one atmosphere (1.013 bars) pressure and at higher temperatures. U.S. Geol. Survey Bull. **1259**.
ROELOFSEN, D. P. (1972) Molecular sieve zeolites-Properties and applications in organic synthesis. Ph. D. thesis, Technical Univ. Delft. Delftsche Uitgeversmaatschappij N.V. Delft, The Netherlands.
SAHA, P. (1959) Geochemical and X-ray investigation of natural and synthetic analcites. Amer. Miner. **44**: 300–313.
SCHRAMM, V. (1973) Refinement of laumontite by DLS- and least-squaresmethods. Third Int. Conf. Mol. Sieve Zeolites, Paper **101** (Preprint).
SCHRAMM, V. and K. F. FISCHER (1970) Refinement of the crystal structures of laumontite.

Sec. Int. Conf. Mol. Sieve Zeolites (Worcester) Preprints: 517–523.
SCHULZ, R. K., R. OVERSTREET and I. BARSHAD (1965) Some unusual ionic exchange properties of certain salt-effected soils. Soil Sci. **99**: 161–165.
SEKI, Y. (1969) Facies series in low-grade metamorphism. J. Geol. Soc. Japan **75**: 225–260.
SHEPARD, A. O. and H. C. STARKEY (1964) Effect of cation exchange on the thermal behaviour of heulandite and clinoptilolite. U.S. Geol. Surv. Prof. Paper **475-D**: 89–92.
SHEPPARD, R. A. and A. J. GUDE (1968) Distribution and genesis of authigenic silicate minerals in tuffs of pleistocene Lake Tecopa, Inyo County, Calif. U.S. Geol. Surv. Prof. Paper **597**.
SIMONOT-GRANGE, M.-H., G. WATELLE-MARION et A. COINTOT (1968) Caractères physico-chimiques de l'eau dans la heulandite. Étude diffractométrique des phases observées au cours de la déshydratation et de la réhydratation. Bull. Soc. Chim. de France **1968**: 2747-2754.
SLAUGHTER, M. (1970) Crystal structure of stilbite. Amer. Miner. **55**: 387–397.
SMITH, G. W. and R. WALLS (1971) A redetermination of the unit-cell geometry of scolecite. Min. Mag. **38**: 72–75.
SMITH, J. V. (1962) Crystal structures with a chabazite framework. I. Dehydrated Ca-chabazite. Acta Cryst. **15**: 835–845.
SMITH, J. V. (1963) Structural classification of zeolites. Min. Soc. Amer. Spec. Paper **1**: 281–290.
SMITH, J. V. (1968) Structure of sorption complexes in zeolites. S.C.I. Monograph Mol. Sieves: 28–35.
SMITH, J. V. and O. F. TUTTLE (1957) The nepheline-kalsilite system. I. X-ray data for the crystalline phases. Amer. J. Sci. **255**, 282–305.
SMITH, J. V., F. RINALDI and L. S. DENT GLASSER (1963) Crystal structures with a chabazite framework. II. Hydrated Ca-chabazite at room temperature. Acta Cryst. **16**: 45–53.
STEBUTT, A. (1930) Lehrbuch der allgemeinen Bodenkunde. Verlag Gebr. Borntraeger, Berlin.
STEINFINK, H. (1962) The crystal structure of the zeolite phillipsite. Acta Cryst. **15**: 644–651.
TAYLOR, W. H. (1930) The structure of analcite ($NaAlSi_2O_2 \cdot H_2O$). Zeit. Krist. **74**: 1–19.
TAYLOR, W. H. (1938) Note on the structure of analcite and pollucite. Zeit. Krist. **99**: 283–290.
TAYLOR, W. H. and R. JACKSON (1933) The structure of edingtonite. Zeit. Krist. **86**: 53–64.
TAYLOR, W. H., C. A. MEEK and W. W. JACKSON (1933) The structures of the fibrous zeolites. Zeit. Krist. **84**: 373–398.
TISELIUS, A. (1936) Adsorption and diffusion in zeolite crystals. J. Phys. Chem. **40**: 223–232.
TISELIUS, A. and S. BROHULT (1934) Sorption von Wasserdampf an Chabasit bei verschiedenen Temperaturen. Zeit. Phys. Chem. Abt. A. **168**: 248–256.
UBBELOHDE, A. R. (1957) Thermal transformations in solids. Quarterly Rev. **11**: 246–272.
VAN REEUWIJK, L. P. (1967) Pedogenetic and clay mineralogical studies: II Properties of synthetic and natural amorphous alumino-silicates. M.Sc. diss., Dept. of Soil Science, Univ. of Natal, Pietermaritzburg, South Africa.
VAN REEUWIJK, L. P. (1971) The dehydration of gismondite. Amer. Miner. **56**: 1655–1659.
VAN REEUWIJK, L.P. (1972) High-temperature phases of zeolites of the natrolite group. Amer. Miner. **57**: 499–510.
VAN REEUWIJK, L. P. and J. M. DE VILLIERS (1968) Potassium fixation by amorphous alumino-silica gels. Soil Sci. Soc. Amer. Proc. **32**: 238–240.
VENUTO, P. B. (1970) Some perspectives on zeolite catalysis. Second Int. Conf. Mol. Sieves (Worcester) Preprints: 186–209.
VISSER, J. W. (1969) A fully automatic program for finding the unit cell from powder data. J. Appl. Cryst. **2**: 89–95.
WEBER, J. N. and R. ROY (1965) Complex stable $\rightleftarrows$ metastable solid reactions illustrated with the $Mg(OH)_2 \rightleftarrows MgO$-reaction. Am. J. Sci. **263**: 668–677.
WEISBROD, A. (1968) Détermination rapide des variations réactionnelles d'entropie et d'enthalpie à partir des courbes expérimentales d'équilibre; tracé rapide des courbes théoriques d'équilibre. Soc. française Miner. et Cristall. Bull. **91**: 444–452.
WENDLANDT, W. W. (1970) The detection of quadruple points in metal salt hydrate systems by

electrical conductivity measurements. Thermochim. Acta **1**: 11–17.
ZEN, E-AN (1971) Comments on the thermodynamic constants and hydrothermal stability relations of antophyllite. Am. J. Sci. **270**: 136-150.
ZEN, E-AN (1972) Gibbs free energy, enthalpy, and entropy of ten rockforming minerals: calculations, discrepancies, implications. Amer. Miner. **57**: 524–553.

PERSOONLIJKE GEGEVENS

De auteur werd op 11 december 1941 geboren te Haarlemmermeer. Na het behalen van het diploma HBS-b aan het Laurens Coster Lyceum (1e Gem. HBS-b) te Haarlem ging hij in 1959 studeren aan de Landbouwhogeschool te Wageningen. In 1964 werd het kandidaatsexamen in de richting Bodemkunde en Bemestingsleer afgelegd. De praktijktijd van 1965 t/m 1967 werd gecombineerd met een studie aan de Universiteit van Natal (Rep. van Zuid-Afrika) onder supervisie van Dr. J. M. DE VILLIERS, waar hij cum laude de graad van Master of Science in Agriculture ontving. Het ingenieursexamen in eerdergenoemde richting werd in 1968 afgelegd (hoofdvak regionale bodemkunde; bijvakken bodemscheikunde en -natuurkunde en geologie) waarna hij als wetenschappelijk assistent en vanaf 1971 als wetenschappelijk medewerker werkzaam was bij de Vakgroep Bodemkunde en Geologie van de Landbouwhogeschool. Sedert 1 januari 1974 is hij verbonden aan het International Soil Museum te Utrecht.